Materialwerte - Zusammenstellung zum Optoelektronikseminar GaAs - $Ga_xIn_{1-x}As$ - $Al_xIn_{1-x}As$ - InP

Dipl.- Ing. Björnstjerne Zindler, M.Sc.

www.Zenithpoint.de

Erstellt: 1. Oktober 2009 – Letzte Revision: 30. Juni 2021

Inhaltsverzeichnis

Literatur

[002] http://www.ioffe.ru/SVA/NSM/Semicond/.

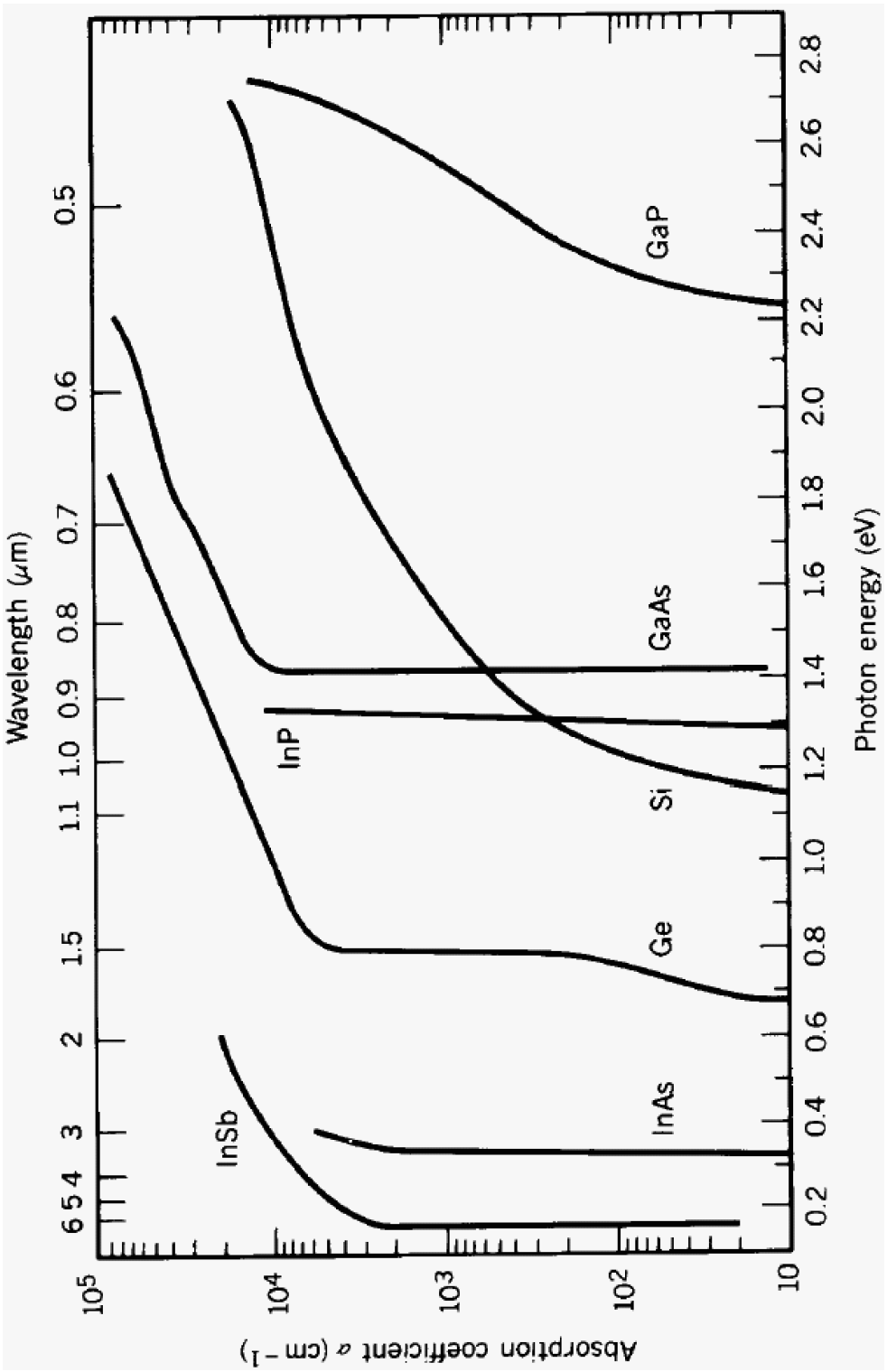
Absorption coefficient α (cm⁻¹)
Wavelength (μm)
Photon energy (eV)
InSb
InAs
Ge
InP
Si
GaAs
GaP

1 GaAs

[002]ff.

1.1 Originaltexte

Dokument nächste Seite folgend.

Si	- Silicon	Ge	- Germanium
GaP	- Gallium Phosphide	GaAs	- Gallium Arsenide
InAs	- Indium Arsenide	C	- Diamond
GaSb	- Gallium Antimonide	InSb	- Indium Antimonide
InP	- Indium Phosphide	$GaAs_{1-x}Sb_x$	- Gallium Arsenide Antimonide
$Al_xGa_{1-x}As$	- Aluminium Gallium Arsenide		
AlN	- Aluminium Nitride	InN	- Indium Nitride
BN	- Boron Nitride	GaN	- Gallium Nitride

We are going to add new data for:

$Ga_xIn_{1-x}As_ySb_{1-y}$	- Gallium Indium Arsenide Antimonide	$Ga_xIn_{1-x}P$	- Gallium Indium Phosphide
$Ga_xIn_{1-x}As$	- Gallium Indium Arsenide	$Ga_xIn_{1-x}Sb$	- Gallium Indium Antimonide
$InAs_{1-x}Sb_x$	- Indium Arsenide Antimonide	$Ga_xIn_{1-x}As_yP_{1-y}$	- Gallium Indium Arsenide Phosphide
$Si_{1-x}Ge_x$	- Silicon Germanium	SiC	- Silicon Carbide

This section is intended to systematize parameters of semiconductor compounds and heterostructures based on them. Such a WWW-archive has a number of advantages: in particular, it enables physicists, both theoreticians and experimentalists, to rapidly retrieve the semiconducting material parameters they are interested in. In addition, physical parameters - optical, electrical, mechanical, etc. - will be presented in the framework of the electronic archive for both the known and new semiconducting compounds. As the starting point in creating the database served the voluminous reference book *"Handbook Series on Semiconductor Parameters"* vol. 1,2 edited by M. Levinstein, S. Rumyantsev and M. Shur, World Scientific, London, 1996, 1999. We express sincere gratitude to M.E. Levinstein for help and attention to this work. A great number of reference books and original papers cited at the end of this section have been used in compiling the information database.

We would like to express our warmest gratitude to all colleages presented their original data and literature references to complete these archive. If you find these archive pages helpful, and use the data retrieved through the server for your reseach, we would appreciate acknowledging it in your papers.

We would be indebted very much for any of your further suggestions and comments.

Authors

GaAs - Gallium Arsenide

GaAs - Gallium Arsenide

Basic Parameters at 300 K

Crystal structure	Zinc Blende
Group of symmetry	T_d^2-F43m
Number of atoms in 1 cm^3	$4.42 \cdot 10^{22}$
de Broglie electron wavelength	240 A
Debye temperature	360 K
Density	5.32 g cm^{-3}
Dielectric constant (static)	12.9
Dielectric constant (high frequency)	10.89
Effective electron mass m_e	$0.063m_o$
Effective hole masses m_h	$0.51m_o$
Effective hole masses m_{lp}	$0.082m_o$
Electron affinity	4.07 eV
Lattice constant	5.65325 A
Optical phonon energy	0.035 eV

GaAs - Gallium Arsenide

Band structure and carrier concentration

Basic Parameters

Energy gap	1.424 eV
Energy separation ($E_{\Gamma L}$) between Γ and L valleys	0.29 eV
Energy separation ($E_{\Gamma X}$) between Γ and X valleys	0.48 eV
Energy spin-orbital splitting	0.34 eV
Intrinsic carrier concentration	$2.1 \cdot 10^{6}$ cm^{-3}
Intrinsic resistivity	$3.3 \cdot 10^{8}$ Ω·cm
Effective conduction band density of states	$4.7 \cdot 10^{17}$ cm^{-3}
Effective valence band density of states	$9.0 \cdot 10^{18}$ cm^{-3}

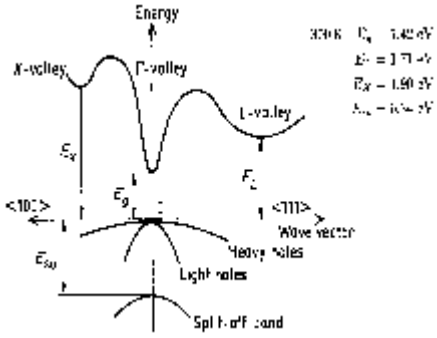

Band structure and carrier concentration of GaAs. 300 K
E_g = 1.42 eV
E_L = 1.71 eV
E_X= 1.90 eV
E_{so} = 0.34 eV

Temperature Dependences

Temperature dependence of the energy gap

$E_g=1.519-5.405 \cdot 10^{-4} \cdot T^2/(T+204)$ (eV)
where T is temperatures in degrees K ($0 < T < 10^3$).

Temperature dependence of the energy difference between the top of the valence band and the bottom of the L-valley of the conduction band

$E_L=1.815-6.05 \cdot 10^{-4} \cdot T^2/(T+204)$ (eV)

Temperature dependence of the energy difference between the top of the valence band and the bottom of the X-valley of the conduction band

$E_L=1.981-4.60 \cdot 10^{-4} \cdot T^2/(T+204)$ (eV)

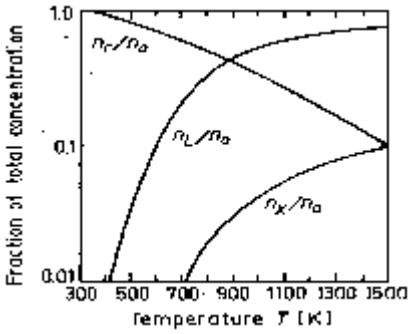

The temperature dependences of the relative populations of the Γ, L and X valleys.
(Blakemore [1982]).

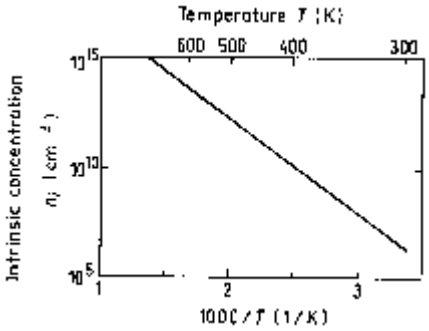

The temperature dependences of the intrinsic carrier concentration.
(Shur [1990]).

Intrinsic Carrier Concentration

$n_i = (N_c \cdot N_v)^{1/2} exp(-E_g/(2k_bT))$

Effective density of states in the conduction band taking into account the nonparabolicity of the Γ-valley and contributions from the X and L-valleys
$N_c = 8.63 \cdot 10^{13} \cdot T^{3/2} [1 - 1.9310^{-4} \cdot T - 4.19 \cdot 10^{-8} \cdot T^2 + 21 \cdot exp(-E_{\Gamma L}/(2k_bT)) + 44 \cdot exp(-E_{\Gamma X}/(2k_bT))$ (cm^{-3})

Effective density of states in the valence band

$N_v = 1.83 \cdot 10^{15} \cdot T^{3/2}$ (cm^{-3})

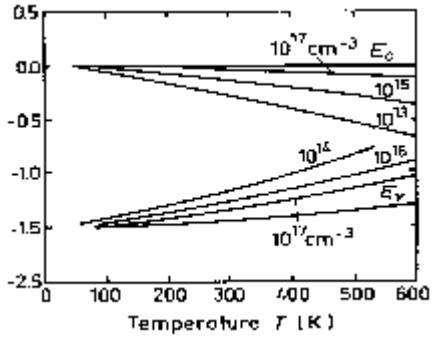

Fermi level versus temperature for different concentrations of shallow donors and acceptors.

Dependences on Hydrostatic Pressure

$E_g = E_g(0) + 0.0126 \cdot P - 3.77 \cdot 10^{-5} P^2$ (eV)
$E_L = E_L(0) + 5.5 \cdot 10^{-3} P$ (eV)
$E_X = E_X(0) + 1.5 \cdot 10^{-3} P$ (eV)
where P is pressure in kbar.

Energy Gap Narrowing at High Doping Levels

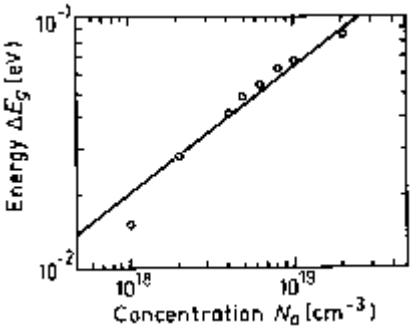

Energy gap narrowing at high doping levels.
(Tiwari and Wright [1990])

$\Delta Eg \approx 2 \cdot 10^{-11} \cdot N_a^{-1/2}$ (eV) (N_a- in cm.$^{-3}$)

Effective Masses

Electrons:

For Γ-valley	$m_\Gamma = 0.063 m_o$
In the L-valley the surfaces of equal energy are ellipsoids	
	$m_l = 1.9 m_o$
	$m_t = 0.075 m_o$
Effective mass of density of states	
$m_L=(16 m_l m_t^2)^{1/3}$	$m_L=0.85 m_o$
In the X-valley the surfaces of equal energy are ellipsoids	
	$m_l = 1.9 m_o$
	$m_t = 0.19 m_o$
Effective mass of density of states	
$m_X=(9 m_l m_t^2)^{1/3}$	$m_X=0.85 m_o$

Holes:

Heavy	$m_h = 0.51 m_o$
Light	$m_{lp} = 0.082 m_o$
Split-off band	$m_{so} = 0.15 m_o$
Effective mass of density of states	$m_v = 0.53 m_o$

Donors and Acceptors

Ionization energies of shallow donors (eV)
(Milnes [1973])

S	Se	Si	Ge	Sn	Te
~0.006	~0.006	~0.006	~0.006	~0.006	~0.03

Ionization energies of shallow acceptors (eV)
(Milnes [1973])

C	Si	Ge	Zn	Sn
~0.02	~0.03/0.1/0.22	~0.03	~0.025	~0.2

GaAs - Gallium Arsenide

Electrical properties

Basic Parameters

Breakdown field	$\approx 4 \cdot 10^5$ V/cm
Mobility electrons	≤ 8500 cm^2 V^{-1}s^{-1}
Mobility holes	≤ 400 cm^2 V^{-1}s^{-1}
Diffusion coefficient electrons	≤ 200 cm^2/s
Diffusion coefficient holes	≤ 10 cm^2/s
Electron thermal velocity	$4.4 \cdot 10^5$ m/s
Hole thermal velocity	$1.8 \cdot 10^5$m/s

Mobility and Hall Effect

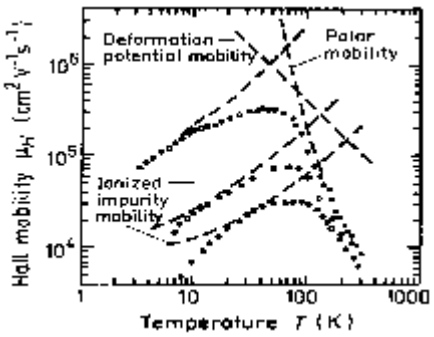

Electron Hall mobility versus temperature for different doping levels. *(Stillman et al. [1970]*

1. Bottom curve: $N_d=5 \cdot 10^{15}$cm^{-3};

2. Middle curve : $N_d=10^{15}$cm^{-3};

3. Top curve : $N_d=5 \cdot 10^{15}$cm^{-3}

For weakly doped GaAs at temperature close to 300 K, electron Hall mobility

$\mu_H=9400(300/T)$ cm^2 V^{-1} s^{-1}

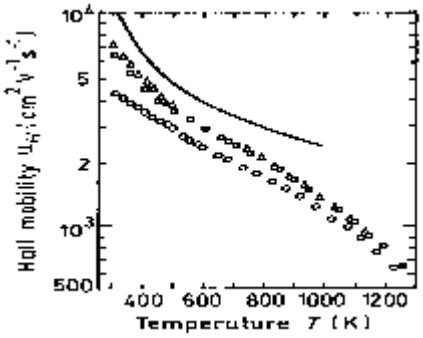

Electron Hall mobility versus temperature for different doping levels and degrees of compensation (high temperatures):

Open circles: $N_d=4N_a=1.2 \cdot 10^{17}$ cm^{-3};

Open squares: $N_d=4N_a=10^{16}$ cm^{-3};

Open triangles: $N_d=3N_a=2 \cdot 10^{15}$ cm^{-3};

Solid curve represents the calculation for pure GaAs *(Blakemore[1982])*.

For weakly doped GaAs at temperature close to 300 K, electron drift mobility

$\mu_n=8000(300/T)^{2/3}$ cm^2 V^{-1} s^{-1}

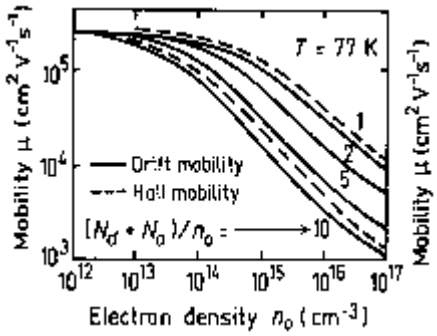

Drift and Hall mobility versus electron concentration for different degrees of compensation T= 77 K
(Rode [1975]).

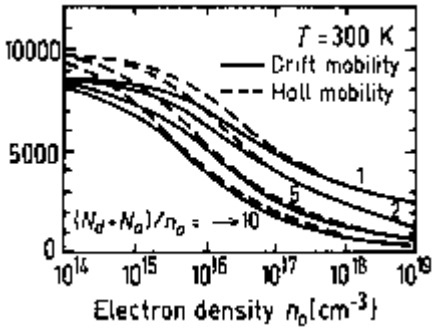

Drift and Hall mobility versus electron concentration for different degrees of compensation T= 300 K
(Rode [1975]).

Approximate formula for the Hall mobility

. $\mu_n = \mu_{OH}/(1+N_d \cdot 10^{-17})^{1/2}$, where $\mu_{OH} \approx 9400$ ($cm^2\ V^{-1}\ s^{-1}$), N_d- in cm^{-3}
(Hilsum [1974]).

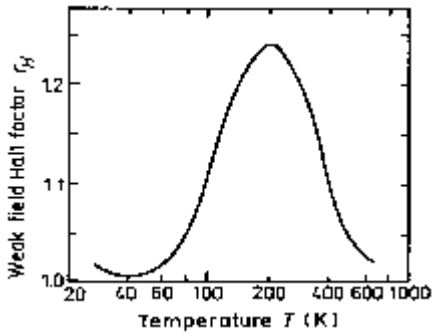

Temperature dependence of the Hall factor for pure *n*-type GaAs in a weak magnetic field
(Rode [1975]).

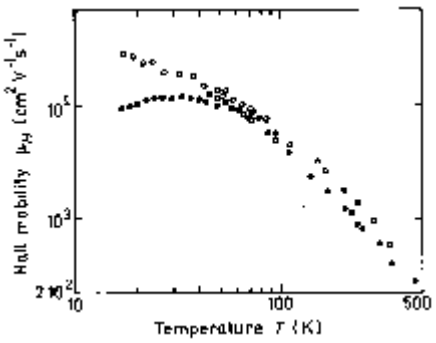

Temperature dependence of the Hall mobility for three high-purity samples
(Wiley [1975])

For GaAs at temperatures close to 300 K, hole Hall mobility

$$\mu_{pH} = \left[0.0025 \left(\frac{T}{300} \right)^{2.3} + 4 \times 10^{21} p \left(\frac{T}{300} \right)^{1.5} \right]^{-1}$$ ($cm^2 V^{-1} s^{-1}$), (p - in cm^{-3})

For weakly doped GaAs at temperature close to 300 K, Hall mobility
$\mu_{pH} = 400(300/T)^{2.3}$ ($cm^2\ V^{-1}\ s^{-1}$).

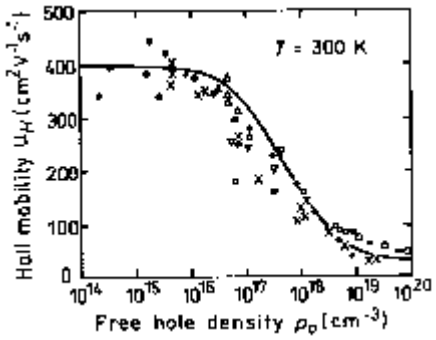

The hole Hall mobility versus hole density.
(Wiley [1975])

At *T*= 300 K, the Hall factor in pure GaAs

r_H=1.25.

Transport Properties in High Electric Fields

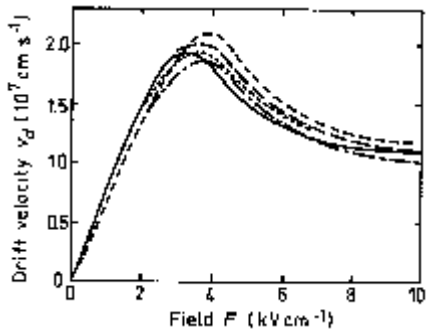

Field dependences of the electron drift velocity.
(Blakemore[1982]).
Solid curve was calculated by *(Pozhela and Reklaitis[1980])*.
Dashed and dotted curves are measured data, 300 K

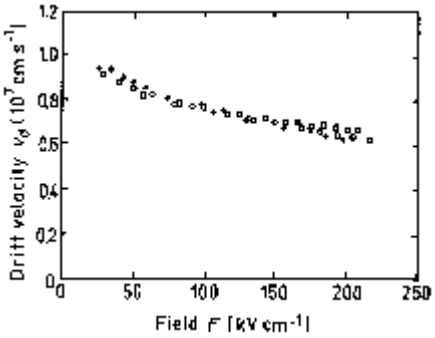

Field dependences of the electron drift velocity for high electric fields, 300 K.
(Blakemore[1982]).

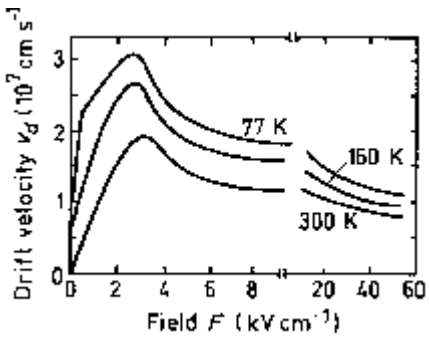

Field dependences of the electron drift velocity at different temperatures.
(Pozhela and Reklaitis[1980]).

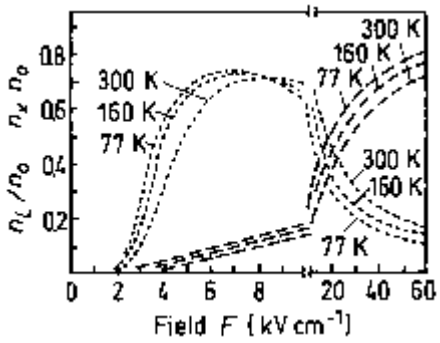

Fraction of electrons in *L* and *X* valleys. n_L and n_X as a function of electric field *F* at 77, 160, and 300 K, N_d=0
(Pozhela and Reklaitis[1980]).
Dotted curve - *L* valleys, dashed curve - *X* valleys.

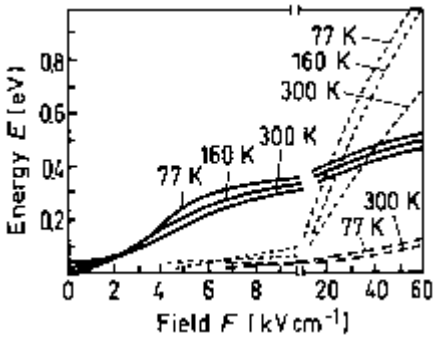

Mean energy *E* in *Γ*, *L*, and *X* valleys as a function of electric field *F* at 77, 160, and 300 K, N_d=0
(Pozhela and Reklaitis[1980]).
Solid curve - Γ valleys, dotted curve - *L* valleys, dashed curve - *X* valleys.

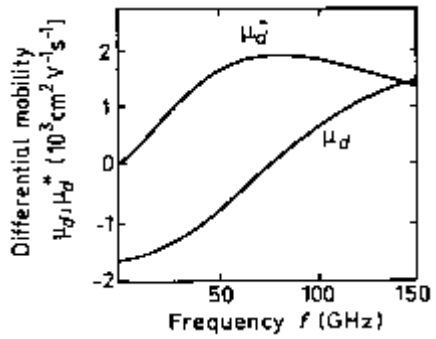

Frequency dependences of electron differential mobility.
μ_d is real part of the differential mobility; μ_d^* is imaginary part of differential mobility.
F= 5.5 kV cm^{-1}
(Rees[1969]).

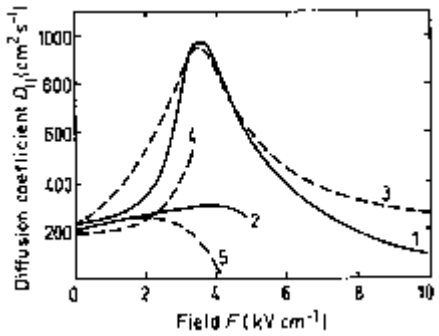

The field dependence of longitudinal electron diffusion coefficient *D*||*F*.
Solid curves 1 and 2 are theoretical calculations. Dashed curves 3, 4, and 5 are experimental data.
Curve 1 - from *(Pozhela and Reklaitis[1980])*.
Curve 2 - from *(Fauquembergue et al.[1980])*.
Curve 3 - from *(Ruch and Kino[1968])*.
Curve 4 - from *(Bareikis et al.[1978])*.
Curve 5 - *(from de Murcia[1991])*.

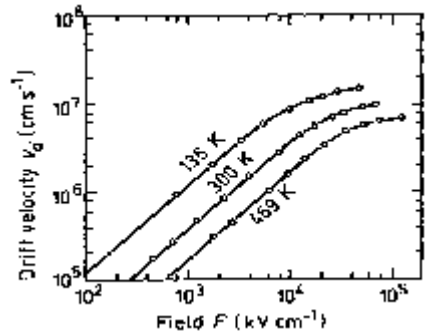

Field dependences of the hole drift velocity at different temperatures.
(Datal et al. [1971]).

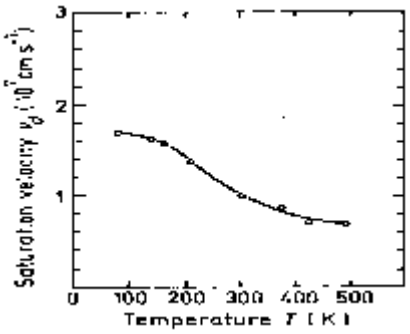

Temperature dependence of the saturation hole velocity in high electric fields
(Datal et al. [1971]).

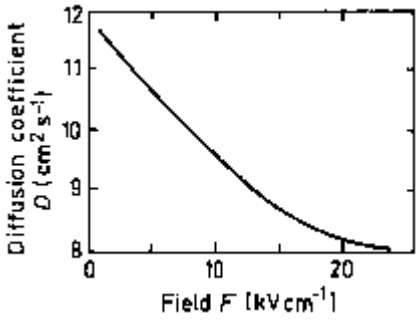

The field dependence of the hole diffusion coefficient.
(Joshi and Crendin [1989]).

Impact Ionization

There are two schools of thought regarding the impact ionization in GaAs.

The first one states that impact ionization rates α_i and β_i for electrons and holes in GaAs are known accurately enough to distinguish such subtle details such as the anisothropy of α_i and β_i for different crystallographic directions. This approach is described in detail in the work by Dmitriev et al.[1987].

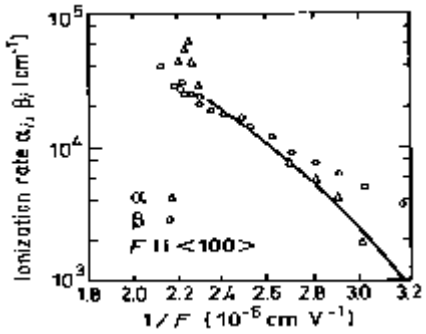

Experimental curves α_i and β_i versus $1/F$ for GaAs.
(Pearsall et al. [1978]).

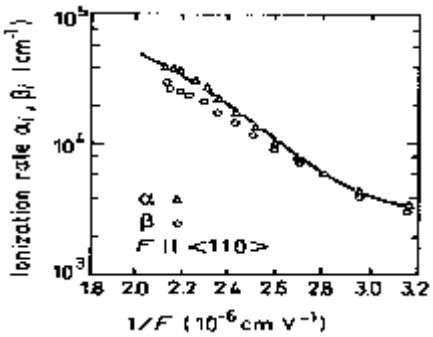

Experimental curves α_i and β_i versus $1/F$ for GaAs.
(Pearsall et al. [1978]).

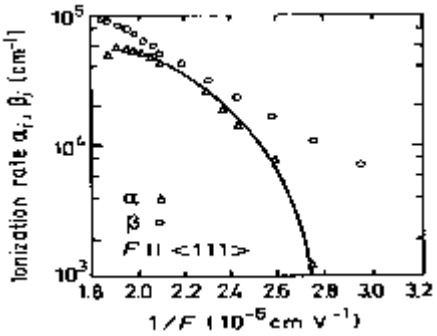

Experimental curves α_i and β_i versus *1/F* for GaAs.
(Pearsall et al. [1978]).

The second school focuses on the values of α_i and β_i for the same electric field reported by different researches differ by an order of magnitude or more. This point of view is explained by Kyuregyan and Yurkov [1989]. According to this approach we can assume that $\alpha_i = \beta_i$. Approximate formula for the field dependence of ionization rates:

$\alpha_i = \beta_i = \alpha_o exp[\delta - (\delta^2 + (F_0 / F)^2)^{1/2}]$

where $\alpha_o = 0.245 \cdot 10^6$ cm^{-1}; $\beta = 57.6\ F_o = 6.65 \cdot 10^6$ V cm^{-1} (Kyuregyan and Yurkov [1989]).

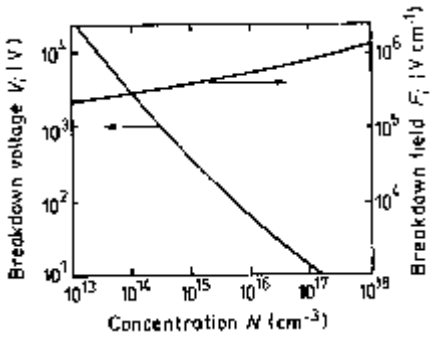

Breakdown voltage and breakdown field versus doping density for an abrupt *p-n* junction.
(Kyuregyan and Yurkov [1989]).

Recombination Parameter

Pure n-type material ($n_o \sim 10^{14}$cm^{-3})	
The longest lifetime of holes	$\tau_p \sim 3 \cdot 10^{-6}$ s
Diffusion length $L_p = (D_p \cdot \tau_p)^{1/2}$	$L_p \sim$30-50 µm.
Pure p-type material	
(a)Low injection level	
The longest lifetime of electrons	$\tau_n \sim 5 \cdot 10^{-9}$ s
Diffusion length $L_n = (D_n \cdot \tau_n)^{1/2}$	$L_n \sim$10 µm
(b) High injection level (filled traps)	
The longest lifetime of electrons	$\tau \sim 2.5 \cdot 10^{-7}$ s
Diffusion length L_n	$L_n \sim$ 70 µm

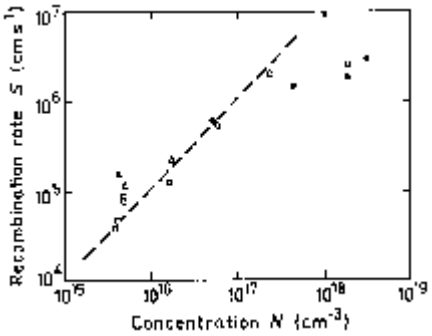

Surface recombination velocity versus doping density *(Aspnes [1983])*.
Different experimental points correspond to different surface treatment methods.

Radiative recombination coefficient *(Varshni[1967])*

90 K $1.8 \cdot 10^{-8} cm^3/s$
185 K $1.9 \cdot 10^{-9} cm^3/s$
300 K $7.2 \cdot 10^{-10} cm^3/s$

Auger coefficient

300 K $\sim 10^{-30} cm^6/s$
500 K $\sim 10^{-29} cm^6/s$

GaAs - Gallium Arsenide

Optical properties

Infrared refractive index	3.3
Radiative recombination coefficient	$7 \cdot 10^{-10}$ cm^3/s

Infrared refractive index

$n = k^{1/2} = 3.255 \cdot (1 + 4.5 \cdot 10^{-5} T)$
for 300 K n= 3.299

Long-wave *TO* phonon energy

$h\nu_{TO} = 33.81 \cdot (1 - 5.5 \cdot 10^{-5} T)$ (meV)
for 300 K $h\nu_{TO}$ = 33.2 meV

Long-wave *LO* phonon energy

$h\nu_{LO} = 36.57 \cdot (1 - 4 \cdot 10^{-5} T)$ (meV)
for 300 K $h\nu_{LO}$ = 36.1 meV

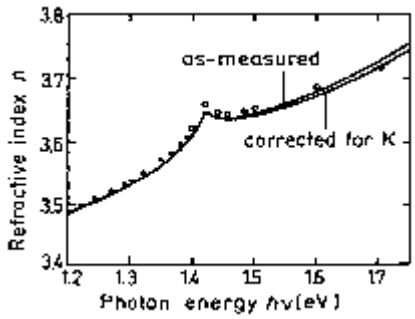

Refractive index *n* versus photon energy for a high-purity GaAs.($n_0 \sim 5 \cdot 10^{13}$ cm^{-3}).
Solid curve is deduced from two-beam reflectance measurements at 279 K. Dark circles are obtained from refraction measurements. Light circles are calculated from Kramers-Kronig analysis
(Blakemore [1982]).

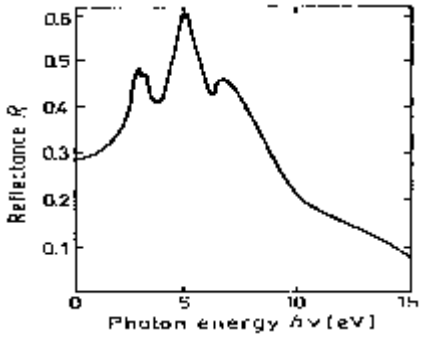

Normal incidence reflectivity versus photon energy.
(Phillip and Ehrenreich [1963]).

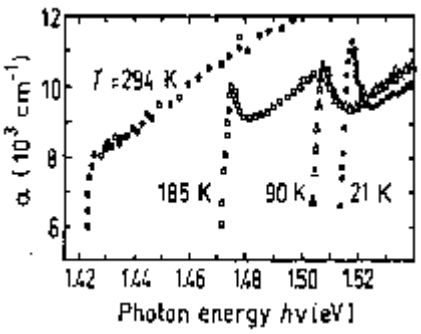

Intrinsic absorption coefficient near the intrinsic absorption edge for different temperatures.
(Sturge [1962]).

A ground state Rydberg energy R_{X1}= 4.2 meV

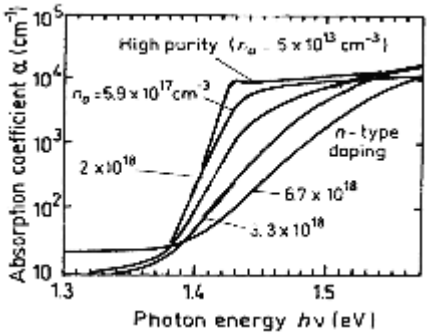

Intrinsic absorption edge at 297 K at different doping levels. *n*-type doping
(Casey et al. [1975]).

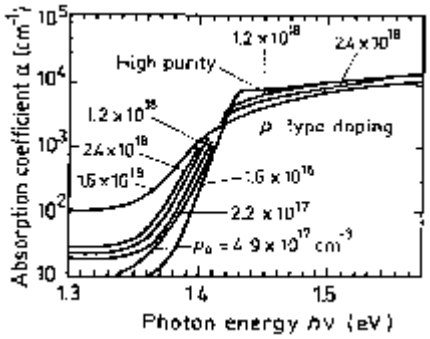

Intrinsic absorption edge at 297 K at different doping levels. *p*-type doping
(Casey et al. [1975]).

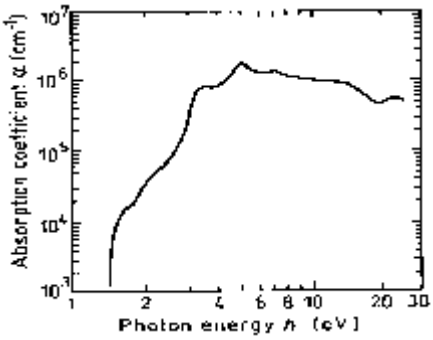

The absorption coefficient versus photon energy from intrinsic edge to 25 eV.
(Casey et al. [1975]).

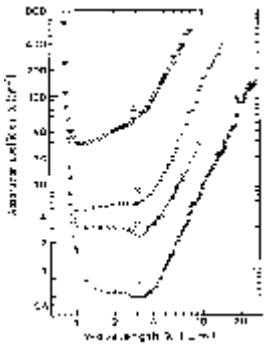

Free carrier absorption versus wavelength at different doping levels, 296 K
(Spitzer and Whelan [1959]).
Conduction electron concentrations are:
1. 1.3·10^{17}cm^{-3}; **2**. 4.9·10^{17}cm^{-3}; **3**. 10^{18}cm^{-3}; **4**. 5.4·10^{18}cm^{-3}

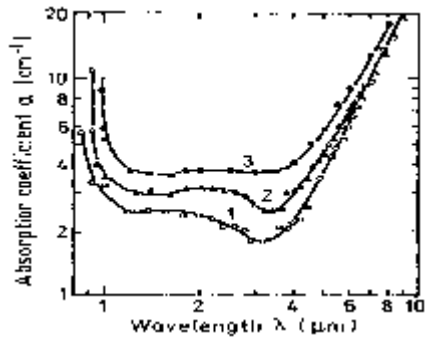

Free carrier absorption versus wavelength at different temperatures.
n_o = 4.9·10^{17}cm^{-3} *(Spitzer and Whelan [1959])*
Temperatures are: **1**. 100 K; **2**. 297 K; **3**. 443 K.

At 300 K

For λ~2 μm α=6·10^{-18} n_o (cm^{-1}) (n_o - in cm^{-1})
For λ > 4μm and 10^{17}<n_o<10^{18}cm^{-3} $\alpha \approx 7.5 \cdot 10^{-20} n_o \cdot \lambda^3$ (cm^{-1}) (n_o - in cm^{-3}, λ - μm)

GaAs - Gallium Arsenide

Thermal properties

Bulk modulus	$7.53 \cdot 10^{11}$ dyn cm^{-2}
Melting point	1240 °C
Specific heat	0.33 J g^{-1}°C $^{-1}$
Thermal conductivity	0.55 W cm^{-1} °C $^{-1}$
Thermal diffusivity	0.31cm^2s^{-1}
Thermal expansion, linear	$5.73 \cdot 10^{-6}$ °C $^{-1}$

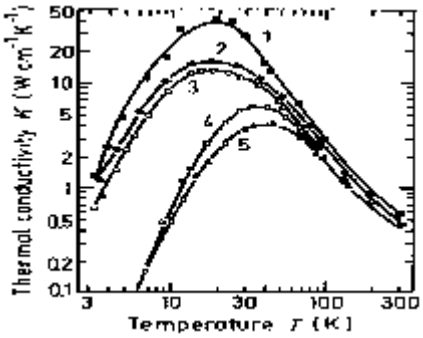

Temperature dependence of thermal conductivity
n-type sample, n_o (cm^{-3}): **1**. 10^{16}; **2**. $1.4 \cdot 10^{16}$; **3**. 10^{18};
p-type sample, p_o (cm^{-3}): **4**. $3 \cdot 10^{18}$; **5**. $1.2 \cdot 10^{19}$.
(Carlson et al [1965]).

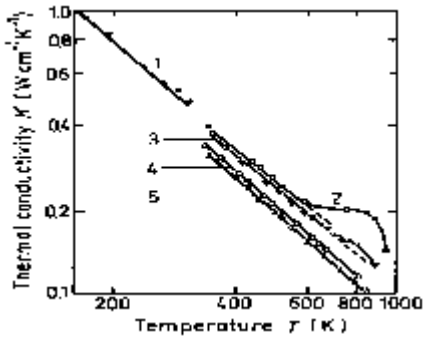

Temperature dependence of thermal conductivity (for high temperature)
n-type sample, n_o (cm^{-3}): **1**. $7 \cdot 10^{15}$; **2**. $5 \cdot 10^{16}$; **3**. $4 \cdot 10^{17}$; **4**. $8 \cdot 10^{18}$;
p-type sample, p_o (cm^{-3}): **5**. $6 \cdot 10^{19}$.
(Blakemore [1982]).

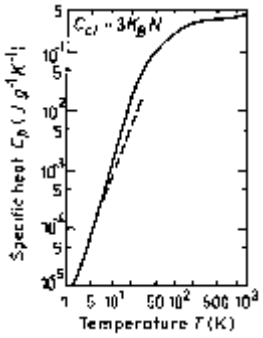

Temperature dependence of specific heat at constant pressure C_{cl}= $3k_bN$ = 0.345 J g^{-1}°C $^{-1}$.
N is the number of atoms in 1 g og GaAs.
Dashed line: $C_p = (4\pi^2 C_{cl} / 5\theta_o^3) \cdot T^3$ for θ_o= 345 K.
(Blakemore [1982]).

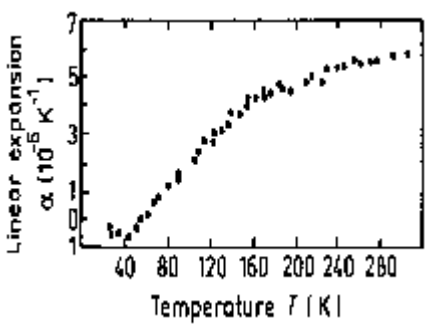

Temperature dependence of linear expansion coefficient α
(Novikova[1961]).

Melting point	T_m=1513 K
For 0 < P < 45 kbar	T_m= 1513 - 3.5P (P in kbar)
Saturated vapor pressure (in Pascals)	
1173 K	1
1323 K	100

GaAs - Gallium Arsenide

Mechanical properties, elastic constants, lattice vibrations

Basic Parameter

Bulk modulus	$7.53 \cdot 10^{11}$ dyn cm^{-2}
Density	5.317 g cm^{-3}
Hardness on the Mohs scale	between 4 and 5
Surface microhardness (using Knoop's pyramid test)	750 kg mm^{-2}
Cleavage plane	{110}
Piezoelectric constant	e_{14}=-0.16 C m^{-2}

Elastic constants 300 K.

C_{11}=11.90$\cdot 10^{11}$ dyn/cm^2
C_{12}=5.34$\cdot 10^{11}$ dyn/cm^2
C_{44}=5.96$\cdot 10^{11}$ dyn/cm^2

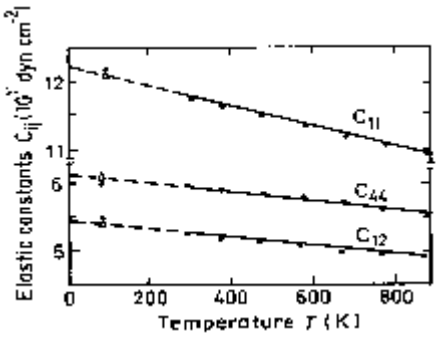

Temperature dependences of elastic constants.
For 0<T<T_m=1513K (in units of 10^{11} dyn cm^{-2})
C_{11}= 12.17 - 1.44$\cdot 10^{-3}T$
C_{12}= 5.46 - 0.64$\cdot 10^{-3}T$
C_{44}= 6.16 - 0.70$\cdot 10^{-3}T$
(Burenkov et al. [1973])

For T = 300 K

Bulk modulus (compressibility^{-1})	B_s= 7.53$\cdot 10^{11}$dyn/cm^2
Shear modulus	C'= 3.285$\cdot 10^{11}$dyn/cm^2
[100] Young's modulus	Y_o= 8.59$\cdot 10^{11}$dyn/cm^2
[100] Poisson ratio	σ_o = 0.31

Acoustic Wave Speeds

Wave propagation	Wave character	Expression for wave speed	Wave speed (in units of

Direction			10^5 cm/s)
[100]	V_L	$(C_{11}/\rho)^{1/2}$	4.73
	V_T	$(C_{44}/\rho)^{1/2}$	3.35
[110]	V_l	$[(C_{11}+C_{l2}+2C_{44})/2\rho]^{1/2}$	5.24
	$V_{t\|\|}$	$V_{t\|\|}=V_T=(C_{44}/\rho)^{1/2}$	3.35
	$V_{t\perp}$	$[(C_{11}-C_{12})/2\rho]^{1/2}$	2.48
[111]	V_l'	$[(C_{11}+2C_{12}+4C_{44})/3\rho]^{1/2}$	5.4
	V_t'	$[(C_{11}-C_{12}+C_{44})/3\rho]^{1/2}$	2.8

Phonon frequencies

(in units of 10^{12} Hz) *(Waugh and Dolling [1963])*

$\nu_{TO}(\Gamma)$ 8.02 ν_{LO} (X) 7.22
$\nu_{LO}(\Gamma)$ 8.55 ν_{TA}(L) 1.86
ν_{TA}(X) 2.36 ν_{LA}(L) 6.26
ν_{LA}(X) 6.80 ν_{TO}(L) 7.84
ν_{TO}(X) 7.56 ν_{LO}(L) 7.15

GaAs - Gallium Arsenide

References:

- Levinshtein M.E., S.L. Rumyantsev *Handbook Series on Semiconductor Parameters*, **vol.1**, M. Levinshtein, S. Rumyantsev and M. Shur, ed., World Scientific, London, 1996, pp. 77-103.
- Dargys A. and J. Kundrotas *Handbook on Physical Properties of Ge, Si, GaAs and InP*, Vilnius, Science and Encyclopedia Publishers, 1994

- Aspnes, D. E., *Surface Sci.* **132**, 1-3 (1983) 406-421.
- Bareikis, V., F. Galdikas, R. Milisyte, and V. Viktoravicius, *Proc. 5th Conf. on Noise in Physical Systems,* Bad Nauheim, West Germany, Mar. 1978, p. 212.
- Blakemore, J. S., *J. Appl. Phys.* **53**, 10 (1982) R123-R181.
- Burenkov, Yu. A., Yu. M. Burdukov, S. Yu. Davidov, and S. P. Nikanorov, *Sov. Phys. Solid State* **15**, 6 (1973) 1175-1177.
- Carlson, R. 0., G. A. Slack, and S. J. Silverman, *J. Appl. Phys.* **36**, 2 (1965) 505.
- Casey, H. C., D. D. Sell, and K. W. Wecht, *J. Appl. Phys.* **46**, 1 (1975) 250.
- Dalal, V. L., A. B. Dreeben, and A. Triano, *J. Appl. Phys.* **42**, 7 (1971) 2864-2867.
- de Murcia, M., D. Gasquet, A. Elamri, J. P. Nougier, and J. Vanbremeerch, *IEEE Trans. Electron. Dev.* **ED-38**, 11 (1991) 2531-2539.
- Dmitriev, A. P., M. P. Mikhailova, and I. N. Yassievich, *Phys. Status Solidi (B)* **140**, 1(1987) 9-137.
- Fauquembergue, R., J. Zimmermann, A. Kaszynski, and E. Constant, *J. Appl. Phys.* **51**, 2 (1980) 1065-1071.
- Hilsum, C., Electron. Lett. 10, 13 (1974) 259-260. Joshi, R. and R. 0. Grendin, *Appl. Phys. Lett.* **54**, 24 (1989) 2438-2439.
- Kyuregyan, A. S. and S. N. Yurkov, *Sov. Phys. Semicond.* **23**, 10 (1989) 1126-1132.
- Milnes, A. G., Deep Impurities in Semiconductors, John Wiley and Sons, N.Y., 1973. Novikova, S. I., *Sov. Phys. Solid State* **3**, 1 (1961) 129.
- Pearsall, T. P., F. Capasso, R. E. Nahory, M. A. Pallack, and J. Chelikowsky, *Solid State Electron.* **21**, 1 (1978) 297-302.
- Phillip, H. R. and H. Ehrenreich, *Phys. Rev.* **129**, 4 (1963) 1550-1560.
- Pozhela, J. and A. Reklaitis, *Solid State Electron.* **23**, 9 (1980) 927-933.
- Rees, H. D., *Solid State Commun.* **7**, 2 (1969) 267-269.
- Rode, D. L., *Semiconductors and Semimetals*, R. K. Willardson and A. C. Beer, eds., *Academic Press*, N.Y., vol. 10, 1975, p. 1.
- Ruch, J. G. and G. S. Kino, *Phys. Rev.* **174**, 3 (1968) 921-931.
- Shur, M., *Physics of Semiconductor Devices*, Prentice Hall, 1990.
- Spitzer, W. G. and J. M. Whelan, *Phys. Rev.* **114**, 1 (1959) 59-63.
- Stillman, G. E., C. M. Waife, and J. 0. Dimmock, *J. Phys. Chem. Solids* **31**, 6 (1970)1199-1204.
- Sturge, M. D., *Phys. Rev.* **127**, 3 (1962) 768.
- Sze, S. M., *Physics of Semiconductor Devices*, John Wiley and Sons, N.Y., 1981.
- Tiwari, S. and S. L. Wright, *Appl. Phys. Lett.* **56**, 6 (1990) 563-565.
- Varshni, V. P., *Phys. Status Solidi* **19**, 2 (1967) 459-514; **20**, 1 (1967) 9-36.
- Waugh, J. L. T. and G. Dolling, *Phys. Rev.* **132**, 6 (1963) 2410.
- Wiley, J. D., *Semiconductor and Semimetals*, R. K. Willardson and A. C. Beer, eds., Academic Press, N.Y., vol. 10, 1975, p. 91.

1.2 Bildvergrößerungen

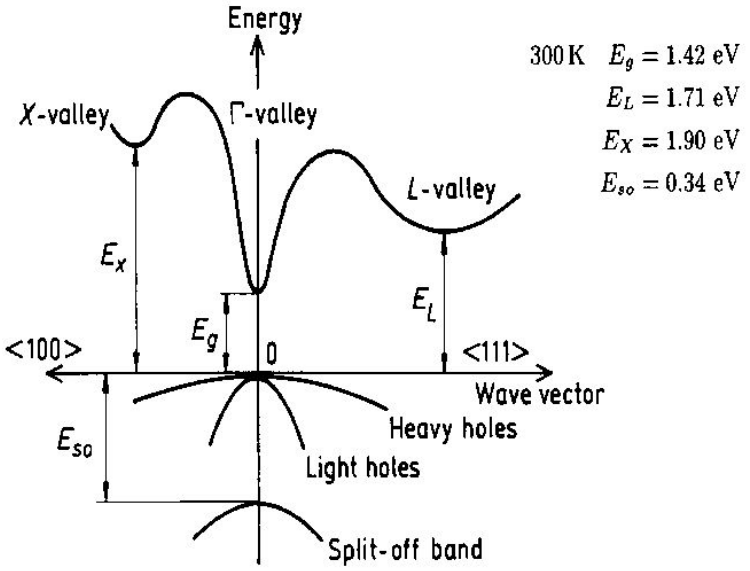

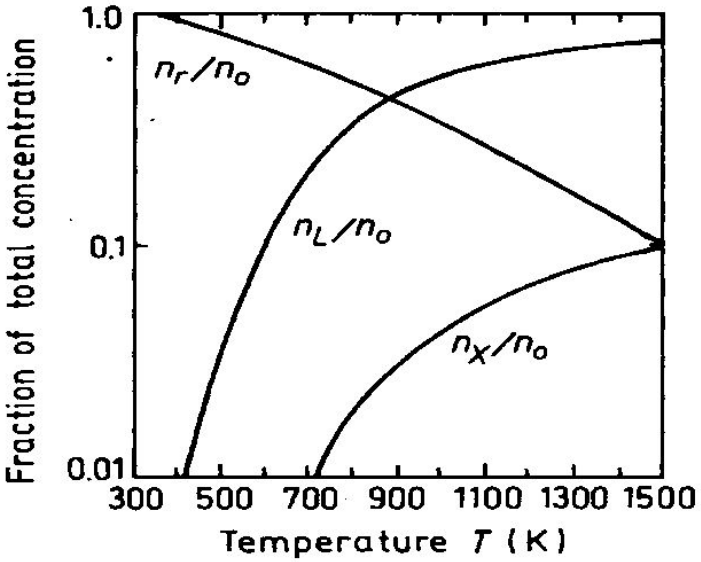

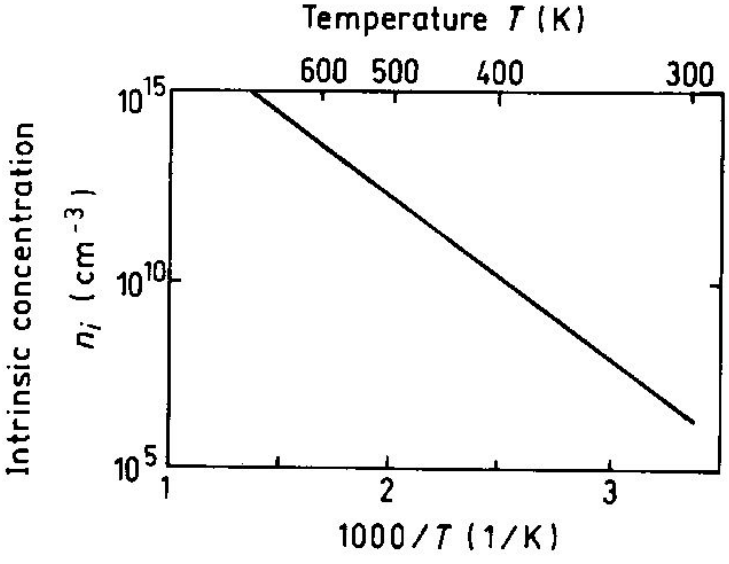

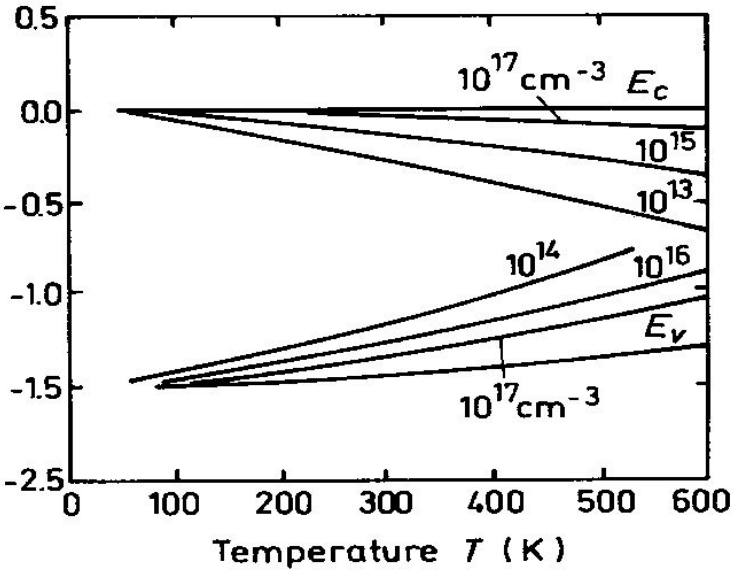
0.5
0.0
-0.5
-1.0
-1.5
-2.5
0
100
200
300
400
500
600
10^{17}cm^{-3} E_c
10^{15}
10^{13}
10^{14}
10^{16}
E_v
10^{17}cm^{-3}
Temperature T (K)

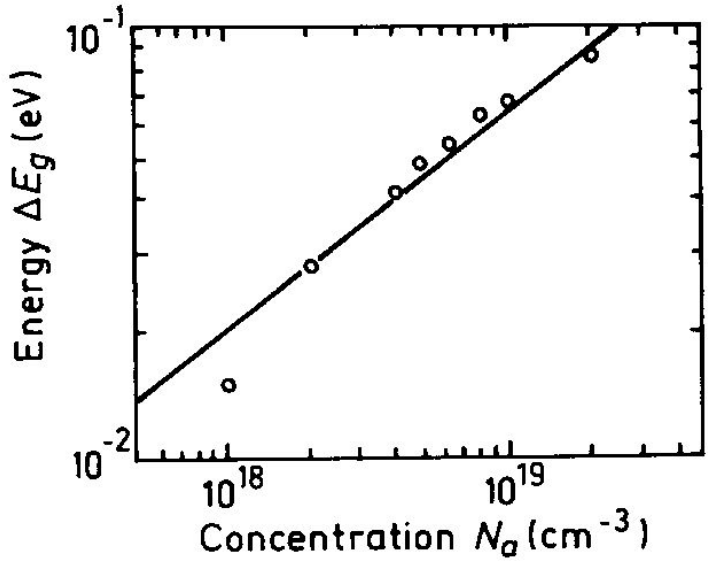
10^{-1}
10^{-2}
10^{18}
10^{19}
Energy ΔE_g (eV)
Concentration N_a (cm^{-3})

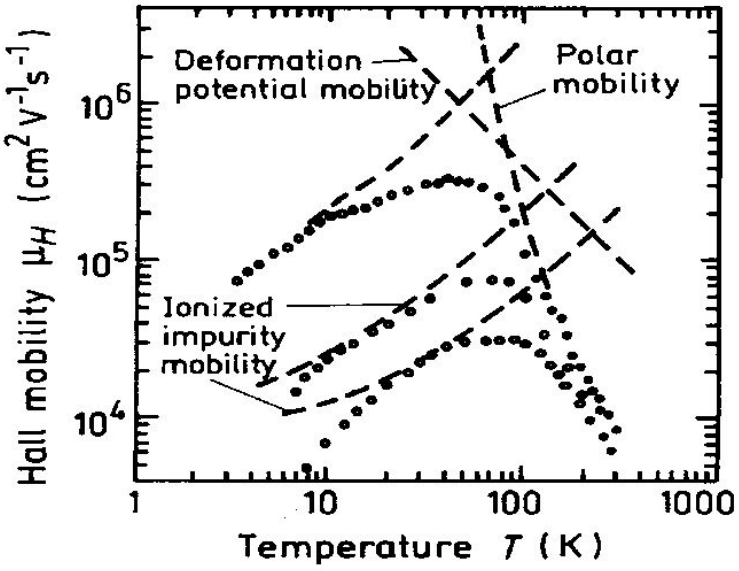
Deformation potential mobility
Polar mobility
Ionized impurity mobility
10^6
10^5
10^4
1
10
100
1000
Hall mobility μ_H (cm^{2}V^{-1}s^{-1})
Temperature T (K)

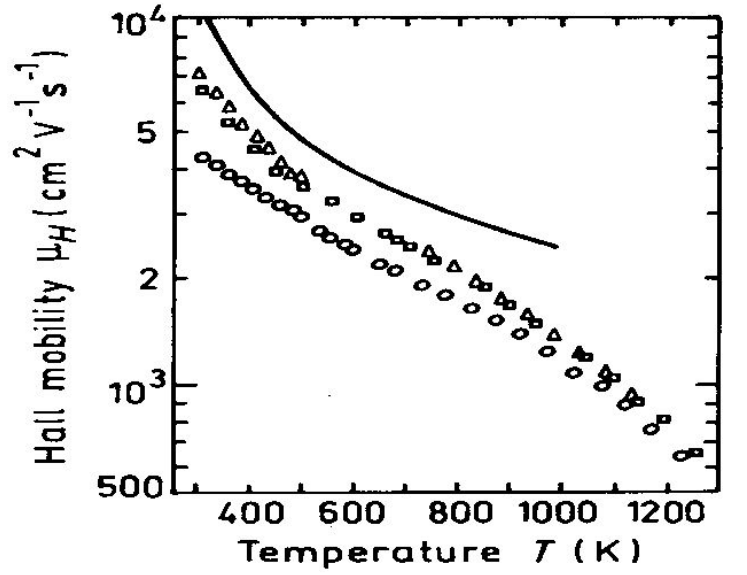
Hall mobility μ_H ($cm^2 V^{-1} s^{-1}$)
10^4
5
2
10^3
500
400 600 800 1000 1200
Temperature T (K)

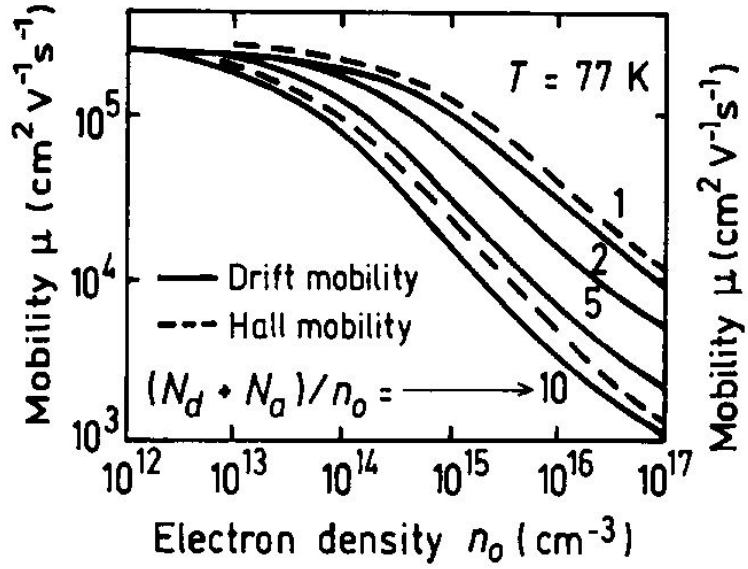
Mobility μ ($cm^2 V^{-1} s^{-1}$)
T = 77 K
10^5
10^4
10^3
Drift mobility
Hall mobility
$(N_d + N_a)/n_o$ = ⟶ 10
1
2
5
10^{12} 10^{13} 10^{14} 10^{15} 10^{16} 10^{17}
Electron density n_o (cm^{-3})
Mobility μ ($cm^2 V^{-1} s^{-1}$)

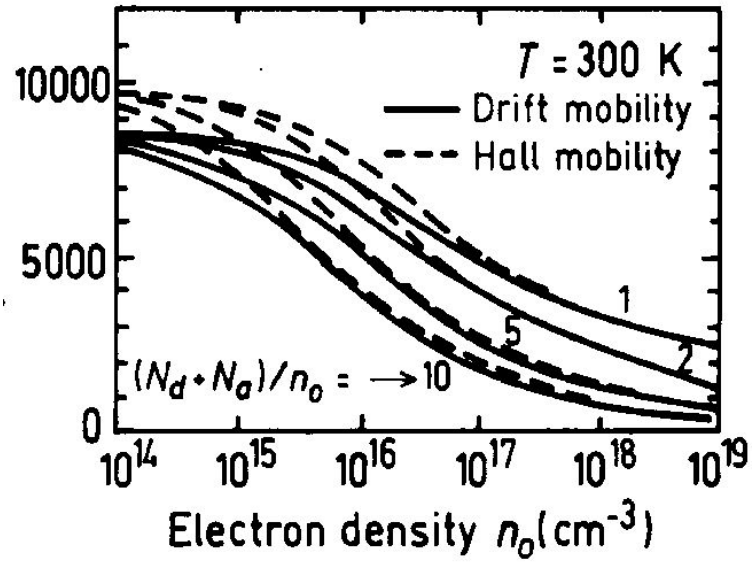
T = 300 K
10000
5000
0
Drift mobility
Hall mobility
$(N_d + N_a)/n_o$ = ⟶ 10
1
2
5
10^{14} 10^{15} 10^{16} 10^{17} 10^{18} 10^{19}
Electron density n_o (cm^{-3})

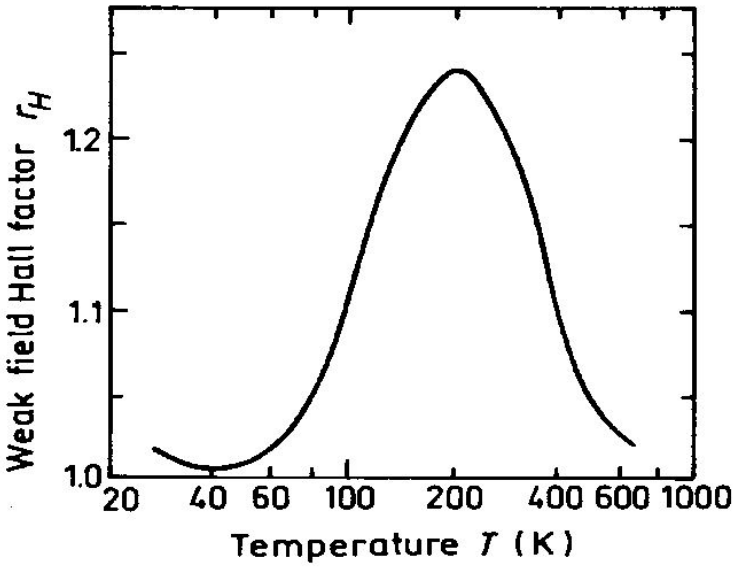
Weak field Hall factor r_H
1.2
1.1
1.0
20 40 60 100 200 400 600 1000
Temperature T (K)

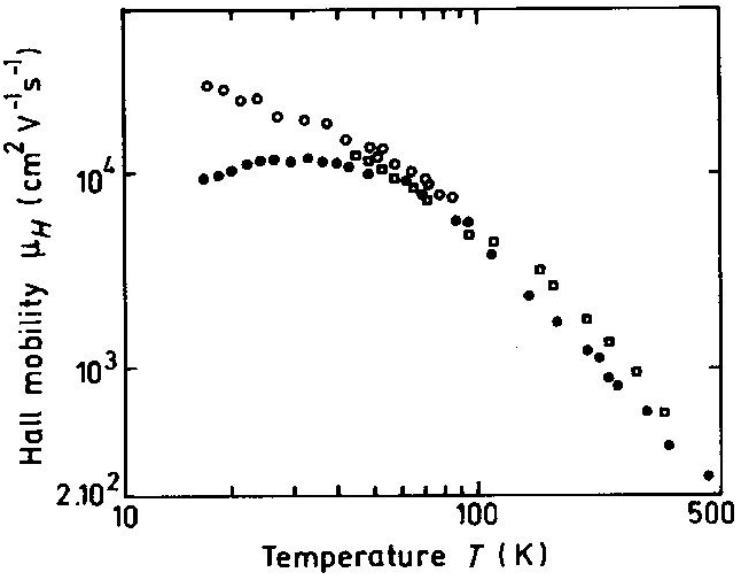
Hall mobility μ_H ($cm^2 V^{-1} s^{-1}$)
10^4
10^3
2.10^2
10
100
500
Temperature T (K)

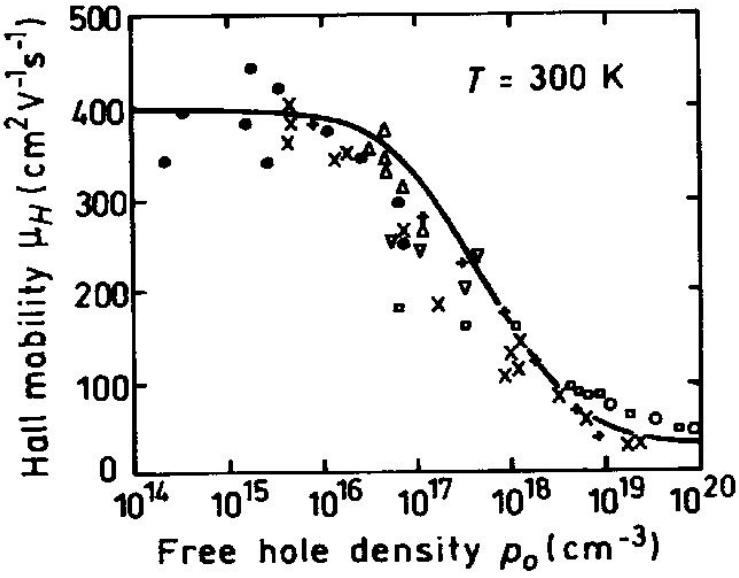
Hall mobility μ_H ($cm^2 V^{-1} s^{-1}$)
500
400
300
200
100
0
T = 300 K
10^{14} 10^{15} 10^{16} 10^{17} 10^{18} 10^{19} 10^{20}
Free hole density p_o (cm^{-3})

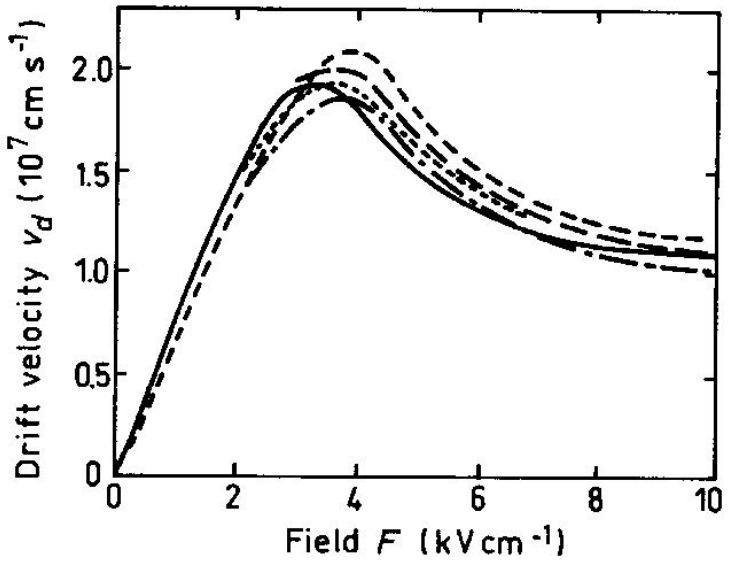
Drift velocity v_d (10^7 cm s^{-1})
2.0
1.5
1.0
0.5
0
0
2
4
6
8
10
Field F (kV cm^{-1})

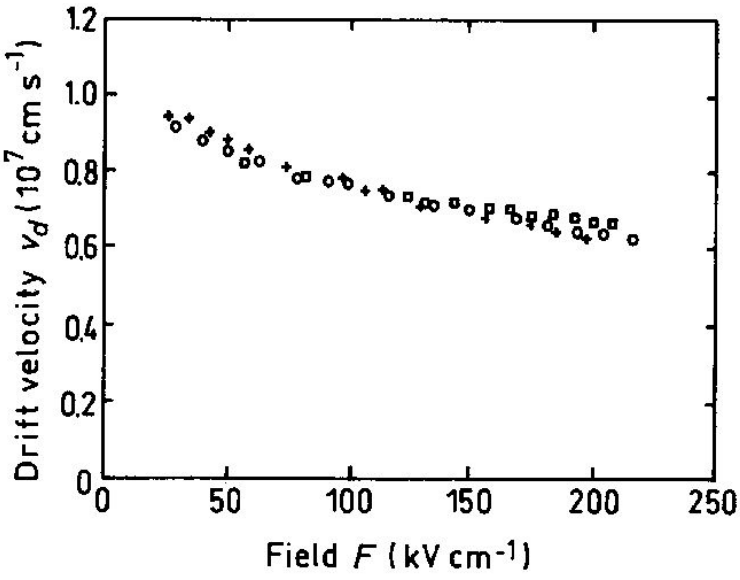
Drift velocity v_d (10^7 cm s^{-1})
1.2
1.0
0.8
0.6
0.4
0.2
0
0
50
100
150
200
250
Field F (kV cm^{-1})

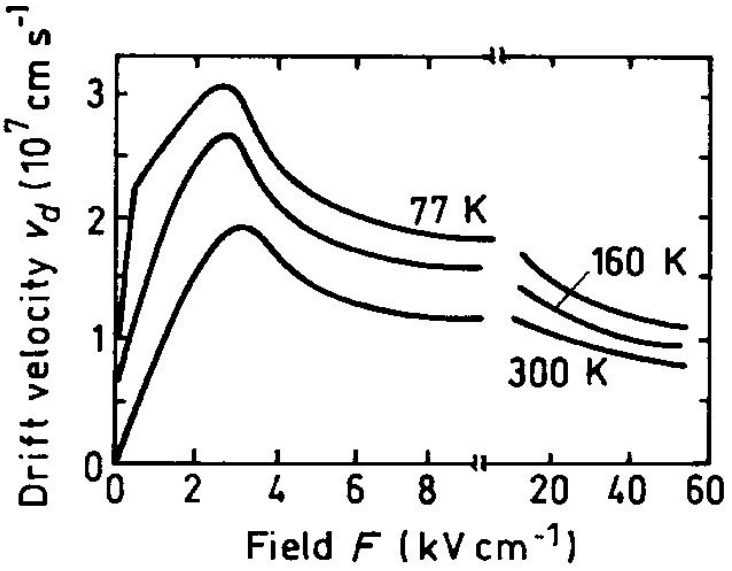
Drift velocity v_d (10^7 cm s^{-1})
3
2
1
0
77 K
160 K
300 K
0
2
4
6
8
20
40
60
Field F (kV cm^{-1})

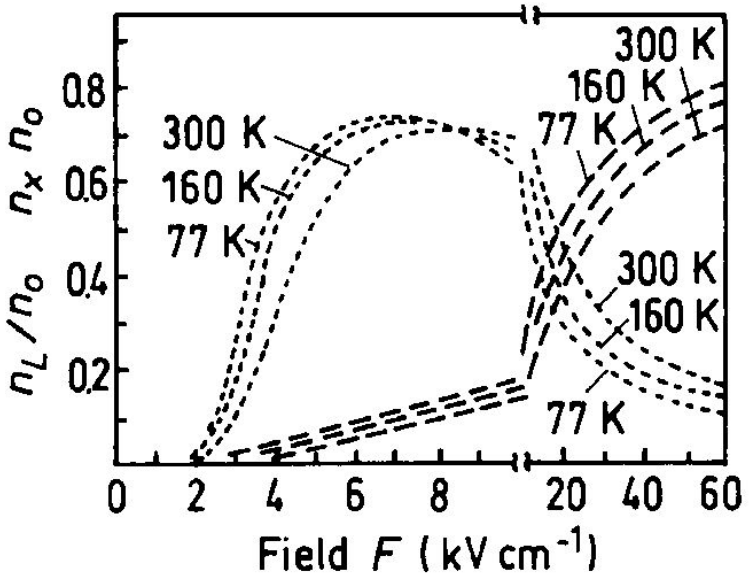
n_L/n_o n_x/n_o
0.8
0.6
0.4
0.2
300 K
160 K
77 K
300 K
160 K
77 K
300 K
160 K
77 K
0 2 4 6 8 20 40 60
Field F (kV cm^{-1})

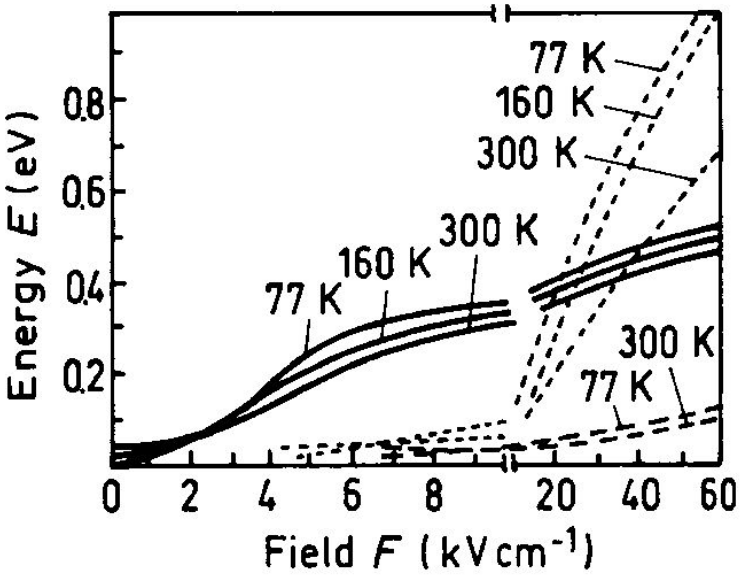
Energy E (eV)
0.8
0.6
0.4
0.2
77 K
160 K
300 K
300 K
160 K
77 K
300 K
77 K
0 2 4 6 8 20 40 60
Field F (kV cm^{-1})

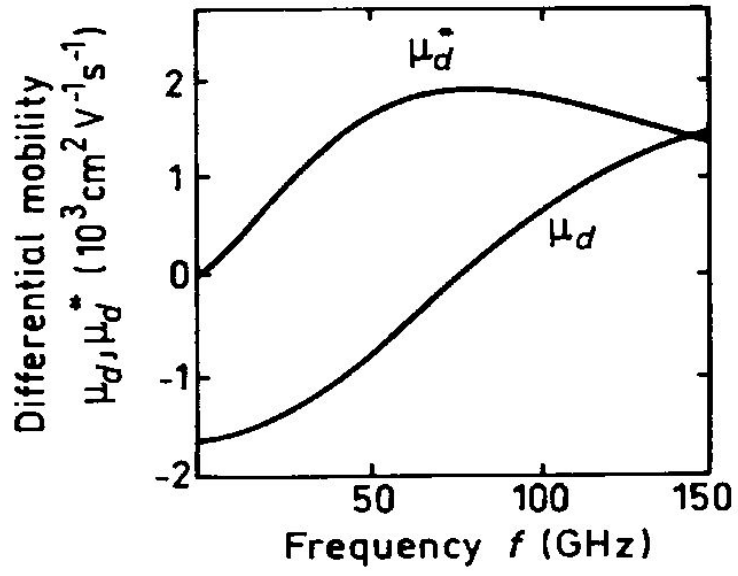
Differential mobility
μ_d, μ_d^* (10^3cm^{2}V^{-1}s^{-1})
μ_d^*
μ_d
2
1
0
-1
-2
50 100 150
Frequency f (GHz)

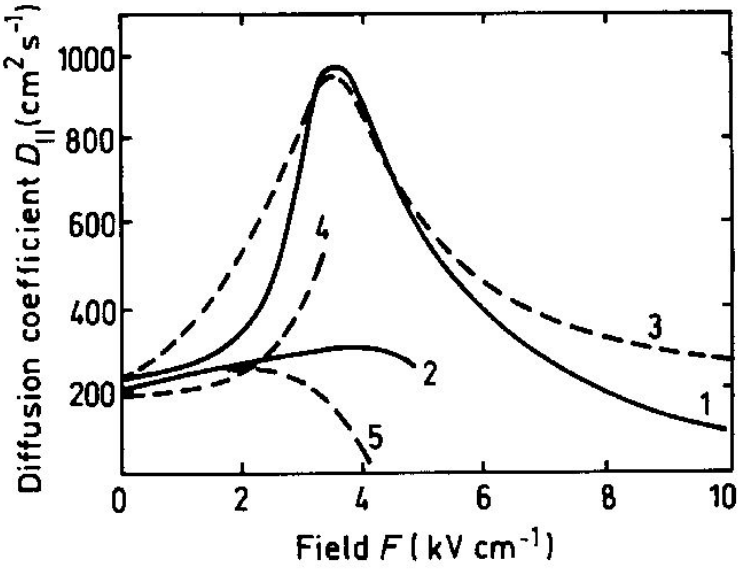
Diffusion coefficient $D_{\parallel}$ ($cm^2 s^{-1}$)
1000
800
600
400
200
0
2
4
6
8
10
Field F (kV cm^{-1})
1
2
3
4
5

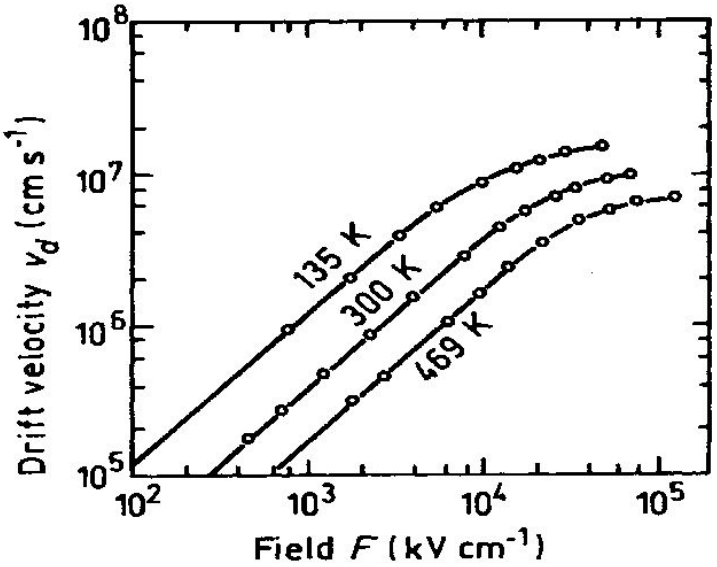
Drift velocity v_d ($cm\ s^{-1}$)
10^8
10^7
10^6
10^5
10^2
10^3
10^4
10^5
Field F (kV cm^{-1})
135 K
300 K
469 K

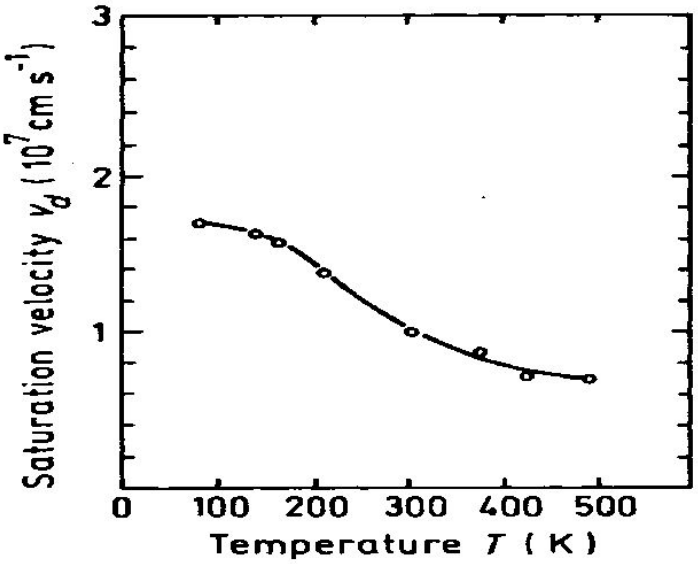
Saturation velocity v_d (10^7 $cm\ s^{-1}$)
3
2
1
0
100
200
300
400
500
Temperature T (K)

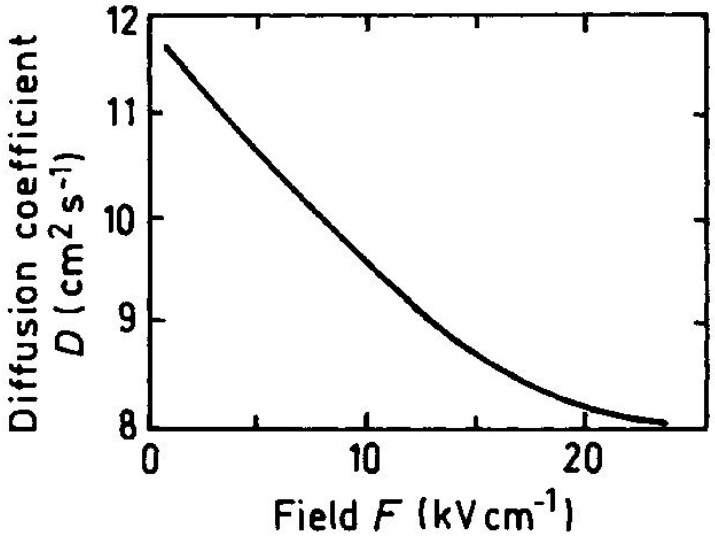
Diffusion coefficient
D (cm² s⁻¹)
12
11
10
9
8
0
10
20
Field F (kV cm⁻¹)

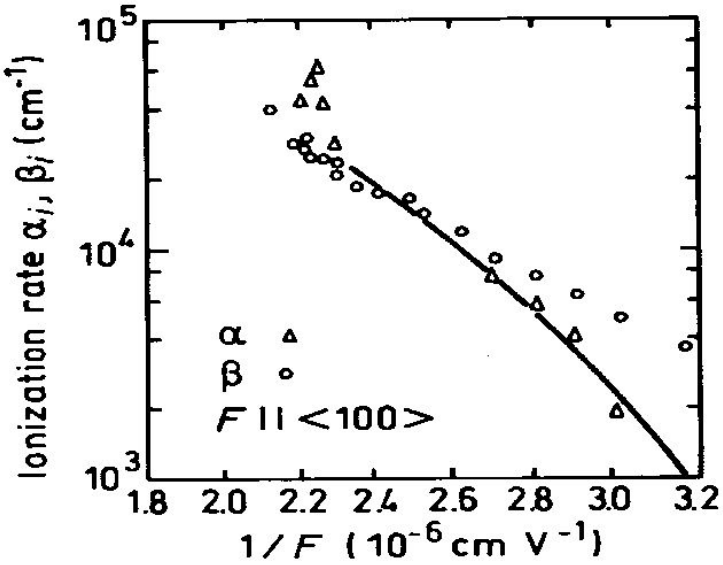
Ionization rate αi, βi (cm⁻¹)
10⁵
10⁴
10³
α
β
F ∥ <100>
1.8
2.0
2.2
2.4
2.6
2.8
3.0
3.2
1/F (10⁻⁶ cm V⁻¹)

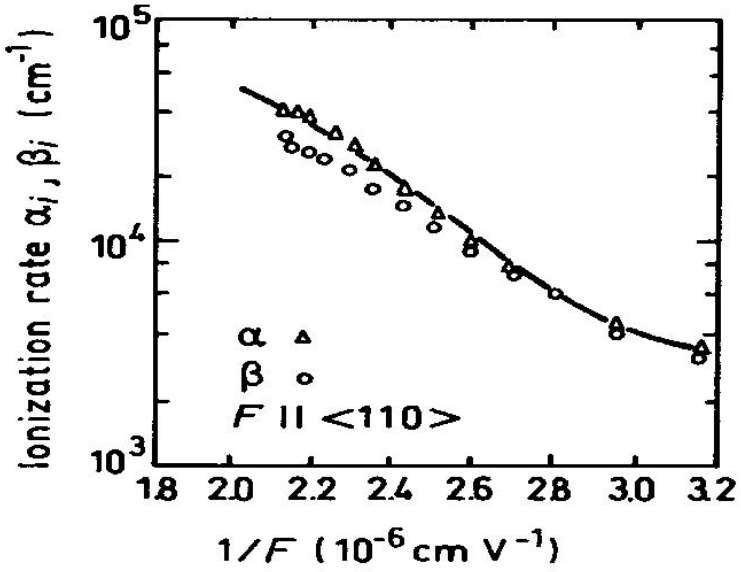
Ionization rate αi, βi (cm⁻¹)
10⁵
10⁴
10³
α
β
F ∥ <110>
1.8
2.0
2.2
2.4
2.6
2.8
3.0
3.2
1/F (10⁻⁶ cm V⁻¹)

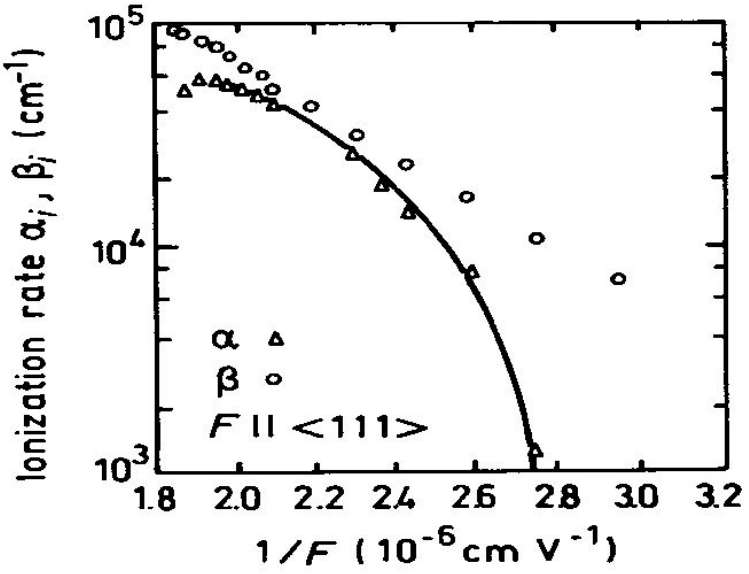
Ionization rate α_i, β_i (cm^{-1})
10^5
10^4
10^3
α △
β ○
F ∥ <111>
1.8 2.0 2.2 2.4 2.6 2.8 3.0 3.2
1/F (10^{-6} cm V^{-1})

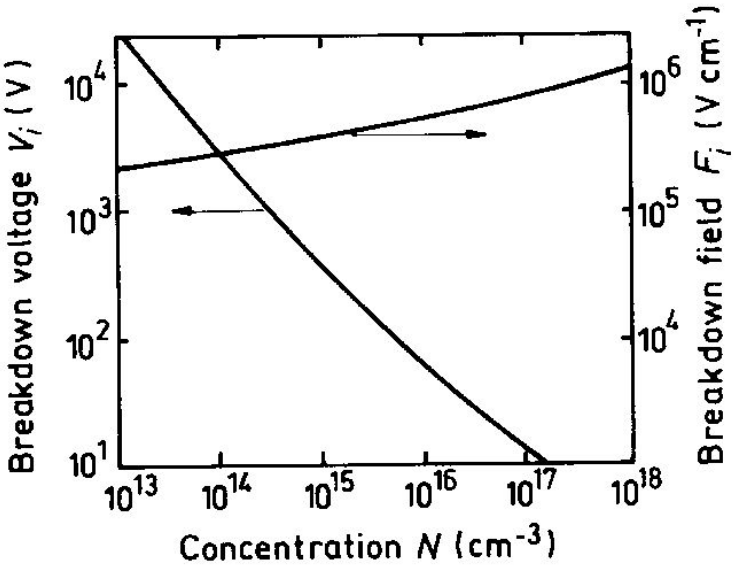
Breakdown voltage V_i (V)
Breakdown field F_i (V cm^{-1})
10^4
10^3
10^2
10^1
10^6
10^5
10^4
10^{13} 10^{14} 10^{15} 10^{16} 10^{17} 10^{18}
Concentration N (cm^{-3})

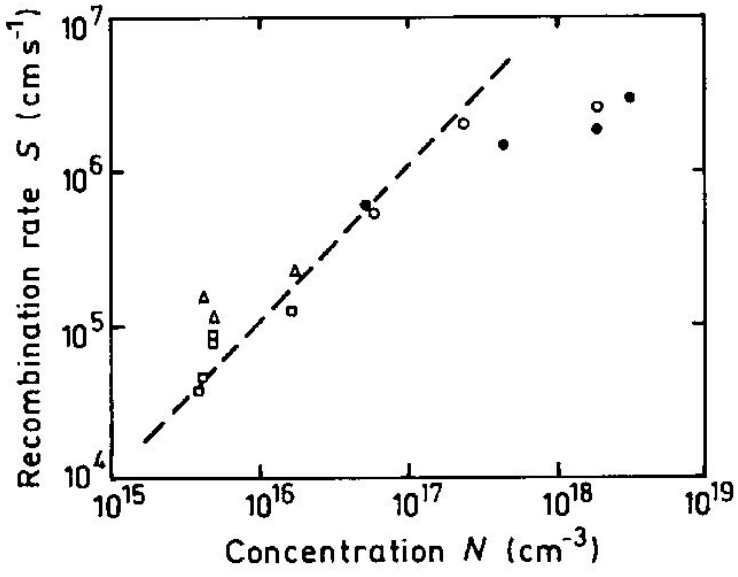
Recombination rate S ($cm\,s^{-1}$)
10^7
10^6
10^5
10^4
10^{15} 10^{16} 10^{17} 10^{18} 10^{19}
Concentration N (cm^{-3})

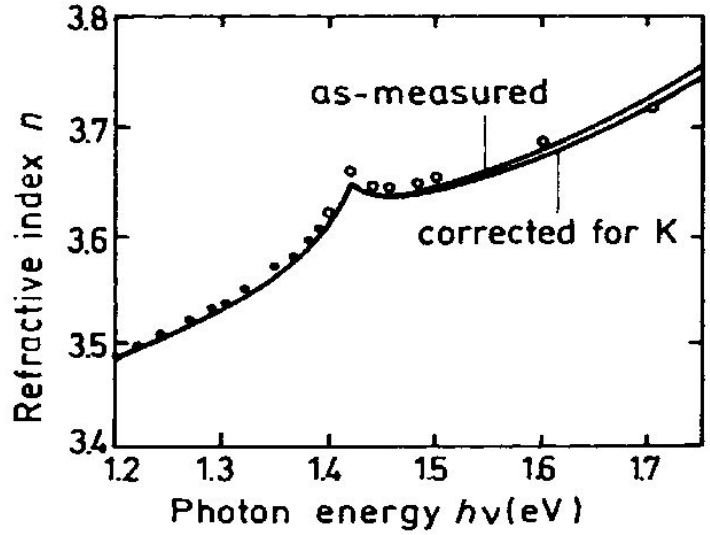
Refractive index n
as-measured
corrected for K
Photon energy hν(eV)

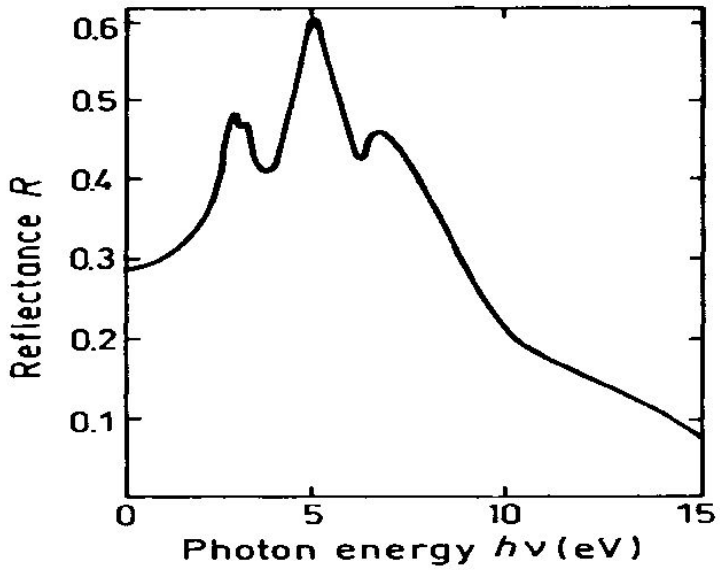
Reflectance R
Photon energy hν(eV)

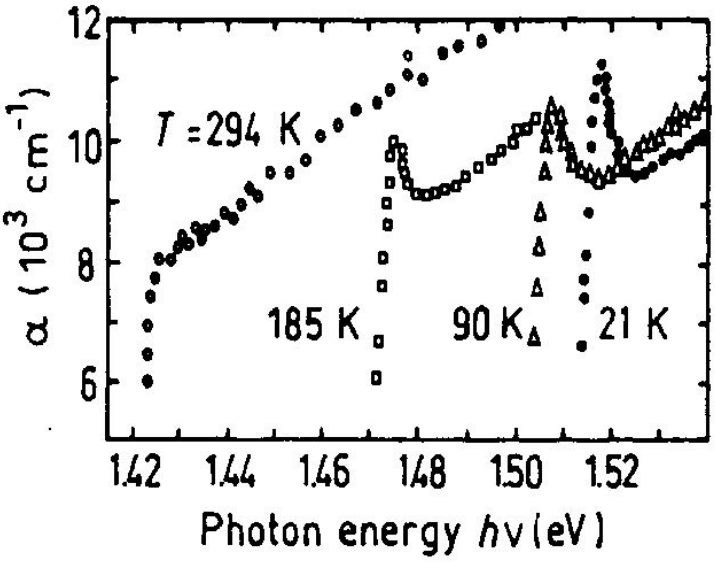
T = 294 K
185 K
90 K
21 K
Photon energy hν(eV)

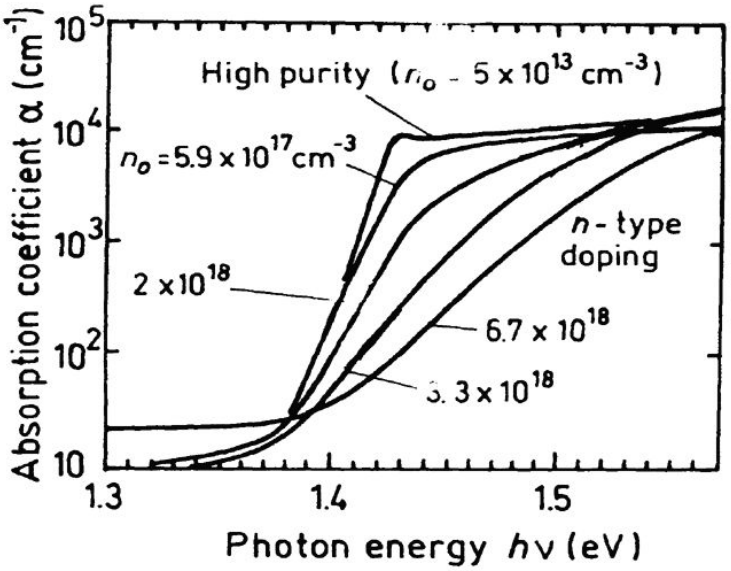
Absorption coefficient α (cm⁻¹)
10⁵
10⁴
10³
10²
10
High purity (n_o - 5 x 10¹³ cm⁻³)
n_o = 5.9 x 10¹⁷ cm⁻³
2 x 10¹⁸
6.7 x 10¹⁸
5.3 x 10¹⁸
n - type doping
1.3
1.4
1.5
Photon energy hν (eV)

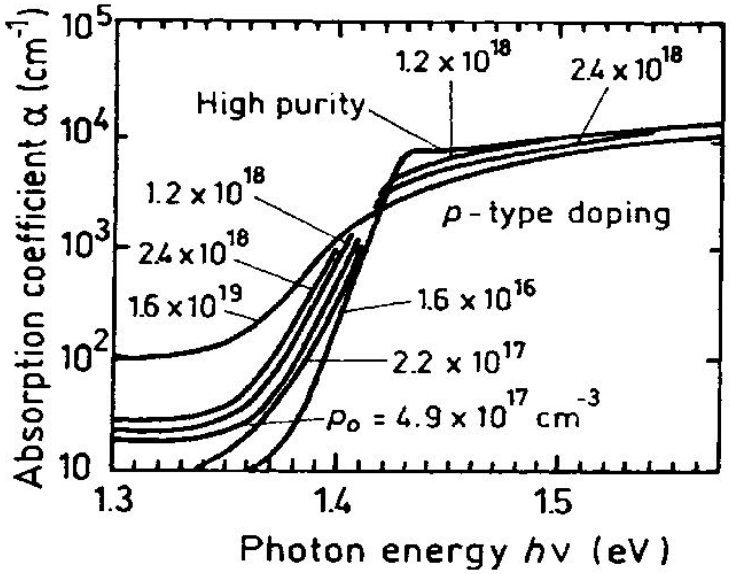
Absorption coefficient α (cm⁻¹)
10⁵
10⁴
10³
10²
10
1.2 x 10¹⁸
2.4 x 10¹⁸
High purity
1.2 x 10¹⁸
2.4 x 10¹⁸
1.6 x 10¹⁹
1.6 x 10¹⁶
2.2 x 10¹⁷
p_o = 4.9 x 10¹⁷ cm⁻³
p - type doping
1.3
1.4
1.5
Photon energy hν (eV)

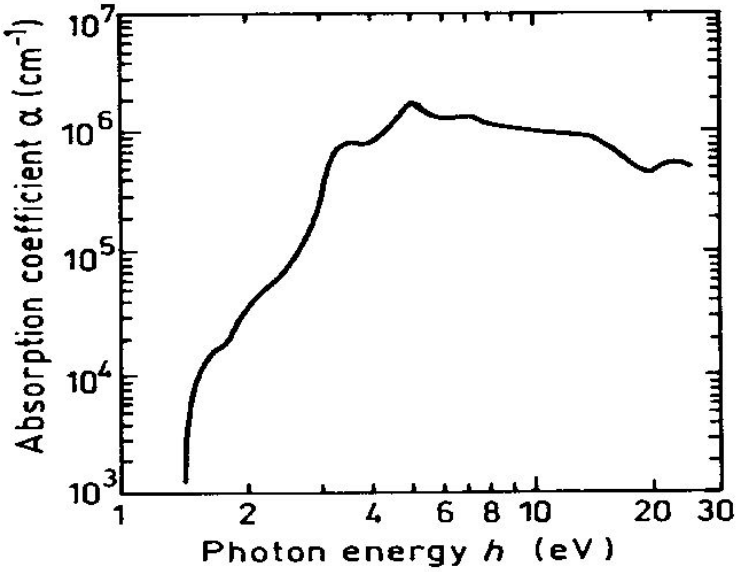
Absorption coefficient α (cm⁻¹)
10⁷
10⁶
10⁵
10⁴
10³
1
2
4
6
8
10
20
30
Photon energy h (eV)

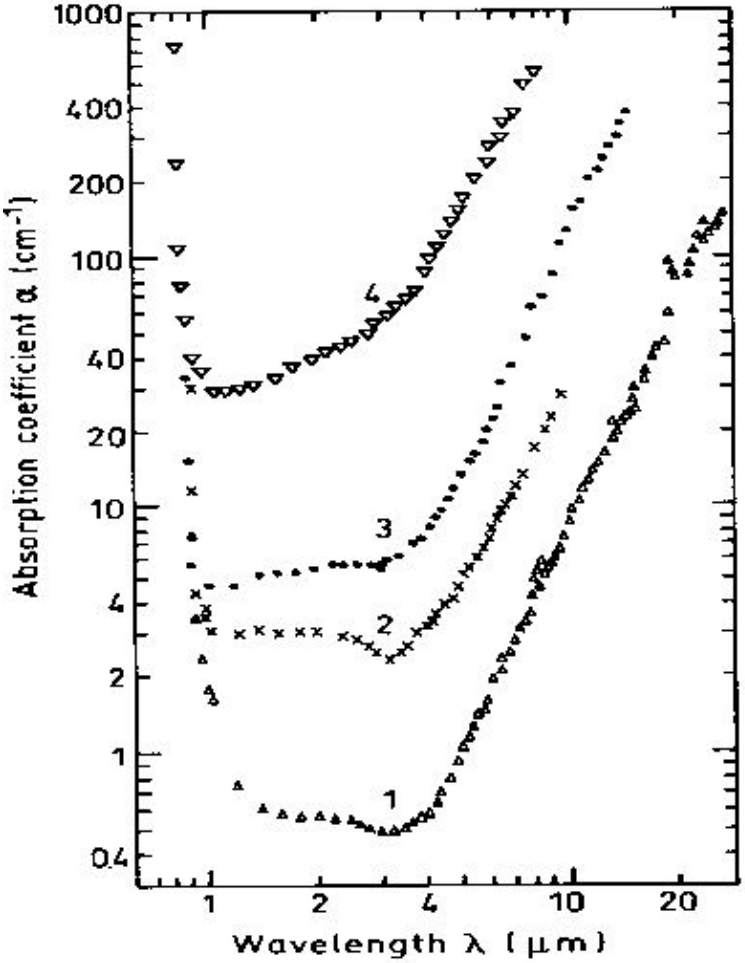
Absorption coefficient α (cm⁻¹)
1000
400
200
100
40
20
10
4
2
1
0.4
1
2
4
10
20
Wavelength λ (μm)
4
3
2
1

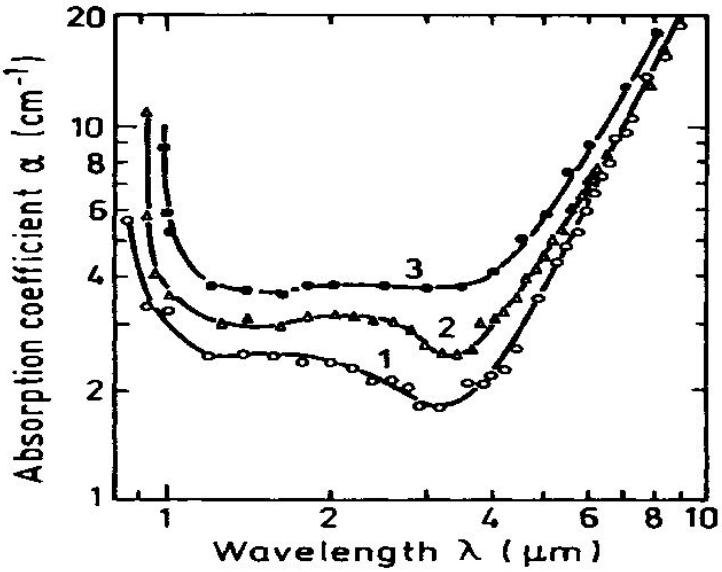
Absorption coefficient α (cm⁻¹)
20
10
8
6
4
2
1
1
2
4
6
8
10
Wavelength λ (μm)
3
2
1

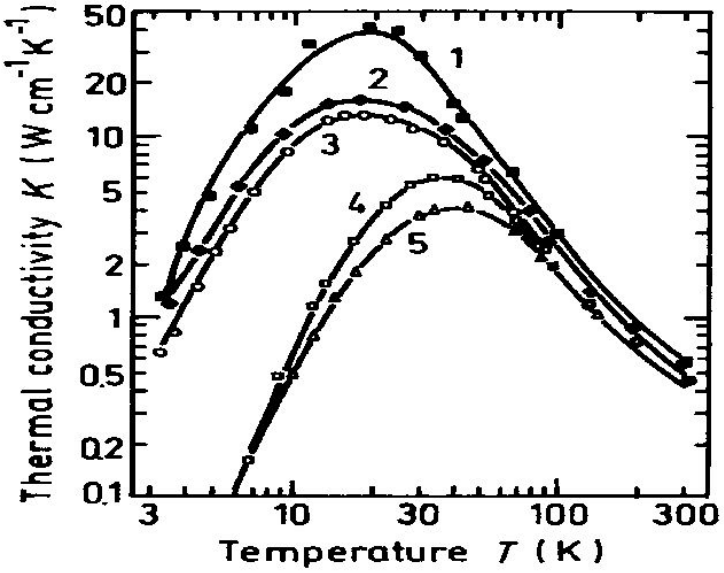
Thermal conductivity K (W cm⁻¹K⁻¹)
50
20
10
5
2
1
0.5
0.2
0.1
3
10
30
100
300
Temperature T (K)
1
2
3
4
5

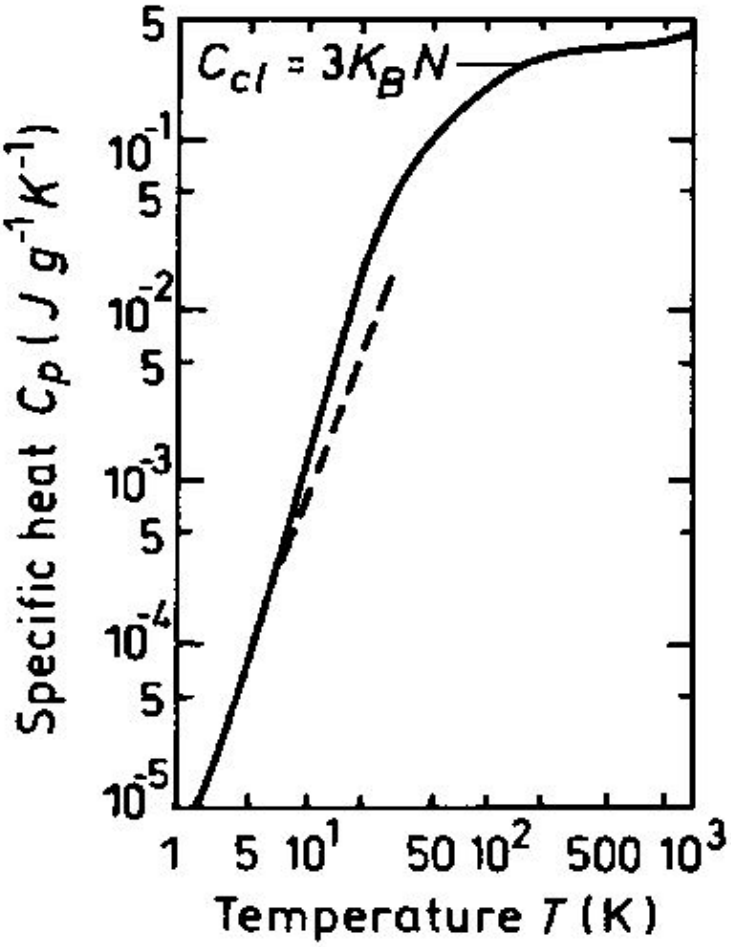
Specific heat Cp (J g⁻¹K⁻¹)
Ccl = 3KBN
5
10⁻¹
5
10⁻²
5
10⁻³
5
10⁻⁴
5
10⁻⁵
1
5
10¹
50
10²
500
10³
Temperature T (K)

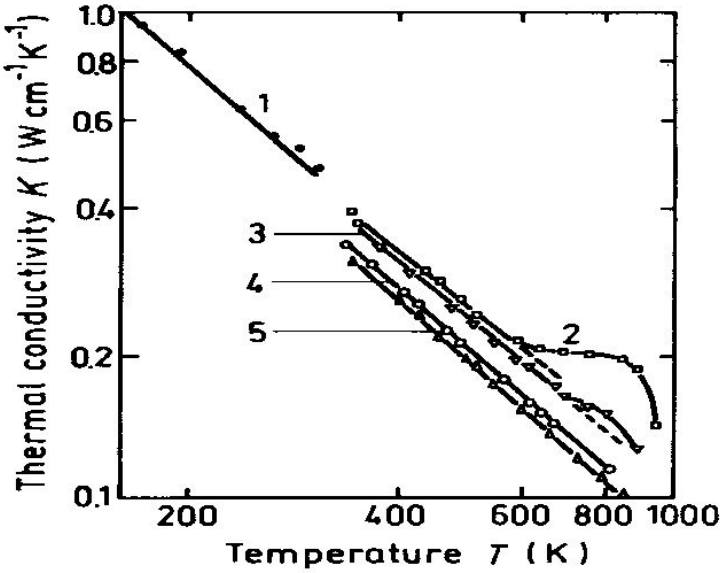
Thermal conductivity K (W cm⁻¹K⁻¹)
1.0
0.8
0.6
0.4
0.2
0.1
1
2
3
4
5
200
400
600
800
1000
Temperature T (K)

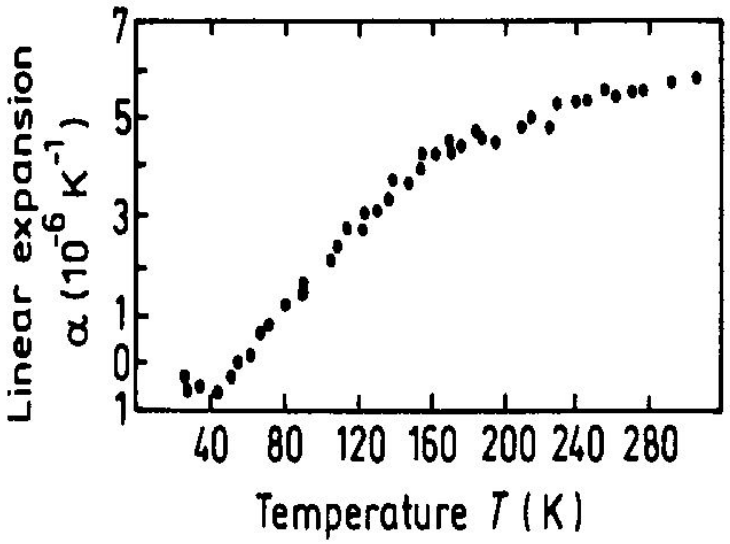
Linear expansion
α (10⁻⁶ K⁻¹)
7
5
3
1
0
1
40
80
120
160
200
240
280
Temperature T (K)

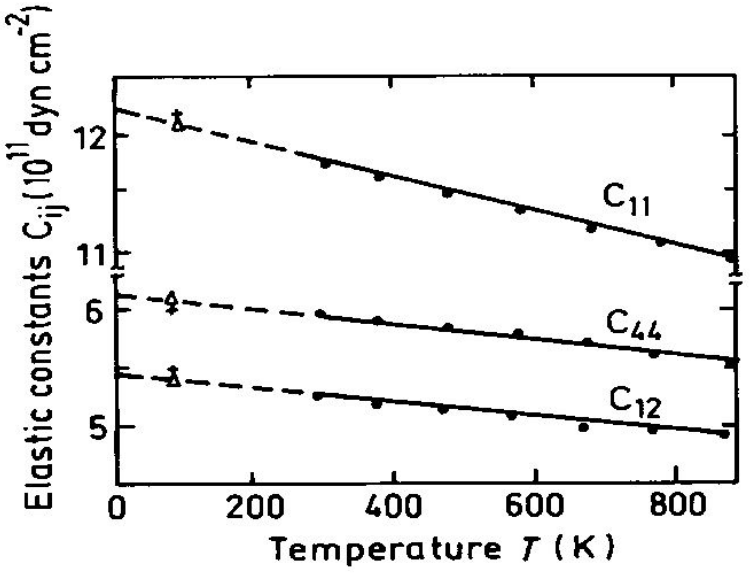
Elastic constants Cij (10¹¹ dyn cm⁻²)
12
11
6
5
C11
C44
C12
0
200
400
600
800
Temperature T (K)

2 $Ga_xIn_{1-x}As$

[002]ff.

2.1 Originaltexte

Dokument nächste Seite folgend.

$Ga_x In_{1-x} As$

$Ga_x In_{1-x} As$

Basic Parameters at 300 K

	$Ga_{0.47}In_{0.53}As$	$Ga_xIn_{1-x}As$	*Remarks*	*Referens*
Crystal structure	Zinc Blende	Zinc Blende	300 K	
Group of symmetry	T_d^2-F43m	T_d^2-F43m	300 K	
Number of atoms in 1 cm^3	$3.98 \cdot 10^{22}$	$(3.59-0.83x) \cdot 10^{22}$	300 K	
Bulk modulus	$6.62 \cdot 10^{11}$ dyn/cm^2	$(5.81+1.72x) \cdot 10^{11}$ dyn/cm^2	300 K	*Goldberg Yu.A. & N.M. Schmidt (1999)*
Debye temperature	330 K	(280+110*x*) K	300 K	
Density	5.50 g·cm^{-3}	(5.68-0.37*x*) g·cm^{-3}	300 K	
Melting point, T_m		~= 1100° C		
Specific heat	0.3 J g^{-1}°C^{-1}		300 K	
Thermal conductivity	0.05 W cm^{-1} °C^{-1}	see *Temerature dependences*		
Thermal expansion coefficient, linear	$5.66x10^{-6}$ °C^{-1}	see *Temerature dependences*		
Dielectric constant (static)	13.9	$15.1-2.87x+0.67x^2$	300 K	
Dielectric constant (high frequency)	11.6	12.3-1.4*x*	300 K	
Infrared refractive index *n*	3.43 cm^2 $V^{-1}s^{-1}$	(3.51-0.16*x*) $V^{-1}s^{-1}$	300 K	
Radiative recombination coefficient	0.96 x 10^{-10} cm^2/s	see *Impact Ionization*	300 K	
Energy gaps, E_g	0.74 eV	$(0.36+0.63x+0.43x^2)$ eV $(0.4105+0.6337x+0.475x^2)$ eV	300 K 2 K	*Goetz et al.(1983)*
Effective electron mass m_e	0.041 m_o (at n= $2 \cdot 10^{17}$ cm^{-3})	$(0.023+0.037x+0.003x^2)$ m_o	300 K	*Pearsall (1982)*
Effective hole masses m_h	0.45 m_o	(0.41+0.1*x*) m_o	300 K	*Goldberg Yu.A. & N.M. Schmidt (1999)*
Effective hole masses m_{lp}	0.052 m_o	(0.026+0.056*x*) m_o	300 K	
Effective hole masses (split-off band) m_{so}		~= 0.15 m_o	300 K	
Electron affinity	4.5 eV	(4.9-0.83*x*) eV	300 K	
Lattice constant	5.8687 A	(6.0583-0.405*x*) A	300 K	
Piezoelectric constant		e_{14}= -(0.045+0.115*x*) C/m^2	300 K	
Optical phonon energy	34 meV	see *Raman-active phonon modes*	300 K	

$Ga_x In_{1-x} As$

Band structure and carrier concentration

Basic Parameters for $Ga_xIn_{1-x}As_yP_{1-y}$

Zinc Blende crystal structure

	$Ga_{0.47}In_{0.53}As$	$Ga_xIn_{1-x}As$	*Remarks*	*Referens*
Energy gaps, E_g	0.74 eV	$(0.36+0.63x+0.43x^2)$ eV	300 K	*Goetz et al.(1983)*
Energy gaps, E_g		$(0.4105+0.6337x+0.475x^2)$ eV	2 K	*Goetz et al.(1983)*
Electron affinity	4.5 eV	$(4.9-0.83x)$ eV	300 K	
Conduction band				
Energy separation between X valley and top of the valence band E_X	1.33 eV	$(1.37-0.63x+1.16x^2)$ eV	300 K	*Goetz et al.(1983)*
Energy separation between L valley and top of the valence band E_L	1.2 eV	$(1.08-0.02x+0.65x^2)$ eV	300 K	*Goetz et al.(1983)*
Effective conduction band density of states	$2.1 \cdot 10^{17}$ cm^{-3}	see *Temerature dependences*		
Valence band				
Energy separation of spin-orbital splitting E_{so}	***	***		
Effective valence band density of states	$7.7 \cdot 10^{18}$ cm^{-3}	see *Temerature dependences*		
Intrinsic carrier concentration	$6.3 \cdot 10^{11}$ cm^{-3}	see *Temerature dependences*		

Band structure for $Ga_xIn_{1-x}As$

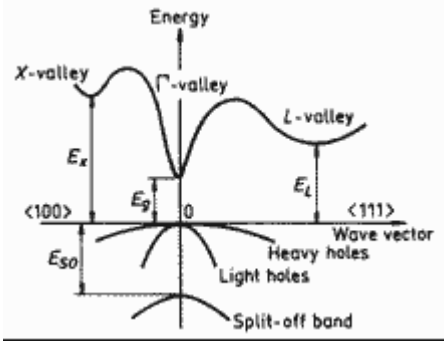

$Ga_xIn_{1-x}As$ (zinc blende, cubic). Band structure
Important minima of the conduction band and maxima of the valence band..

For details see *Goldberg Yu.A. & N.M. Schmidt (1999)* .

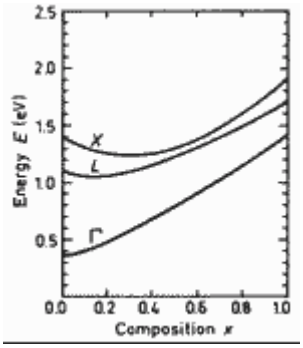

$Ga_xIn_{1-x}As$. Energy gap E_g Energy separations between Γ- ,X-, and L -conduction band minima and top of the valence band vs. composition parameter *x*.

Porod and Ferry (1983)

Interfacial elastic strain induced by lattice parameter mismatch between epilayer and substrate results in significant band-gap shifts:

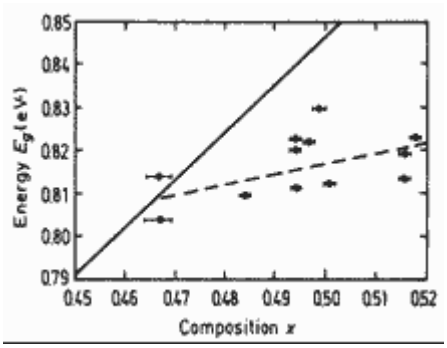

$Ga_xIn_{1-x}As$. Energy band gap Eg of unstrained (solid line) and strained (dashed line and experimental points) vs. composition parameter *x*.
Solid line is calculated according to Eg= $(0.4105+0.6337x+0.475x^2)$ eV.
Experimental points are obtained at **4K.**
Kuo et al.(1985)

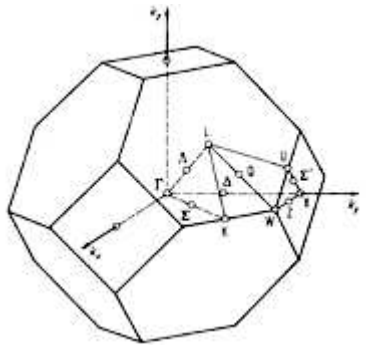

Brillouin zone of the face centered cubic lattice, the Bravais lattice of the diamond and zincblende structures.

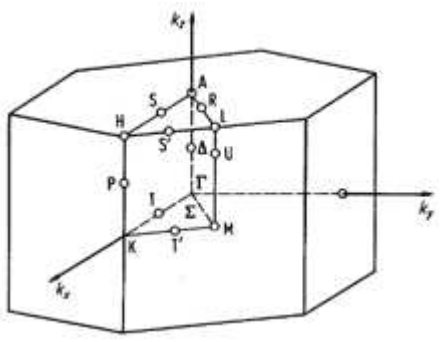

Brillouin zone of the hexagonal lattice.

Temperature Dependences

$E_g\,(x,T)= 0.42 + 0.625x - [5.8/(T+300)-4.19/(T+271)]\cdot 10^{-4}T^2x - 4.19\cdot 10^{-4}T^2/(T+271) + 0.475x^2$ (eV)	$Ga_xIn_{1-x}As$	Paul et al.(1991)
$E_g\,(x,T)= E_g\,(0) + (6x^2 - 8.6x + 5.2)\cdot 10^{-4}\,T^2/(337x^2 - 455x + 196)$	$Ga_xIn_{1-x}As$ on Ga As	Karachevtseva et al.(1994)
$E_g\,(x,T)= 0.42 + 0.625x - [5.8/(T+300)-4.19/(T+271)]\cdot 10^{-4}T^2x - 4.19\cdot 10^{-4}T^2/(T+271) + 0.475x^2$ (eV)	$Ga_xIn_{1-x}As$	

where T is temperature in degrees K

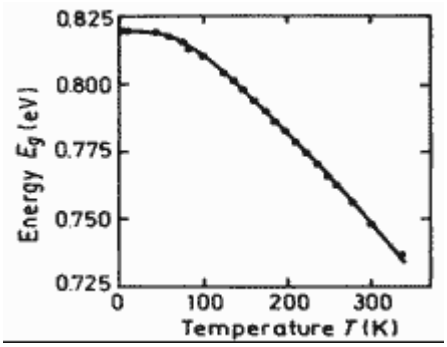

$Ga_{0.47}In0.53As$. Energy gap E_g of vs. temperature
Points are experimental data.
Solid line is theoretical calculation.
$E_g(0)$=821.5 ± 0.2 meV.
Zielinski et al.(1986)

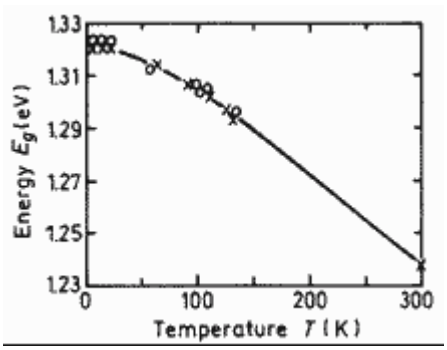

$Ga_{0.87}In0.13As$. Energy gap E_g of vs. temperature
Points are experimental data.
Solid line -- $1.321 - 4.1\cdot 10^{-4}\,T^2/(T+139)$
Karachevtseva et al.(1994)

Lasing wavelength λ_0

Intrinsic carrier concentration:

$n_i = (N_c\cdot N_v)^{1/2}exp(-E_g/(2k_BT)) \sim= 4.82 \times 10^{15}\cdot [(0.41-0.09x)^{3/2} + (0.027+0.047x)^{3/2}]1^{/2} \times x(0.025+0.043x)^{3/4}[\,T^{3/2}\exp(-\nu/2)(1+3.75/\nu + 3.28/\nu^2 - 2.46/\nu^3)^{1/2}\,]\ (cm^{-3})$,
where $\nu=E(x,T)/2kT$
Paul et al.(1991).

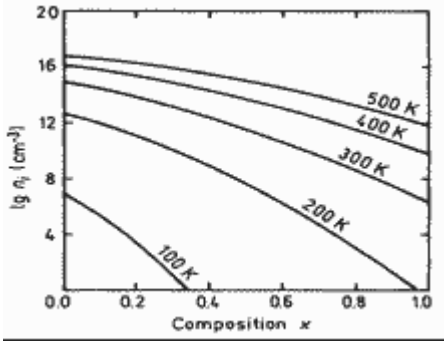

$Ga_xIn_{1-x}As$. Intrinsic carrier concentration vs. temperature for $Ga_xIn_{1-x}As$.
T = 100K; 200K; 300K; 400K; 500K;
Paul et al.(1991)

n_i = 6.3x1011 cm-3 for **$Ga_{0.47}In_{0.53}As$** at **300K**

Effective density of states in the conduction band: N_c

N_c ~= 4.82 x 10^{15} · $(m_\Gamma/m_0)^{3/2}T^{3/2}$ (cm^{-3}) ~= 4.82 x 10^{15} · $(0.023+0.037x+0.003x^2)^{3/2}$ $T^{3/2}$ (cm^{-3}) :

Effective density of states in the valence band: N_v

N_v ~= 4.82 x 10^{15} · $(m_h/m_0)^{3/2}$ $T^{3/2}$ (cm^{-3})= 4.82 x 10^{15} · $(0.41-0.1x)^{3/2}$ $T^{3/2}$ (cm^{-3}) :

Dependence on Hydrostatic Pressure

E_g (0.47,P)~= (0.796+10.9x 10^{-3} ·P -30x10^{-6} ·P^2) eV	80K, **$Ga_{0.47}In_{0.53}As$**	x=0.47	*Lambkin and Dunstan (1988)*
E_g (0.47,P)~= (0.733+11.0x 10^{-3} ·P -27x10^{-6} ·P^2) eV	300K, **$Ga_{0.47}In_{0.53}As$**	x=0.47	
E_g (0.0, P)~= (E_g (0)+4.8x 10^{-3} ·P) eV	300K, **InAs**	x=0.	
E_g (1.0, P)~= (E_g (0)+12.6x 10^{-3} ·P -37.7x10^{-6} ·P^2) eV	300K, **GaAs**	x=1.	

where P is pressure in kbar.

Energy gap narrowing at high doping levels

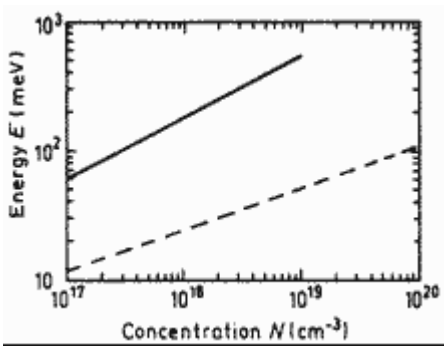

$Ga_{0.47}In0.53As$. Energy gap narrowing E_g vs. donor (solid line) **and acceptor** (dashed line) **doping density**
solid line -- donor doping density;
dashed line -- acceptor doping density
Jain et al. (1990)

ΔE_g ~= $(A \cdot N^{1/3}\, 10^{-9} + B \cdot N^{1/4}\, 10^{-7} + C \cdot N^{1/2}\, 10^{-12})$ meV	300K, **$Ga_{0.47}In_{0.53}As$**	x=0.47

where

n : A=15.5; B=1.95; C=159	300K, **$Ga_{0.47}In_{0.53}As$**	x=0.47
p : A= 9.2; B=3.57; C=3.65	300K, **$Ga_{0.47}In_{0.53}As$**	x=0.47

N -- carrier concentration in cm^{-3}

Band Discontinuities at Heterointerfaces

Band discontinuities at **$Ga_xIn_{1-x}As/Al_yGa_{1-y}As$** heterointerface *Shur (1990)*.

		Referens
Conduction band discontinuity	ΔE_v =(ΔE_g -ΔE_v) eV	*Shur (1990)*
Valence band discontinuity	ΔE_c = (0.44 ΔE_{gg}) eV	*Shur (1990)*

where ΔE_{gg} (eV) = [1.247y + 1.5(1-x) - 0.4(1-x)^2] (eV) is the difference between Γ-valleys in $Ga_xIn_{1-x}As$ and $Al_{yGA1-y}As$.

Energy gap E_g discontinuity :	$\Delta E_g = \Delta E_{gg}$	for y<0.45	
Energy gap E_g discontinuity :	ΔE_g = 0.476 +0.125y + 0.143y^2 +1.5(1-x) - 0.4(1-x)^2	for y>0.45	
Band discontinuities	ΔE_v ~= 0.38 eV ΔE_c ~= 0.22 eV	at **$Ga_{0.47}In_{0.53}As/InP$** heterointerface	*Adachi (1992); Hybertsen (1991)*
Band discontinuities	ΔE_v ~= 0.2 eV ΔE_c ~= 0.52 eV	at **$Ga_{0.47}In_{0.53}As/Al_{0.48}In_{0.52}As$** heterointerface	*Adachi (1992); Hybertsen (1991)*
	ΔE_c /ΔE_g = [0.653 + 0.1(1-x)] eV	at **$Ga_xIn_{1-x}As/Al_xIn_{1-x}As$** heterointerface	*Wolak et al.(1991)*

Effective Masses and Density of States:

Electrons

For wurtzite crystal structure the surfaces of equal energy in Γ valley should be ellipsoids, but effective masses in z direction and perpendicular directions are estimated to be approximately the same:

Effective Electron Masses		*Remarks*	*Referens*
Effective electron mass $m_e = m_\Gamma$	0.023 -0.037x +0.003x^2 m_o	$Ga_xIn_{1-x}As$; 300K; for Γ - valley	*Goldberg Yu.A. & N.M. Schmidt (1999)*

Effective electron mass m_e	m_l= 0.041 m_o at n= $2x \cdot 10^{17}$ cm^{-3} m_l= 0.074 m_o at n= $6x \cdot 10^{18}$ cm^{-3}	$Ga_{0.47}In_{0.53}As$; x=0.47	*Pearsall (1982)*
	m_L = 0.29 m_o ; (L - valley) m_X = 0.68 m_o ; (X - valley)	$Ga_{0.47}In_{0.53}As$; x=0.47	*Pearsall (1982)*

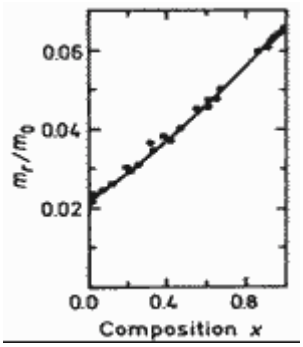

$Ga_xIn_{1-x}As$. Electron effective mass vs. concentration x for $Ga_xIn_{1-x}As$; **300K**
Adachi (1992))

Holes

Effective Masses for Zinc Blende GaN		*Remarks*	*Referens*
Effective hole masses (heavy) m_h	m_h ~= (0.41 -0.1x) m_o	$Ga_xIn_{1-x}As$; 300K;	*Goldberg Yu.A. & N.M. Schmidt (1999)*
Effective hole masses (light) m_{lp}	m_{lp} ~= (0.026 -0.056x) m_o	$Ga_xIn_{1-x}As$; 300K;	
Effective hole masses (split-off band) m_s	m_{so} ~= 0.15 m_o	$Ga_xIn_{1-x}As$; 300K;	

Donors and Acceptors

Ionization energies of Shallow Donors		*Remarks*	
Sn, Ge, Si, C	~ 5 meV	$Ga_{0.47}In_{0.53}As$; x=0.47	*Goldberg Yu.A. & N.M. Schmidt (1999)*
Sn, Ge, Si, S, Se, Te	> 1 meV	InAs; x=0	
Sn, Ge, Si, S, Se, Te	~ 6 meV	GaAs; x=1	
Ionization energies of Shallow Acceptor			
Mg	~ 25 meV	$Ga_{0.47}In_{0.53}As$; x=0.47	*Goldberg Yu.A. & N.M. Schmidt (1999)*
Zn	~ 20 meV	$Ga_{0.47}In_{0.53}As$; x=0.47	
Cd	~ 30 meV	$Ga_{0.47}In_{0.53}As$; x=0.47	

Mn	~ 50 meV	$Ga_{0.47}In_{0.53}As$; x=0.47
Fe	~ 150 meV	$Ga_{0.47}In_{0.53}As$; x=0.47

(above valence band), 280, 370, and 440 below conduction band

Mg	~ 25 meV	$Ga_xIn_{1-x}As$; $0<x<1$
Be	~ 25 meV	$Ga_xIn_{1-x}As$; $0<x<1$
Cd	~ 8-20 meV	$Ga_xIn_{1-x}As$; $0<x<1$

(above valence band), 280, 370, and 440 below conduction band

Sn-10; Ge-14; Si-20; Cd-15; Zn-10 meV	InAs; x=0
C - 20, Si - three acceptor levels ~ 30, 100, and 220, Ge - 30, Zn - 25, Sn - 20.	GaAs; x=1

$Ga_x In_{1-x} As$

Electrical properties

Basic Parameters

	$Ga_{0.47}In_{0.53}As$	**$Ga_xIn_{1-x}As$**	*Remarks*	*Referens*
Breakdown field	$\approx 2\cdot 10^5$ V/cm	$\approx(2\div 4)\cdot 10^5$ V/cm	300 K	*Goldberg Yu.A. & N.M. Schmidt (1999)*
Mobility electrons	$<12\cdot 10^3$ cm^2 V^{-1}s^{-1}	$(40\text{-}80.7x\text{+}49.2x^2)\cdot 10^3$ cm^2 V^{-1}s^{-1}	300 K	
Mobility holes	<300 cm^2 V^{-1}s^{-1}	$\sim 300\div 400$ cm^2 V^{-1}s^{-1}	300 K	
Diffusion coefficient electrons	<300 cm^2/s	$(10\text{-}20.2x\text{+}12.3x^2)\cdot 10^2$ cm^2/s	300 K	
Diffusion coefficient holes	<7.5 cm^2/s	$\sim 7\div 12$ cm^2/s	300 K	
Electron thermal velocity	$5.5\cdot 10^5$ m/s	$(7.7\text{-}5.9x\text{+}2.6x^2)\cdot 10^5$ m/s	300 K	
Hole thermal velocity	$2\cdot 10^5$m/s	$(1.8\div 2)\cdot 10^5$m/s	300 K	
Surface recombination velocity		$<10^6$ cm/s	300 K	
Radiative recombination coefficient	$0.96\cdot 10^{-10}$ cm^3/s		300 K	
Auger coefficient	$7\cdot 10^{-29}$ cm^6/s		300 K	

$Ga_x In_{1-x} As$

Optical properties

	$Ga_{0.47}In_{0.53}As$	$Ga_xIn_{1-x}As$	*Remarks*	*Referens*
Dielectric constant (static)	13.9	$15.1-2.87x+0.67x^2$	300 K	
Dielectric constant (high frequency)	11.6	$12.3-1.4x$	300 K	
Infrared refractive index *n*	3.43 $cm^2\ V^{-1}s^{-1}$	$(3.51-0.16x)\ V^{-1}s^{-1}$	300 K	*Goldberg Yu.A. & N.M. Schmidt (1999)*
Radiative recombination coefficient	0.96×10^{-10} cm^2/s	see *Impact Ionization*	300 K	
Optical phonon energy	34 meV	see *Raman-active phonon modes*	300 K	

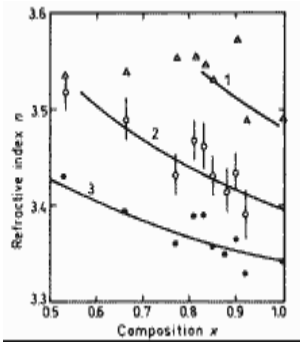

Refractive index *n* versus alloy composition *x* at different photon energies
1 1.2 eV
2 0.9 eV
3 0.6 eV.
Takagi (1978)

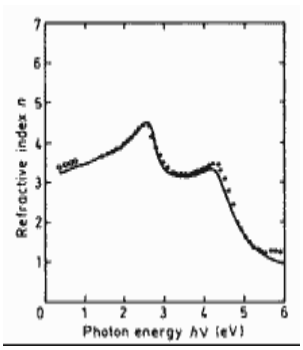

Refractive index *n* versus photon energy for *x*=0.47. 300 K.
Adachi (1992)

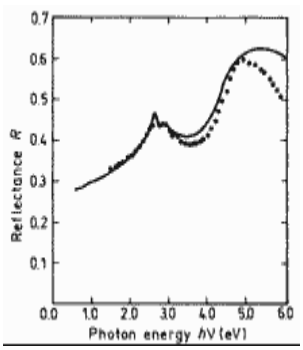

Normal incidence reflectivityversus photon energy for *x*=0.47. 300 K.
Adachi (1992)

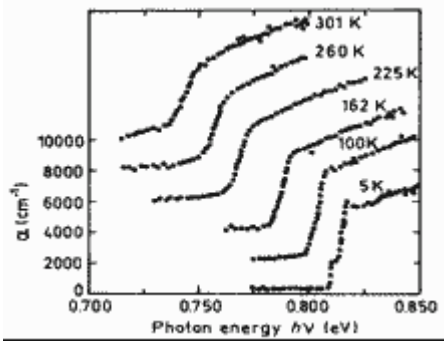

The absorption coefficient versus photon energy at different temperatures for *x*=0.47.
Electron concentration n_o=8·10^{14} cm^{-3}.
Curves are shifted vertically for clarity.
Zielinski et al. (1986)

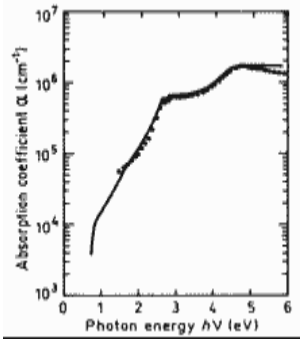

The absorption coefficient versus photon energy for *x*=0.47, 300 K.
Adachi (1992)

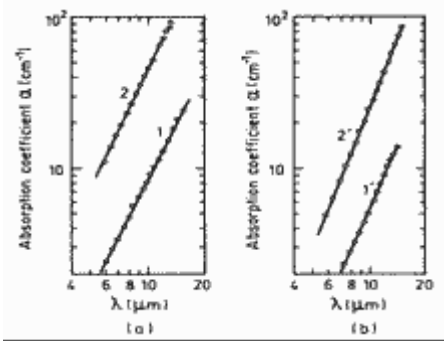

Free carrier absorption coefficient versus wavelength.
a - T=300 K, b - T=92 K.
1 *x*=0.08, N_d=1.4·10^{17} cm^{-3}
2 *x*=0.1 N_d=5.4·10^{17} cm^{-3}.
Aliev et al. (1987)

A ground state Rydberg energy R_{x1}=2.5 meV (for *x*=0.47).

$Ga_x In_{1-x} As$

Thermal properties

Basic parameters

	$Ga_{0.47}In_{0.53}As$	$Ga_xIn_{1-x}As$	*Remarks*	*Referens*
Bulk modulus	$6.62 \cdot 10^{11}$ dyn/cm^2	$(5.81+1.72x) \cdot 10^{11}$ dyn/cm^2	300 K	*Goldberg Yu.A. & N.M. Schmidt (1999)*
Debye temperature	330 K	(280+110*x*) K		
Density	5.50 g/cm^3	5.68-0.37x g/cm^3	300 K	*Goldberg Yu.A. & N.M. Schmidt (1999)*
Melting point, T_m		~= 1100° C		
Specific heat	0.3 J g^{-1}°C $^{-1}$			
Thermal conductivity	0.05 W cm^{-1} °C $^{-1}$	see *Temerature dependences*		
Thermal expansion coefficient, linear	5.66x10^{-6} °C $^{-1}$	see *Temerature dependences*		
Lattice constant	5.8687 A	(6.0583-0.405*x*) A		

Thermal conductivity

Thermal conductivity 0.05 W cm^{-1} °C $^{-1}$

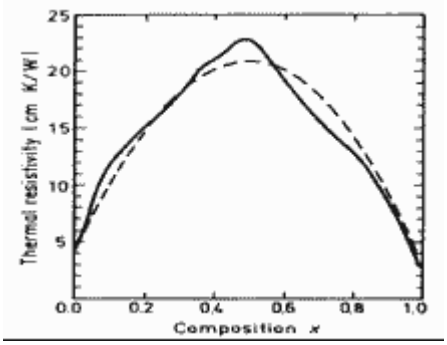

$Ga_xIn_{1-x}As$. Thermal resistivity vs. composition parameter *x* 300K
Solid lines shows the experimental data.
Dashed lines are the results theoretical calculation.
Adachi (1983)

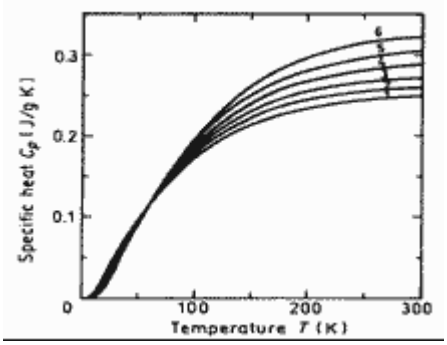

$Ga_xIn_{1-x}As$. Specific heat at constant pressure vs. temperature for different concentrations *x*.
1 - x=0.0;
2 - x=0.2;
3 - x=0.4;
4 - x=0.6;
5 - x=0.8.
6 - x=1.0.
Sirota et al. (1982)

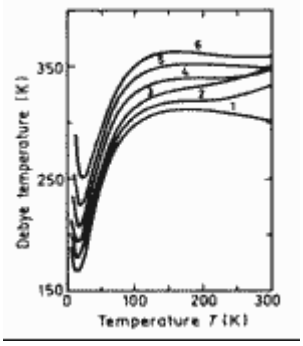

$Ga_xIn_{1-x}As$. Debye temperature vs. temperature for different concentrations *x*.
1 - x=0.0;
2 - x=0.2;
3 - x=0.4;
4 - x=0.6;
5 - x=0.8.
6 - x=1.0.
Sirota et al. (1982)

Lattice properties

Lattice parameters

	Remarks	*Referens*
Lattice constant, *a* (6.0583-0.405*x*) A	$Ga_xIn_{1-x}As$; 300K	*Adachi (1982)*
5.8687 A	$Ga_{0.47}In_{0.53}As$; 300K, *x*=0.47	

Linear thermal expansion coefficient

$Ga_x In_{1-x} As$

Mechanical properties, elastic constants, lattice vibrations

Basic Parameter

	$Ga_{0.47}In_{0.53}As$	$Ga_xIn_{1-x}As$	*Remarks*	*Referens*
Bulk modulus	$6.62 \cdot 10^{11}$ dyn/cm^2	$(5.81+1.72x) \cdot 10^{11}$ dyn/cm^2	300 K	*Goldberg Yu.A. & N.M. Schmidt (1999)*
Debye temperature	330 K	(280+110*x*) K		
Density	5.50 g/cm^3	5.68-0.37x g/cm^3	300 K	*Goldberg Yu.A. & N.M. Schmidt (1999)*
Melting point, T_m		~= 1100° C		
Specific heat	0.3 J g^{-1}°C $^{-1}$			
Thermal conductivity	0.05 W cm^{-1} °C $^{-1}$	see *Temerature dependences*		
Thermal expansion coefficient, linear	$5.66x10^{-6}$ °C $^{-1}$	see *Temerature dependences*		
Hardness on the Mohs scale		***		
Surface microhardness (using Knoop's pyramid test)		see *Micro Hardness*		
Piezoelectric constant		e_{14}= -(0.045+0.115*x*) C/m^2		
Cleavage plane	{110}	{110}		
Lattice constant	5.8687 A	(6.0583-0.405*x*) A		

Elastic constants at 300K

$C_{11} = (8.34 + 3.56x) \cdot 10^{11}$ dyn/cm^2
$C_{12} = (4.54 + 0.8x) \cdot 10^{11}$ dyn/cm^2
$C_{44} = (3.95 + 2.01) \cdot 10^{11}$ dyn/cm^2

Cleavage plane	{110}
Bulk modulus (compressibility^{-1})	
$B_s=(C_{11}+2C_{12})/3$	$B_s = (5.81+1.72x) \cdot 10^{11}$ dyn/cm^2
Anisotropy factor	
$C'=(C_{11}-C_{12})/2$	A = (0.48+0.07*x*)
Shear modulus	
$C'=(C_{11}-C_{12})/2$	$C' = (1.9+1.38x) \cdot 10^{11}$ dyn/cm^2

[100] Young's modulus

$Y_o=(C_{11}+2C_{12})\cdot(C_{11}-C_{12})/(C_{11}+C_{12})$ $Y_o = (5.14+3.39x)\cdot 10^{11}$ dyn/cm^2

[100] Poisson ratio

$\sigma_o=C_{12}/(C_{11}+C_{12})$ $\sigma_o = (0.35-0.04x)$

Micro Hardness

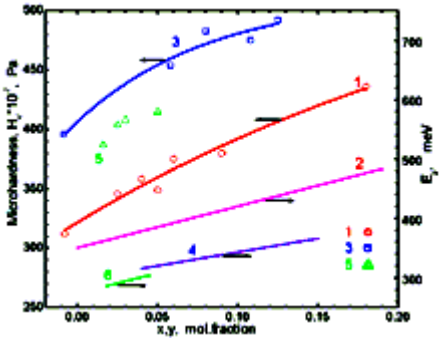

Micro hardness (Hv) and **energy gap values E_g vs composition** of three alloy systems:
$In_{1-x}Ga_xAs$ (1, 2),
$In_{1-x}Ga_xAs_{0.9}Sb_{0.1}$ (3, 4) and
$InAs_{1-x-0.1}Sb_{0.1}P_y$ (5, 6).
Measured using (111) oriented epilayers at 50 g weight (stress) on Vikkers pyramid
*B.A.Matveev et al. Izv.Akad.Nauk SSSR, Neorg.Mater, **26** (1990), 639*
Contact authors: *B.A.Matveev*

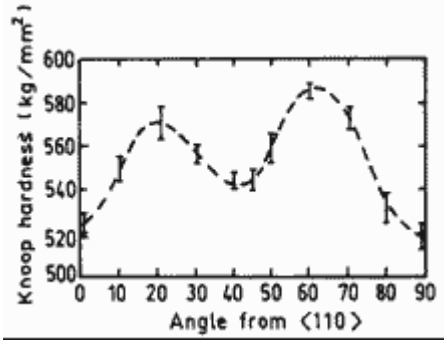

Knoop microhardness anisotropy on the {100} plane for $Ga_{0.47}In_{0.53}As$.
Adachi (1992)

Acoustic Wave Speeds

Wave propagation Direction	Wave character	Expression for wave speed	Wave speed (in units of 10^5 cm/s)
[100]	V_L (longitudinal)	$(C_{11}/\&rho)^{1/2}$	3.83+0.90x
	V_T (transverse)	$(C_{44}/\&rho)^{1/2}$	2.64+0.71x
[100]	V_l	$[(C_{11}+C_{l2}+2C_{44})/2\&rho]^{1/2}$	4.28+0.96x
	$V_{t\|\|}$	$V_{t\|\|}=V_T=(C_{44}/\ρ)^{1/2}$	2.64+0.71x
	$V_t\perp$	$[(C_{11}-C_{12})/2\&rho]^{1/2}$	1.83+0.65x
[111]	V_l'	$[(C_{11}+2C_{12}+4C_{44})/3\&rho]^{1/2}$	4.41+0.99x
	V_t'	$[(C_{11}-C_{12}+C_{44})/3\&rho]^{1/2}$	2.13+0.67x

Phonon frequencies

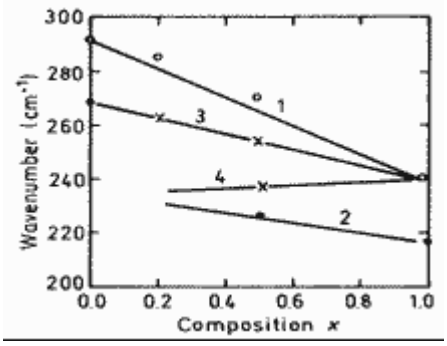

Raman-active phonon modes in $Ga_xIn_{1-x}As$.
The symbols show experimental results.
1 - LO phonon behavior,
2 - TO phonon behavior,
3,4 - mixed mode behavior.
Pearsall et al. (1983)

$Ga_x In_{1-x} As$

Piezoelectric, Thermoelectic and Magnetic Properties

Piezoelectric constant

			Remarks	*Referens*
Piezoelectric constant	e_{14}= -(0.045+0.115*x*)	C/m^2	300 K	*Goldberg Yu.A. & N.M. Schmidt (1999)*

$Ga_x In_{1-x} As$

References:

- Goldberg Yu.A. and N.M. Schmidt *Handbook Series on Semiconductor Parameters*, **vol.2**, M. Levinshtein, S. Rumyantsev and M. Shur, ed., World Scientific, London, 1999, pp. 62-88.

- S. Adachi, *J.Appl. Phys.*, **54**, no.4, pp.1844-1848 (1983).
- S.Adachi, *J. Appl. Phys.*, **66**, no.12, pp.6030-6040(1989).
- S.Adachi, *Physical Properties of III-Y Semiconductor compounds*. John Wiley and Sons.1992.
- M.I.Aliev, Kh.A.Khalilov, G.B.Ibragimov, *Phys. Stat. Sol.(b)*, **140**, no.1, pp.K83-K86(1987).
- P.Ambree, B.Gruska, K.Wandel, *Semicond. Sci. and Technol.*, **7**, pp. 858-860(1992).
- N.Arnold, R.Schmitt, K.Heime, *J.Phys. D*, **17**, no.3, pp.443-474(1984).
- V.Balynas, A.Krotkus, A.Stalnionis, A.T.Gorelionok, N.M.Shmidt, J.A.Tellefsen, *Appl. Phys.A*, **51**, no.4, pp.357-360(1990).
- P.K.Bhattacharya, U.Das, F.Y.Juang, Y.Nashimoto, S.Dhar, *Sol. St. Electr.*, **29**, no.2, pp.261-267(1986).
- P.Bourel, J.L.Thobel, K.Bellahsni, M.Pernisek, R.Fanquembergue. *Journal de Physique. III*, **1**, no.4, pp.511-520(1991).
- D.Chattopadhyay, S.K.Sutradhar, B.R.Nag, *J. Phys. C*, **14**, no.6, pp.891-908(1981).
- A.Chin, T.Y. Chang, *J.Vac.Sci.Technol.*, **B8**, no.2, pp.364-366(1990).
- I.J. Fritz, T.J. Drummond, G.C.Osbourn, J.E.Schirber, E.D.Jones, *Appl. Phys. Lett.*, **48**, no.24, pp.1678-1680(1986).
- G.Gaonach, J.Favre, E.Barbier, D.Adam, M.Champagne, C.Terrier, D.Pons, *Inst.Phys. Conf.Ser. N112*, Gallium Arsenide and Related Compounds 1990. Inst. of Phys., Bristol, Philadelphia and New York, pp. 441-446.
- K-H. Goetz, D. Bimberg, H. Jurgensen, J. Selders, A.V.Solomonov, G.F.Glinskii, M. Razeghi, *J. Appl. Phys.*, **54**, no.8, pp.4543-4552(1983).
- M.A.Haase, V.M. Robbins, N.Tabatabaie, G.E. Stillman, *J.Appl. Phys.*, **57**, no.6, pp.2295-2298(1985).
- C.H. Henry, R.A. Logan, F.R. Merritt, C.G. Bethea, *Electronics Letters*, **20**, no.9, pp.358-359(1984).
- M.S. Hybertsen, *Appl. Phys. Lett.*, **58**, no.16, pp.1759-1761(1991).
- S.C.Jain, J.M.Mc.Gregor, D.J.Roulston, *J. Appl. Phys.*, **68**, no.7, pp.3747-3749(1990).
- M.V. Karatchevtseva, A.S. Ignatiev, V.G.Mokerov, G.S.Nemtsov, V.A.Strakhov, N.G.Yaremenko, *Semiconductors*, **28**, no.7, pp.691-694 (1994).
- C.P.Kuo, S.K.Vong, R.M.Cohen, G.B. Stringfellow, *J. Appl. Phys.*, **57**, no.12, pp.5428-5432 (1985).
- J.D.Lambkin, D.J.Dunstan, *Sol. St. Comm.*, **67**, no.8, pp.827-830(1988).
- T. Matsuoka, E. Kobayashi, K.Taniguchi, C.Hamaguchi, S.Sasa., *Jap. J. Appl. Phys.*, **29**, no.10, pp.2017-2025(1990).
- J.Novak, M.Kuliffayova, M.Morvic, P.Kordos, *J.Cryst.Growth*, **96**, no.3, pp.645-648(1989).
- J.D.Oliver, Jr., L.F.Eastman, P.D.Kirchner, W.J.Schaff, *J.Cryst.Growth.*, **54**, no.1, pp.64-68 (1981).
- F.Osaka, T.Mikawa, T.Kaneda, *IEEE J. Quant. El.*, **QE-21**, no.9, pp.1326-1338(1985).
- J.Pamulapati, R.Lai, G.I.Ng, Y.C.Chen, P.R.Berger, P.K.Bhattacharya, J.Singh, D.Pavlidis, *J. Appl. Phys.*, **68**, no.1, pp.347-350(1990).
- S.Paul, J.B.Roy, P.K.Basu, *J. Appl. Phys.*, **69**, no.2, pp.827-829 (1991).
- T.P.Pearsall, J.P.Hirtz, *J.Cryst. Growth*, **54**, no.1, pp.127-131(1981).
- T.P.Pearsall, *GaInAsP Alloy Semiconductors*. John Wiley and Sons. 1982.
- T.P. Pearsall, R.Carles, J.C.Portal, *Appl. Phys. Lett.*, **42**, no.5, pp.436-438(1983).
- W. Porod, D.K. Ferry, *Phys. Rev.*, **B27**, no.4, pp.2587-2589(1983).
- N.N.Sirota, V.V.Novikov, A.M.Antiukhov, *Doklady Akademii Nauk SSSR*, **263**, no.1, pp.96-100(1982).
- H-M.Shieh, C-L.Wu, W-Ch.Hsu, Y-H.Wu, M-J.Kao, *Jap. J. Appl. Phys.*, **33**, no.4a, pp.1778-1780(1994).
- M.Shur, *Physics of Semiconductor Devices*, Prentice Hall, 1990.
- T.Takagi, *Jap. J. Appl. Phys.*, **17**, no.10, pp.1813-1817(1978).
- J.L.Thobel, L.Baudry, A.Cappy, P.Bourel, R.Fauquembergue, *Appl. Phys. Lett.*, **56**, no.4, pp.346-348(1990).
- E.Wolak, J.C.Harmand, T.Matsuno, K.Inoue, T.Narusawa, *Appl. Phys. Lett.*, **59**, no.1, pp.111-113(1991).
- E.Zielinski, H.Schweizer, K.Streubel, H.Eisele, G.Weimann, *J. Appl. Phys.*, **59**, no.6, pp.2196-2204(1986).

2.2 Bildvergrößerungen

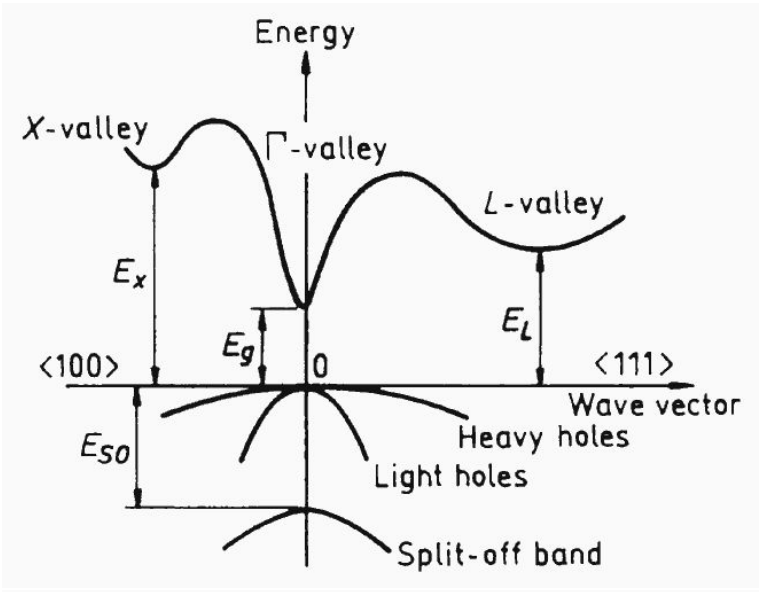

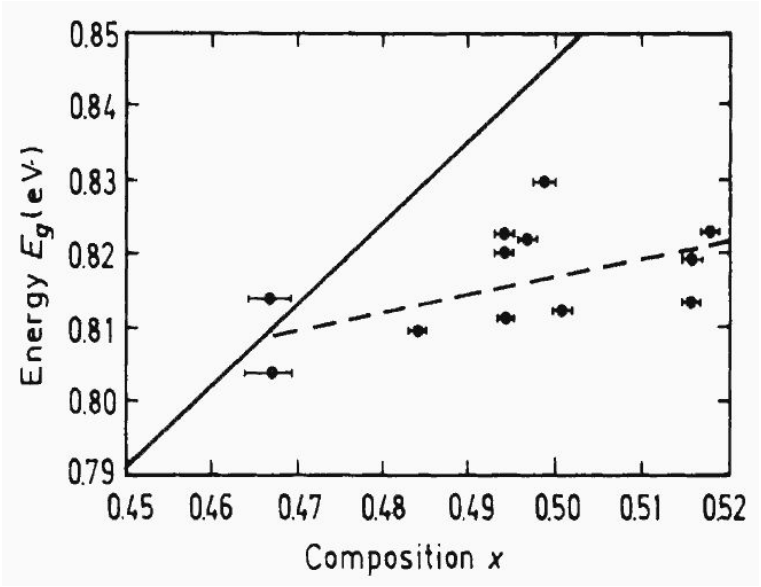

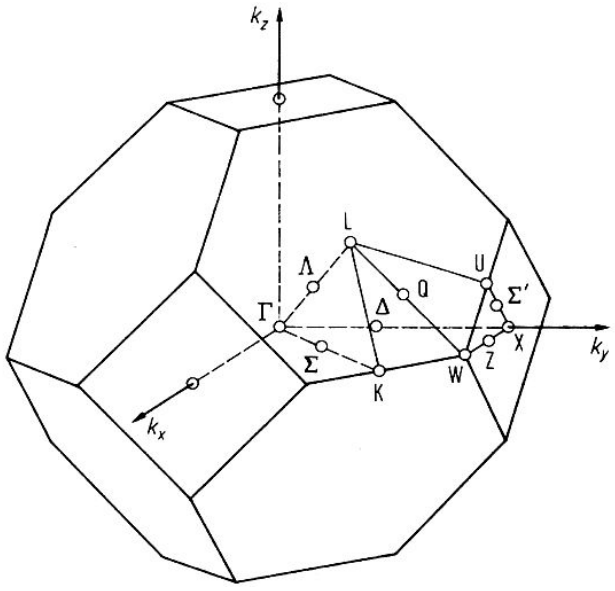

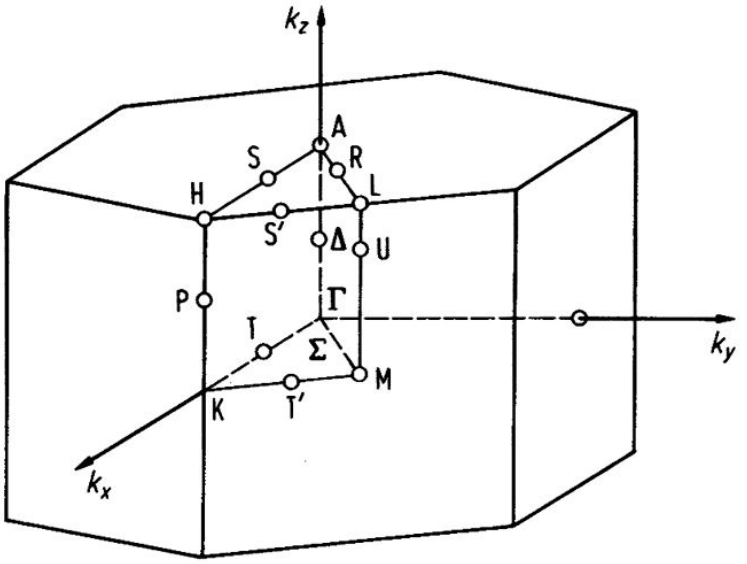
k_z
A
S
R
H
L
S'
Δ
U
P
Γ
T
Σ
M
K
T'
k_y
k_x

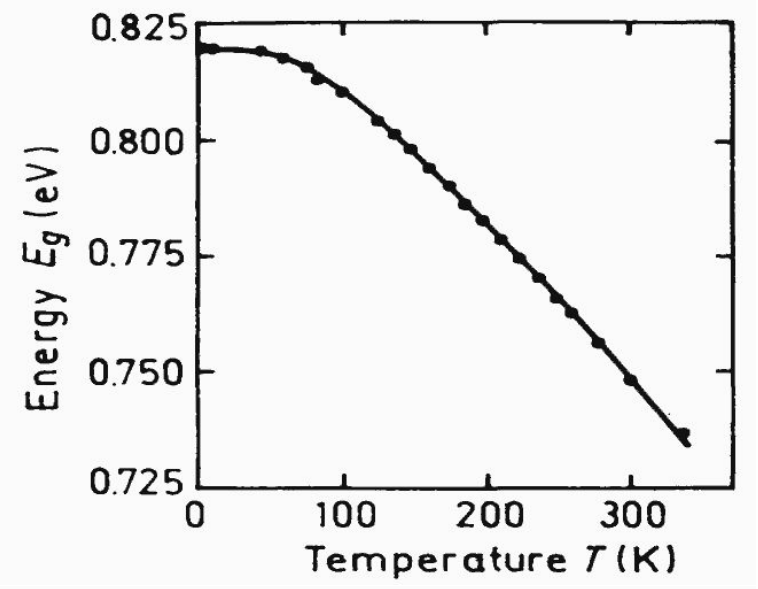
0.825
0.800
0.775
0.750
0.725
Energy E_g (eV)
0
100
200
300
Temperature T (K)

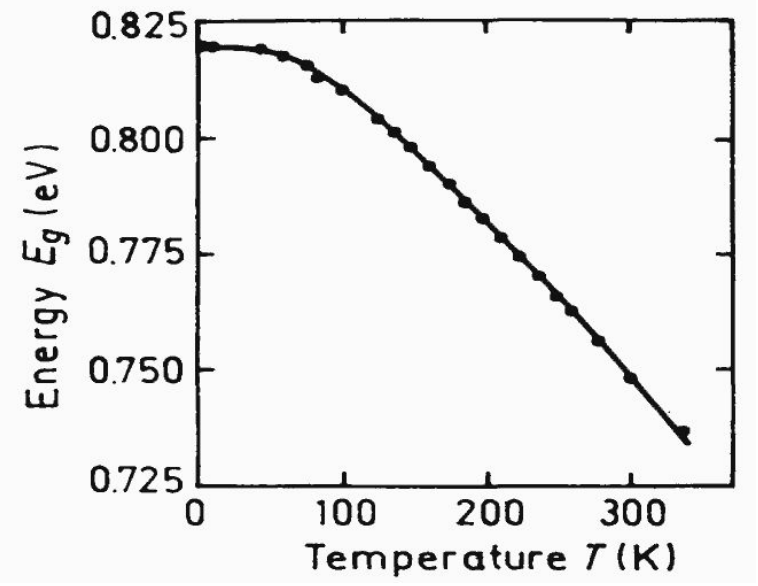
0.825
0.800
0.775
0.750
0.725
Energy E_g (eV)
0
100
200
300
Temperature T (K)

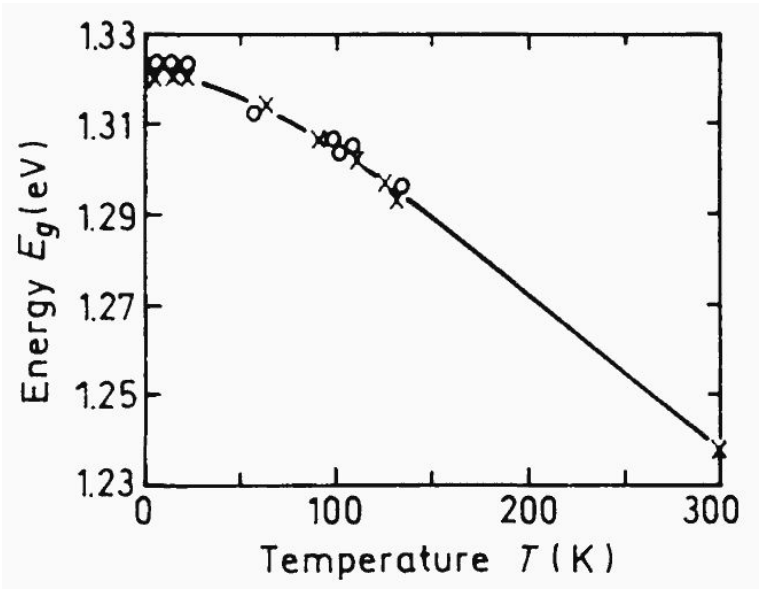
1.33
1.31
1.29
1.27
1.25
1.23
Energy E_g (eV)
0
100
200
300
Temperature T (K)

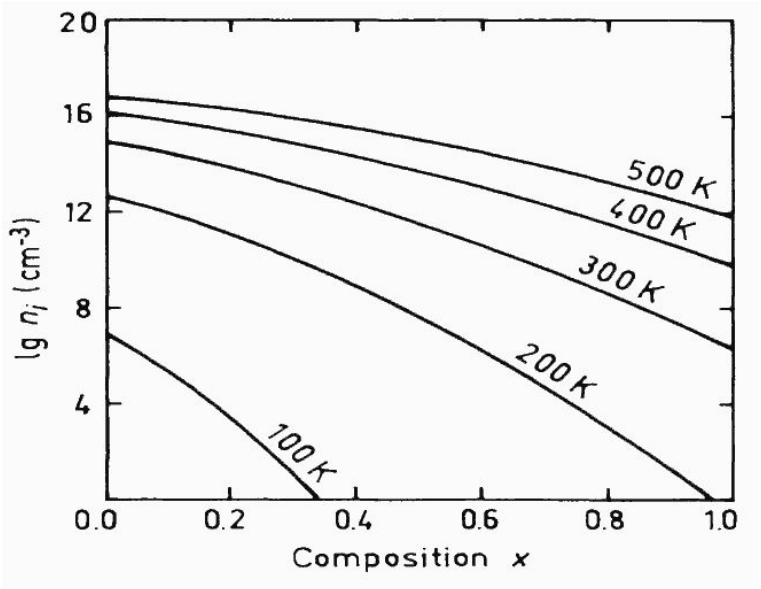
20
16
12
8
4
lg n_i (cm^{-3})
500 K
400 K
300 K
200 K
100 K
0.0
0.2
0.4
0.6
0.8
1.0
Composition x

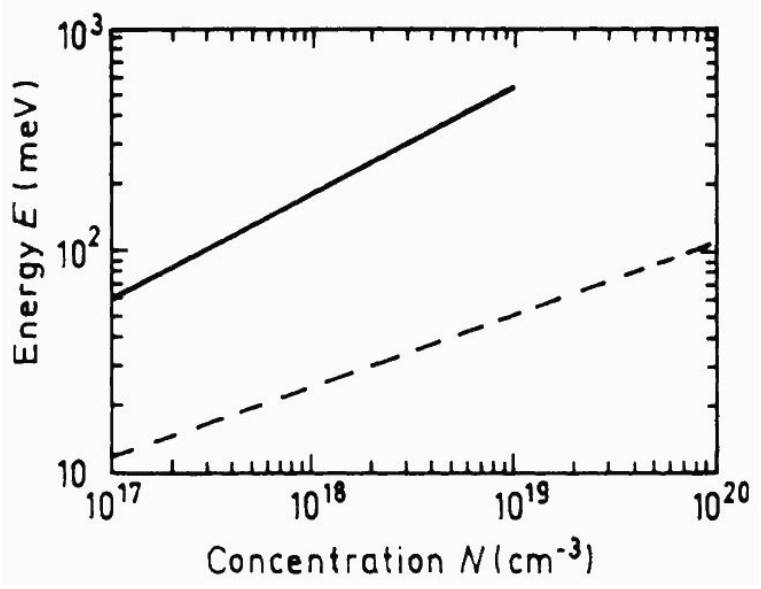
10^3
10^2
10
Energy E (meV)
10^{17}
10^{18}
10^{19}
10^{20}
Concentration N (cm^{-3})

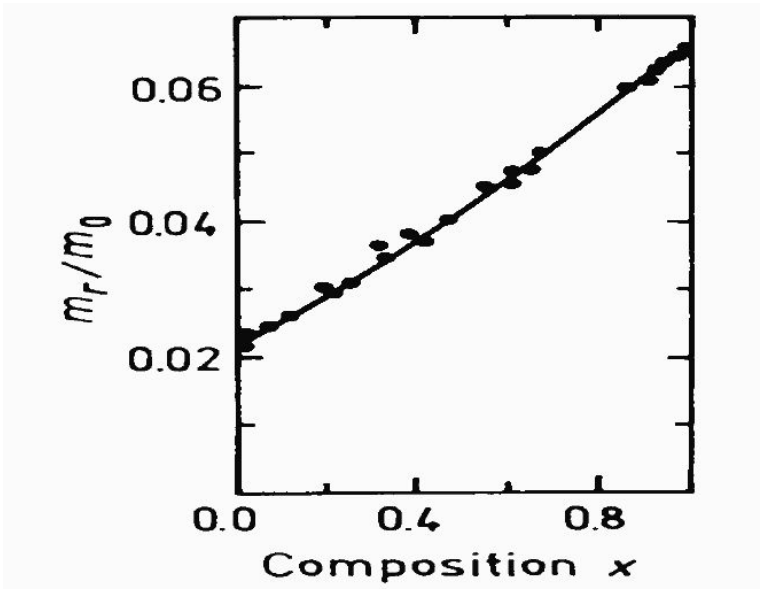
0.06
0.04
0.02
m_r/m_0
0.0
0.4
0.8
Composition x

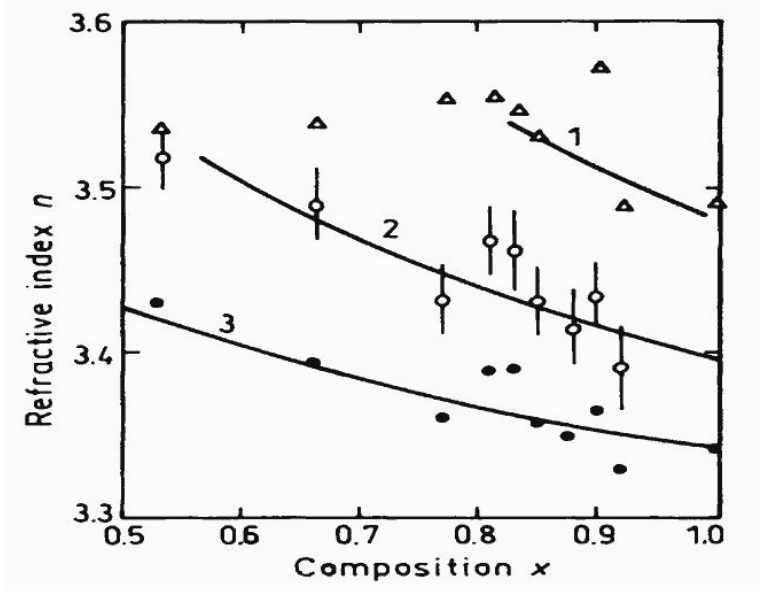
3.6
3.5
3.4
3.3
Refractive index n
1
2
3
0.5
0.6
0.7
0.8
0.9
1.0
Composition x

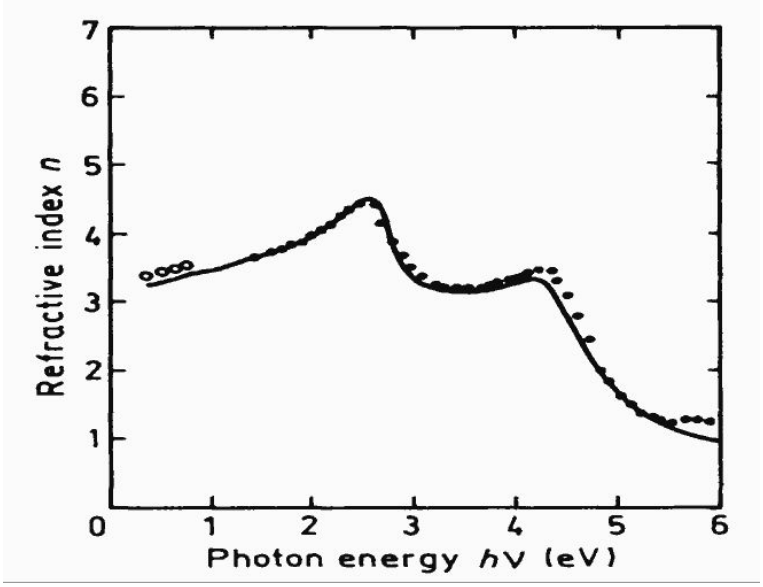
7
6
5
4
3
2
1
0
Refractive index n
0
1
2
3
4
5
6
Photon energy hV (eV)

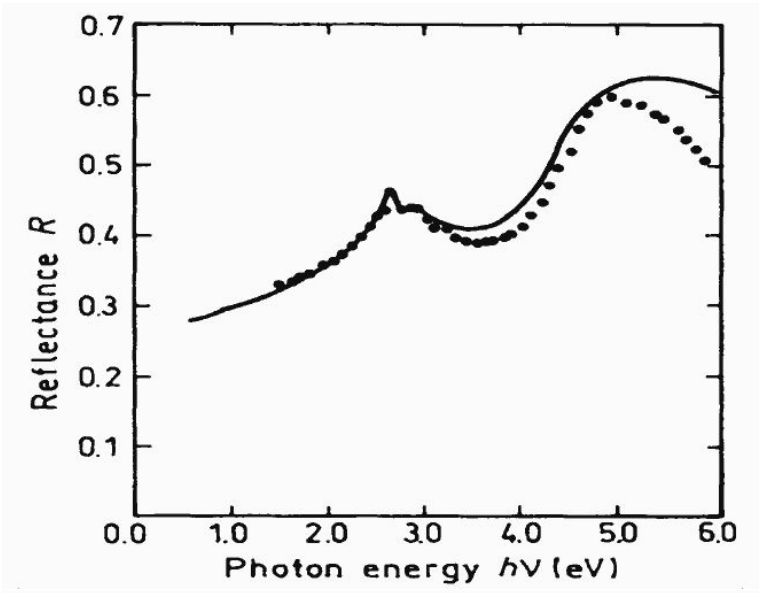
Reflectance R
0.7
0.6
0.5
0.4
0.3
0.2
0.1
0.0
1.0
2.0
3.0
4.0
5.0
6.0
Photon energy hV (eV)

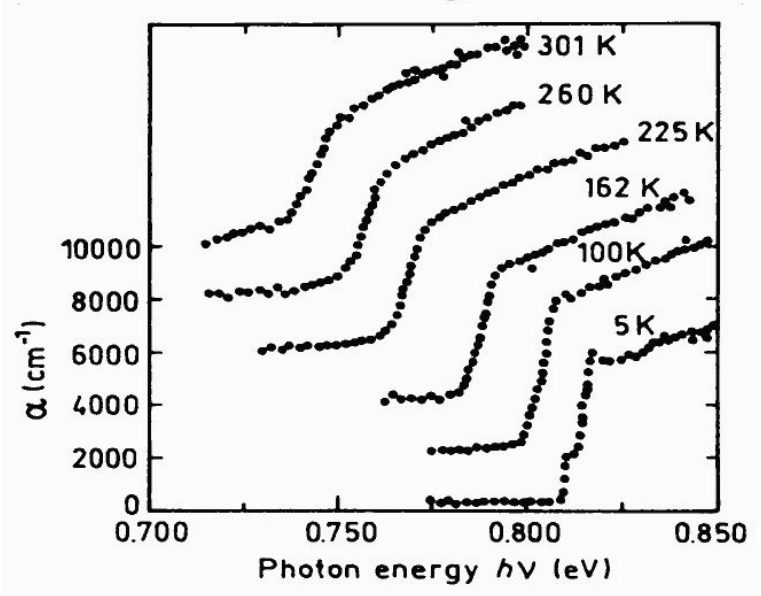
301 K
260 K
225 K
162 K
100K
5K
α (cm⁻¹)
10000
8000
6000
4000
2000
0
0.700
0.750
0.800
0.850
Photon energy hV (eV)

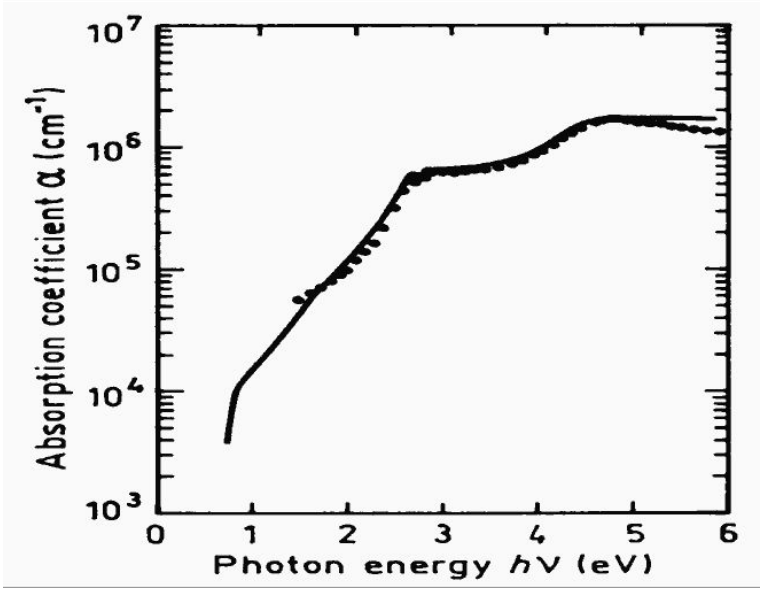
Absorption coefficient α (cm⁻¹)
10⁷
10⁶
10⁵
10⁴
10³
0
1
2
3
4
5
6
Photon energy hV (eV)

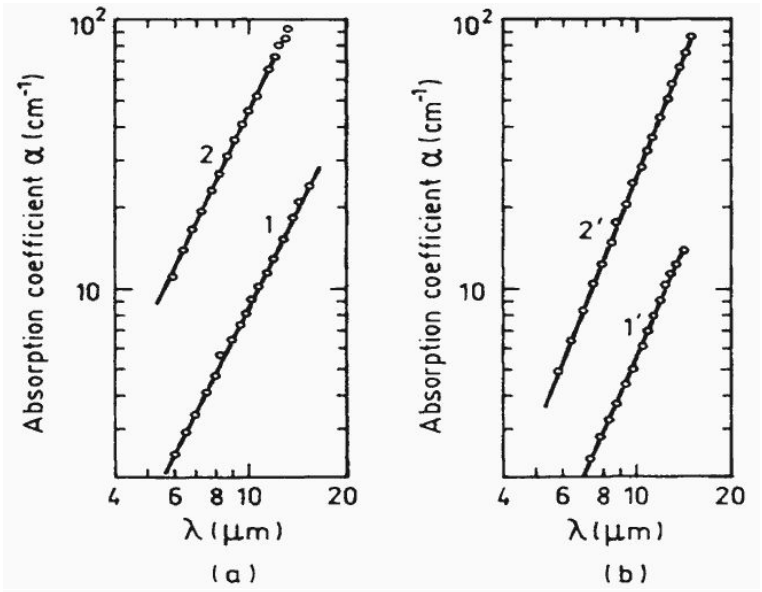
Absorption coefficient α (cm⁻¹)
10²
10
2
1
4 6 8 10 20
λ (μm)
(a)
Absorption coefficient α (cm⁻¹)
10²
10
2'
1'
4 6 8 10 20
λ (μm)
(b)

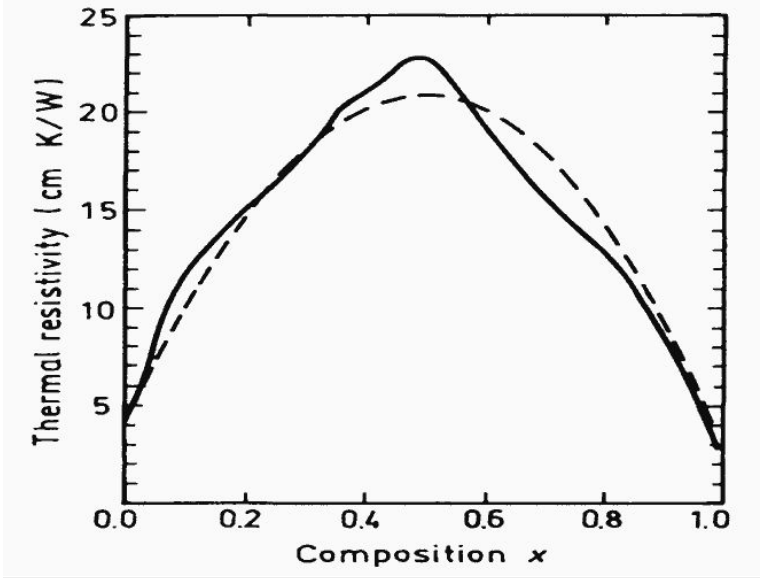
Thermal resistivity (cm K/W)
25
20
15
10
5
0.0 0.2 0.4 0.6 0.8 1.0
Composition x

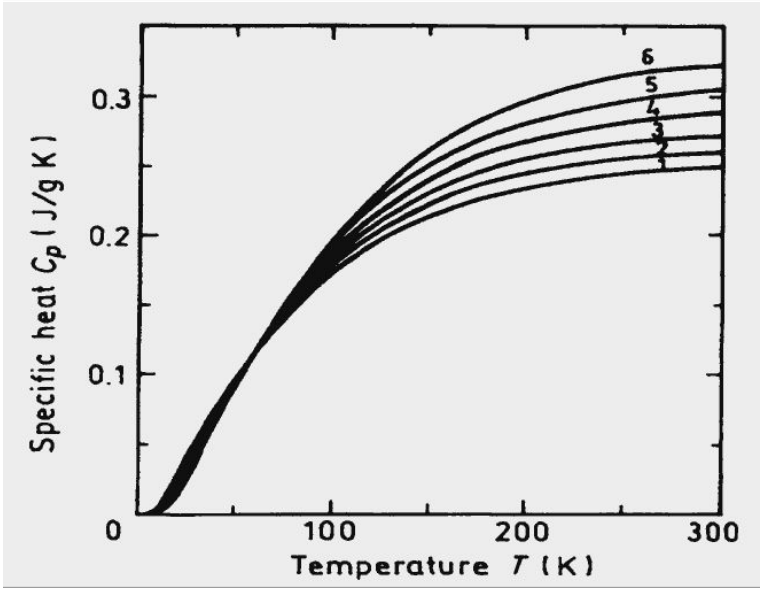
Specific heat C_p (J/g K)
0.3
0.2
0.1
0
6
5
4
3
2
1
100 200 300
Temperature T (K)

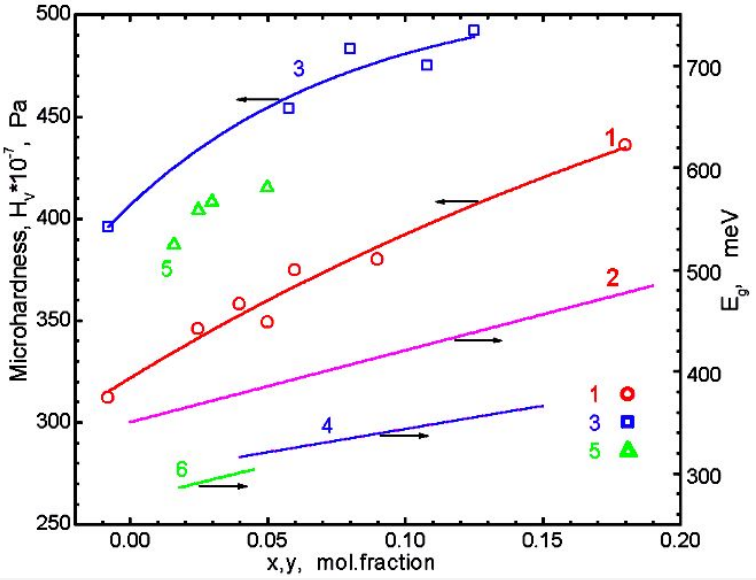
Microhardness, H_v*10^{-7}, Pa
E_g, meV
x,y, mol.fraction
1
2
3
4
5
6

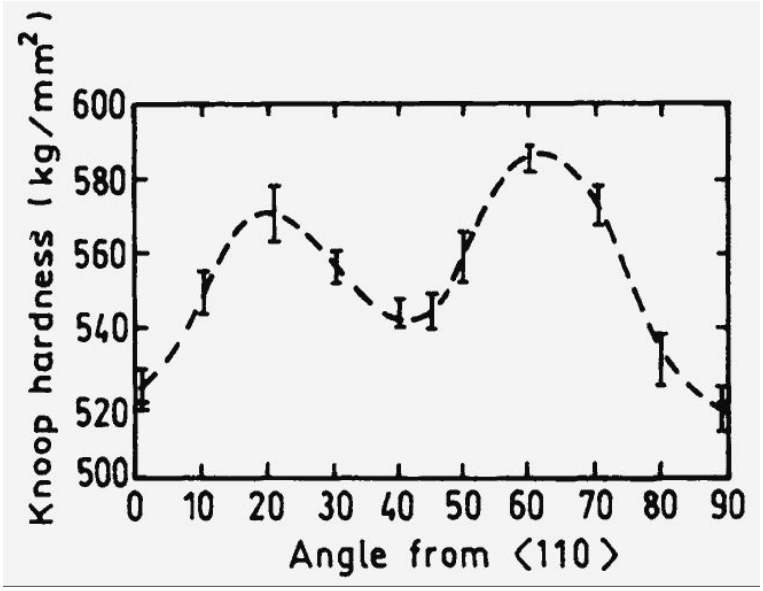
Knoop hardness (kg/mm^2)
Angle from ⟨110⟩

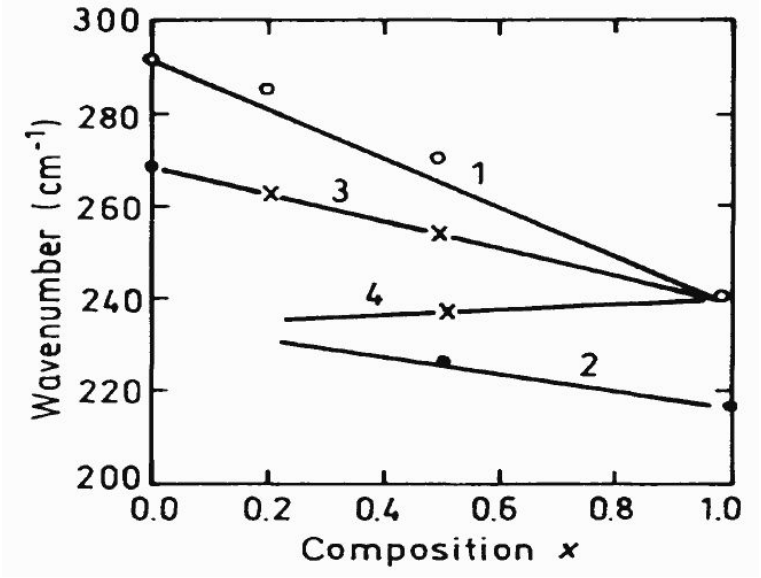
Wavenumber (cm^{-1})
Composition x
1
2
3
4

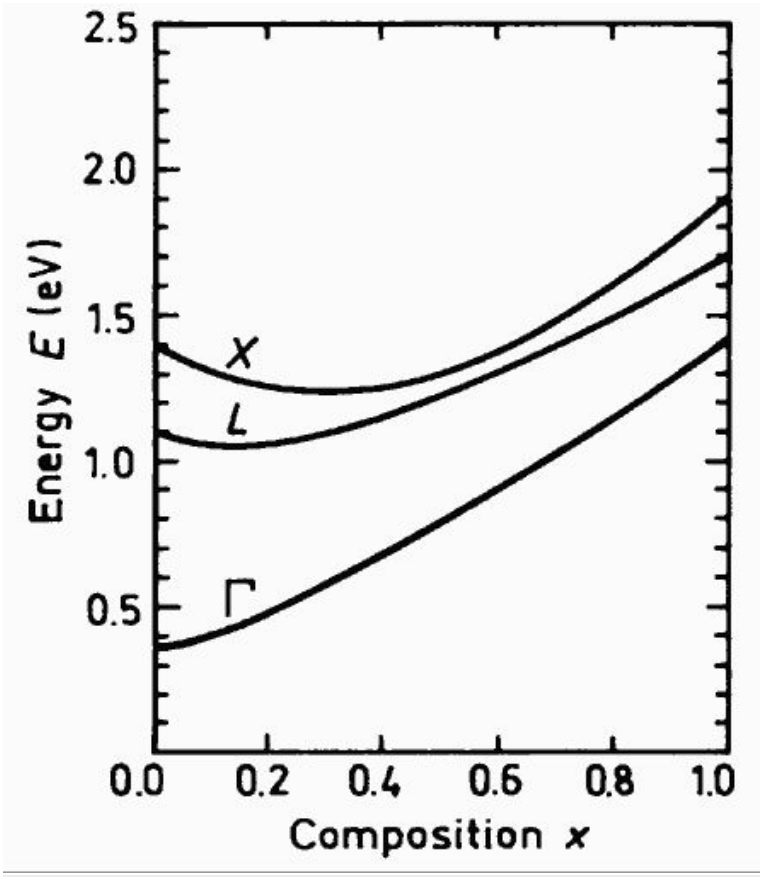
2.5
2.0
1.5
1.0
0.5
Energy E (eV)
X
L
Γ
0.0
0.2
0.4
0.6
0.8
1.0
Composition x

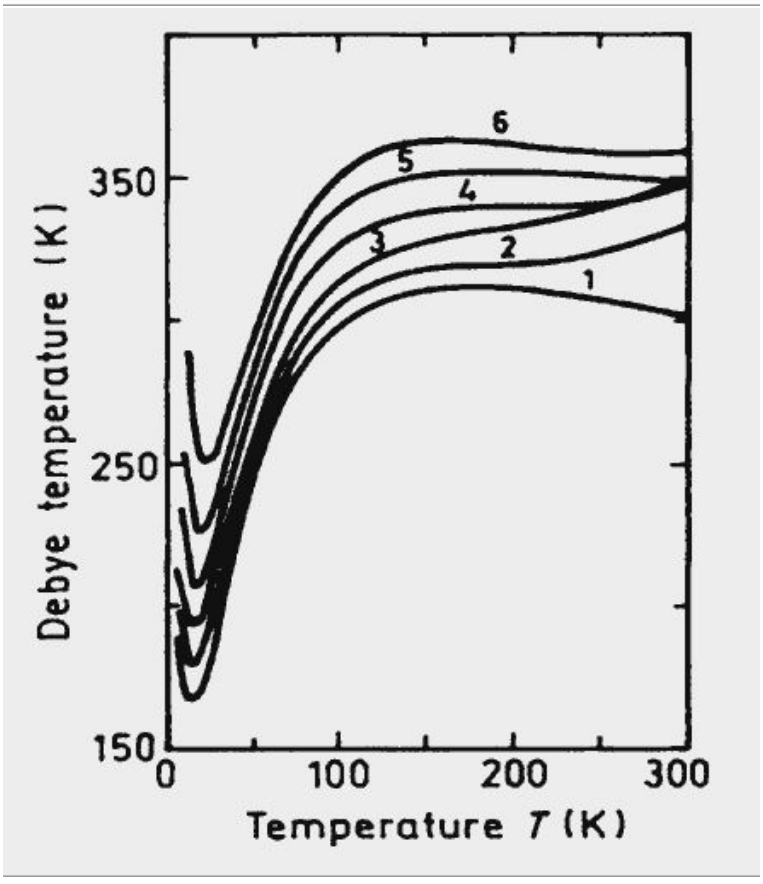
6
5
4
3
2
1
350
250
150
Debye temperature (K)
0
100
200
300
Temperature T (K)

3 $Al_xIn_{1-x}As$

[002]ff.

3.1 Originaltexte

Dokument nächste Seite folgend.

$Al_x Ga_{1-x} As$

$Al_x Ga_{1-x} As$

Basic Parameters at 300 K

Crystal structure	Zinc Blende
Group of symmetry	T_d^2-F43m
Number of atoms in 1 cm^3	$(4.42-0.17x)\cdot 10^{22}$
Debye temperature	$370+54x+22x^2$ K
Density	$5.32-1.56x$ g·cm^{-3}
Dielectric constant (static)	12.90-2.84x
Dielectric constant (high frequency)	10.89-2.73x
Effective electron mass m_e	0.063+0.083x m_o (x<0.45)
Density-of-states electron mass m_{cd}	0.85-0.14x m_o (x>0.45)
Conductivity effective mass m_{cc}	0.26 m_o (x>0.45)
Effective hole masses m_h	0.51+0.25x m_o
Effective hole masses m_{lp}	0.082+0.068x m_o
Electron affinity	4.07-1.1x eV (x<0.45) 3.64-0.14x eV (x>0.45)
Lattice constant	5.6533+0.0078x A
Optical phonon energy	$36.25+1.83x+17.12x^2-5.11x^3$ meV

$Al_x Ga_{1-x} As$

Band structure and carrier concentration

Basic Parameters

Energy gap	x<0.45	1.424+1.247x eV
	x>0.45	$1.9+0.125x+0.143x^2$
Energy separation ($E_{\Gamma L}$) between Γ and L valleys	0.29 eV	
Energy separation (E_Γ) between Γ and top of valence band	$1.424+1.155x+0.37x^2$ eV	
Energy separation (E_X) between X-valley and top of valence band	$1.9+0.124x+0.144x^2$ eV	
Energy separation (E_L) between L-valley and top of valence band	1.71+0.69x eV	
Energy spin-orbital splitting	0.34-0.04x eV	
Intrinsic carrier concentration	x=0.1	$2.1\cdot 10^5$ cm^{-3}
	x=0.3	$2.1\cdot 10^3$ cm^{-3}
	x=0.5	$2.5\cdot 10^2$ cm^{-3}
	x=0.8	$4.3\cdot 10^1$ cm^{-3}
Intrinsic resistivity	x=0.1	$4\cdot 10^9$ Ω·cm
	x=0.3	$1\cdot 10^{12}$ Ω·cm
	x=0.5	$1\cdot 10^{14}$ Ω·cm
	x=0.8	$5\cdot 10^{14}$ Ω·cm
Effective conduction band density of states	x<0.41	$2.5\cdot 10^{19}\cdot(0.063+0.083x)^{3/2}$ cm^{-3}
	x>0.45	$2.5\cdot 10^{19}\cdot(0.85-0.14x)^{3/2}$ cm^{-3}
Effective valence band density of states	$2.5\cdot 10^{19}\cdot(0.51+0.25x)^{3/2}$ cm^{-3}	

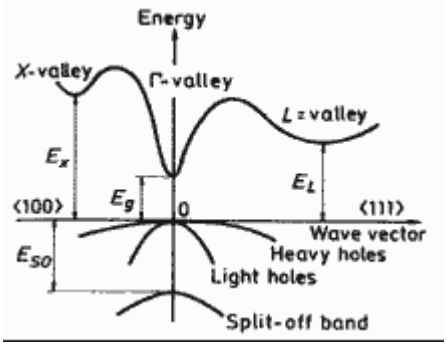

Band structure Al_xGa_{1-x} for x<0.41-0.45. Important minima of the condition band and maxima of the valence band

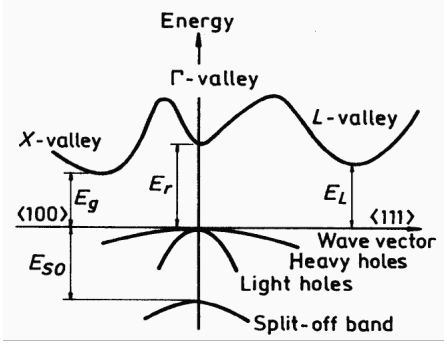

Band structure Al_xGa_{1-x} for x>0.45. Important minima of the condition band and maxima of the valence band

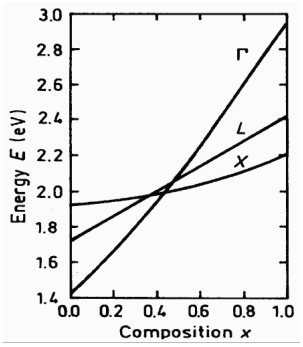

Energy separation between Γ-, X-, and L- conduction band minima and top of the valence band versus composition.
Crossover points:

x_c(L-X) = 0.35 eV E_L=E_X = 1.95 eV

x_c(Γ-X) = 0.41 eV $E_Γ$=E_X = 1.97 eV

x_c(Γ-L) = 0.47 eV $E_Γ$=E_L = 2.04 eV

(Saxena [1980]).

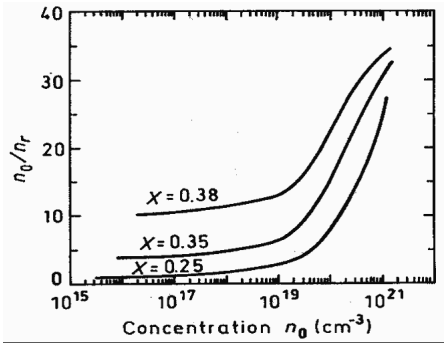

Ratio of the total carrier concentration to the carrier concentration in Γ-valley as a function of equilibrium carrier concentration at 300K *(Zarem et al. [1989])*.

Temperature Dependences

To estimate the temperature dependences of energy difference between the top of the valence band and the bottom of the Γ, X, and L valleys of the conduction band $E_Γ$, E_X and E_L one can use the data for GaAs *(Aspnes [1976])*.

$E_Γ=E_Γ(0)-5.41\cdot10^{-4}\cdot T^2/(T+204)$ (eV)

where $E_Γ(0)=1.519+1.155x+0.37x^2$ (eV)

$E_X=E_X(0)-4.6\cdot10^{-4}\cdot T^2/(T+204)$ (eV)

where $E_X(0)=1.981+0.124x+0.144x^2$ (eV)

$E_L=E_L(0)-6.05\cdot10^{-4}\cdot T^2/(T+204)$ (eV)

where $E_L(0)=1.815+0.0.69x$ (eV)

Temperature dependence of the energy difference between the top of the valence band and the bottom of the L-valley of the conduction band

$E_L=1.815-6.05\cdot10^{-4}\cdot T^2/(T+204)$ (eV)

Temperature dependence of the energy difference between the top of the valence band and the bottom of the X-valley of the conduction band

E_L=1.981-4.60·10^{-4}·T^2/(T+204) (eV)

Effective density of states in the conduction band N_c

X<0.41 $N_c=4.82\cdot 10^{15}\cdot(m_\Gamma/m_o)^{3/2}\cdot T^{3/2} = 4.82\cdot 10^{15}\cdot T^{3/2}\cdot(0.063+0.083x)^{3/2}$ (cm^{-3})

X>0.41 $N_c=4.82\cdot 10^{15}\cdot(m_{cd}/m_o)^{3/2}\cdot T^{3/2} = 4.82\cdot 10^{15}\cdot T^{3/2}\cdot(0.85-0.14x)^{3/2}$ (cm^{-3})

where m_{cd} is effective mass of the density of states;

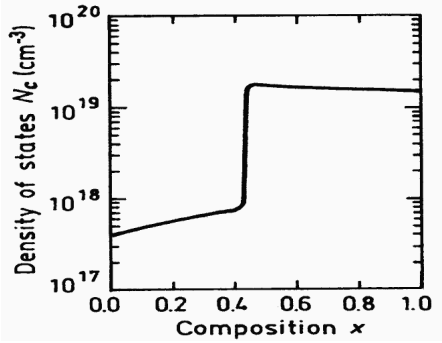

Effective density of states in the conduction band versus x.
(Calculated)

Effective density of states in the valence band N_v

$N_v = 4.82\cdot 10^{15}\cdot T^{3/2}\cdot(0.51+0.25x)^{3/2}$ (cm^{-3}) **X>0.41** $N_c=4.82\cdot 10^{15}\cdot(m_{cd}/m_o)^{3/2}\cdot T^{3/2} = 4.82\cdot 10^{15}\cdot T^{3/2}\cdot(0.85-0.14x)^{3/2}$ (cm^{-3})

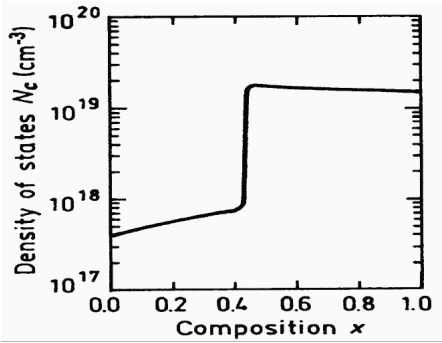

Effective density of states in the conduction band versus x.
(Calculated)

Intrinsic Carrier Concentration

$n_i = (N_c\cdot N_v)^{1/2}\exp[-E_g/(2k_bT)]$

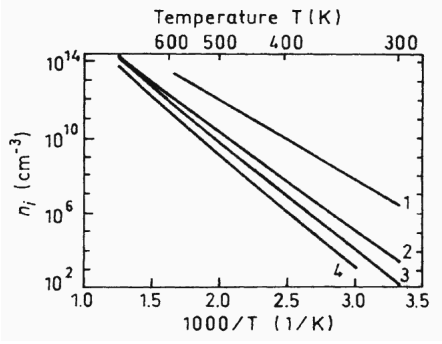

The temperature dependences of the intrinsic carrier concentration.
1. x=0
2. x=0.3
3. x=0.6
4. x=1

Dependences on Hydrostatic Pressure

$E_\Gamma = (11.5 - 1.3\,x)\cdot 10^{-3}\cdot P$ *(eV)*
$E_X = -0.8\cdot 10^{-3}\cdot P$ *(eV)*
$E_L = 2.8\cdot 10^{-3}\cdot P$ *(eV)*
where P is pressure in kbar. *(Adachi [1985])*

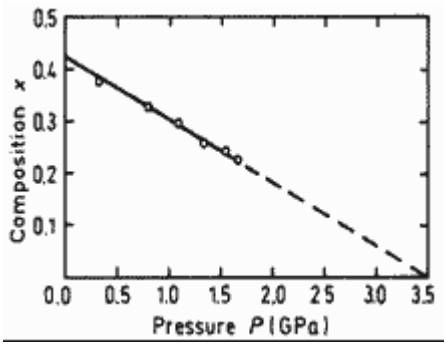

Pressure dependence of the Γ-X crossover. 300 K
(Saxena [1980])

Energy Gap Narrowing at High Doping Levels

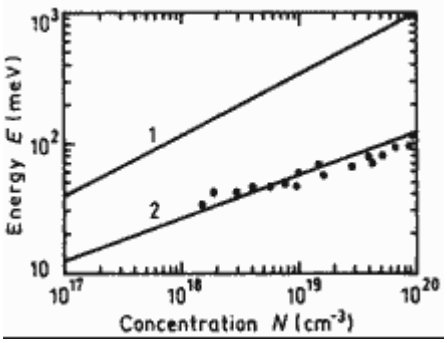

Energy gap narrowing versus donor(curve 1) and acceptor (curve 2) doping density for GaAs (x=0).
Experimental points for p-GaAs are taken from four different papers
(Jain and Roulston [1991])

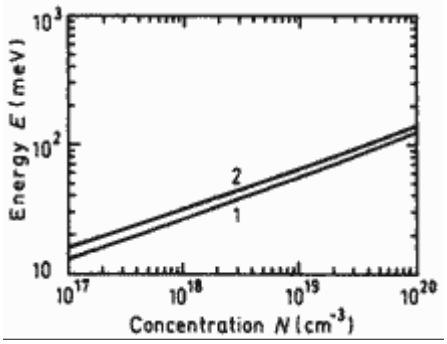

Energy gap narrowing versus donor (curve 1) and acceptor (curve 2)doping density for AlAs (x=1).
The curvesare calculated according *(Jain et al. [1990])*

Band Discontinuities at $Al_xGa_{1-x}As$/GaAs Heterointerface

Valence band discontinuity:

ΔE_v = - 0.46x (eV)

Conduction band discontinuity:

x<0.41 ΔE_c = 0.79x (eV)

x>0.41 ΔE_c = 0.475-0.335x+0.143x^2 (eV)

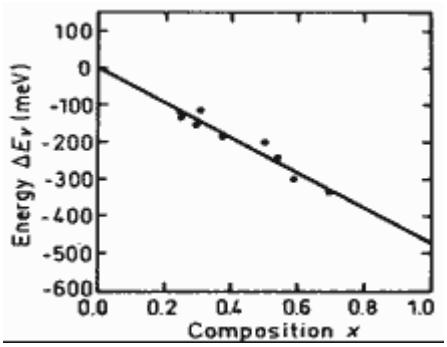

Energy gap narrowing versus donor(curve 1) and acceptor (curve 2) doping density for GaAs (x=0).
Experimental points for p-GaAs are taken from four different papers *(Jain and Roulston [1991])*

$Al_x Ga_{1-x} As$

Electrical properties - Basic Parameters

Breakdown field	$\approx(4 \div 6) \cdot 10^5$ V/cm
Mobility electrons	
0<x<0.45	$8 \cdot 10^3 - 2.2 \cdot 10^4 x + 10^4 \cdot x^2$ cm^2 V^{-1} s^{-1}
0.45<x<1	$-255 + 1160x - 720x^2$ cm^2 V^{-1} s^{-1}
Mobility holes	$370 - 970x + 740x^2$ cm^2 V^{-1} s^{-1}
Diffusion coefficient electrons	
0<x<0.45	$200 - 550x + 250x^2$ cm^2/s
0.45<x<1	$-6.4 + 29x - 18x^2$ cm^2/s
Diffusion coefficient holes	$9.2 - 24x + 18.5x^2$ cm^2/s
Electron thermal velocity	
0<x<0.4	$(4.4 - 2.1x) \cdot 10^5$ m/s
0.45<x<1	$2.3 \cdot 10^5$ m/s
Hole thermal velocity	$(1.8 - 0.5x) \cdot 10^5$ m/s

$Al_x Ga_{1-x} As$

Mobility and Hall Effect

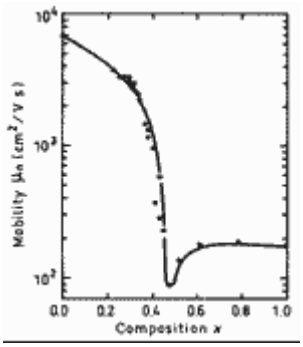

Electron Hall mobility versus alloy composition x. T=300 K.
Electron concentration n_o=(5÷10)· 10^{15} cm^{-3}.
(Saxena (1981b)).

For weakly doped $Al_xGa_{1-x}As$ at 300 K electron Hall mobility.

0<x<0.45 μ_H=-8000 - 22000x+ 10000x^2
0.45<x<1 μ_H=-255+1160x-720x^2
(Shur (1990)).

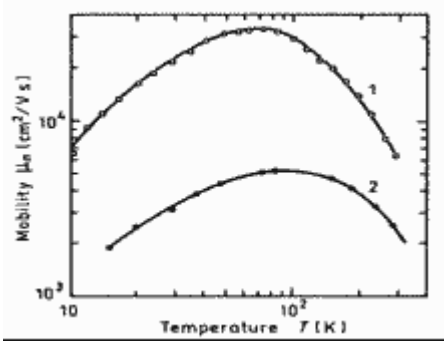

Electron Hall mobility versus temperature.
Curve 1 x=0; n=0.5· 10^{16} cm^{-3} *(Stillman et al. (1970))*.
Curve 2 x=0.32; n=(0.5÷1)· 10^{16} cm^{-3} *(Saxena (1981b))*.

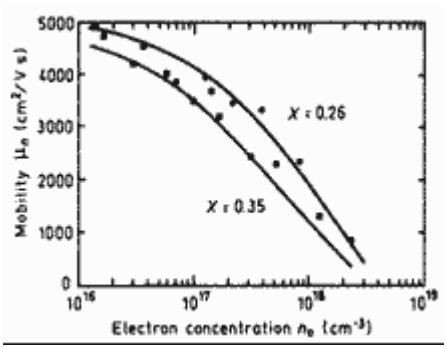

Electron Hall mobility versus electron concentration for two values of x. T=77 K.
(Liu (1990)).

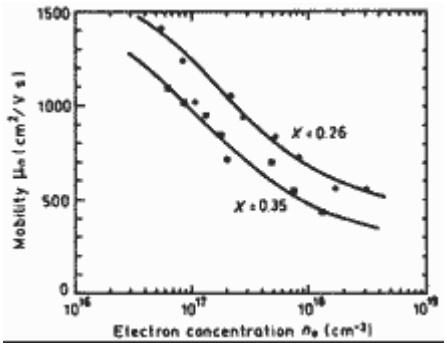

Electron Hall mobility versus electron concentration for two values of x. T=300 K.
(Liu (1990)).

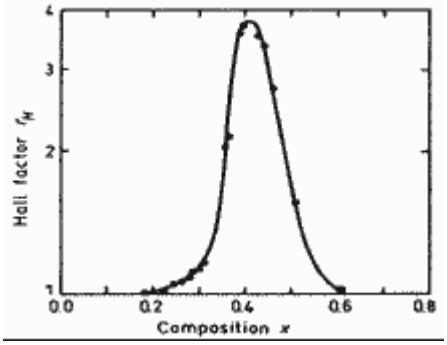

Hall factor versus alloy composition x for n-type $Al_xGa_{1-x}As$ T=300 K
Electron concentration $n_o=(5\div10)\cdot10^{15}$ cm^{-3}.
(Saxena (1981a)).

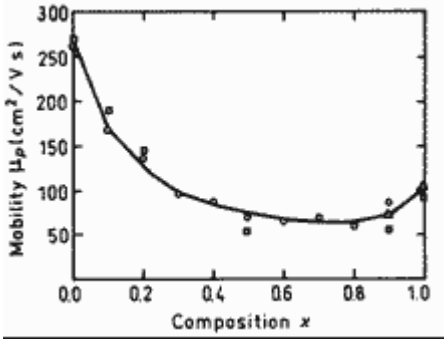

Hole Hall mobility versus alloy composition x. 296 K.
Acceptor density $N_a\approx2.5\cdot10^{17}$ cm^{-3}.
(Look et al. (1992)).

For weakly doped $Al_xGa_{1-x}As$ at 300 K hole Hall mobility.

$\mu_H=-370-970x+740x^2$
(Shur (1990)).

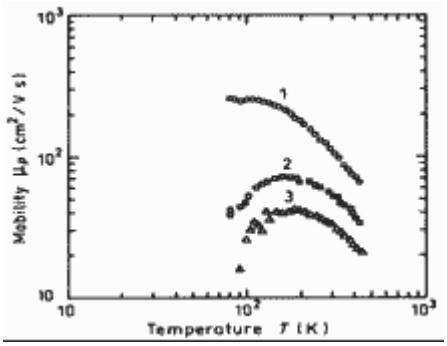

Hole Hall mobility versus temperature.
Curve 1 - x=0; $p_o=7\cdot10^{17}$ cm^{-3}
Curve 2 - x=0.41; $p_o=4.65\cdot10^{17}$ cm^{-3}
Curve 3 - x=0.75; $p_o=2.4\cdot10^{17}$ cm^{-3}
(Yang et al. (1981)).

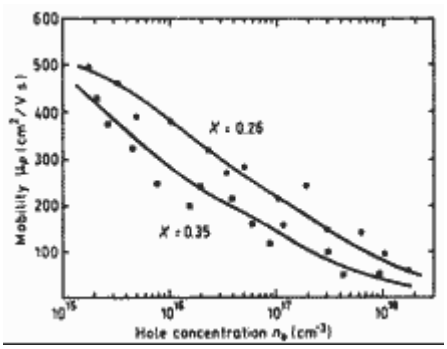

Hole Hall mobility versus hole concentration for two values of x. T=77 K.
(Liu (1990)).

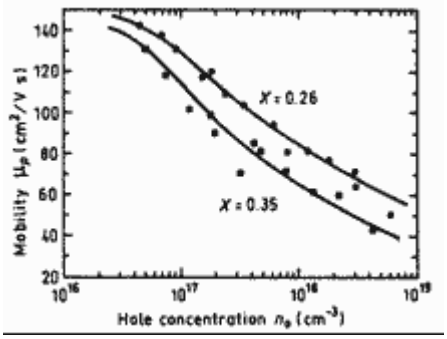

Hole Hall mobility versus hole concentration for two values of x. T=300 K.
(Liu (1990)).

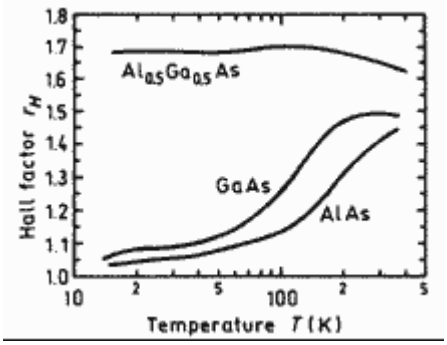

Hall factor versus temperature x for p-type GaAs, AlAs and $Al_{0.5}Ga_{0.5}As$.

Curves are calculated for acceptor concentration $N_a \approx 6.5 \cdot 10^{13}$ cm^{-3}. *(Look et al. (1992))*.

$Al_x Ga_{1-x} As$

Two-dimensional electron and hole gas mobility at $Al_xGa_{1-x}As/GaAs$ interface

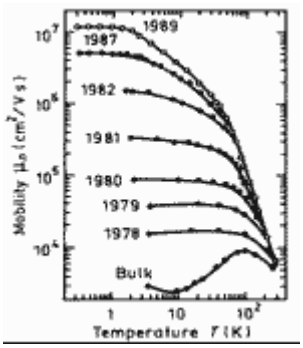

Temperature dependences of the electron Hall mobility in the modulation-doped two-dimensional gas.
(Pfeiffer et al. (1989)).

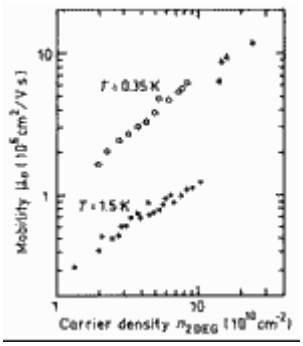

Dependences of electron mobility versus surface carrier density 2D electron gas in the modulation-doped two-dimensional gas.
(Pfeiffer et al. (1989)).

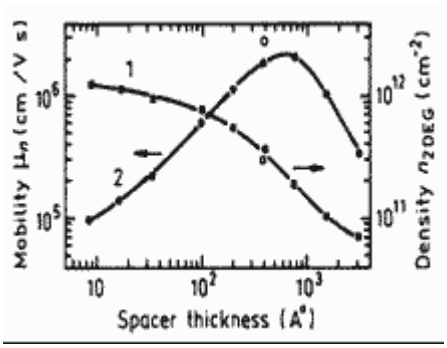

Dependences of surface electron density (Curve 1) and mobility (Curve 2) versus undoped spacer thickness. T=4 K.
(Harris et al. (1987)).

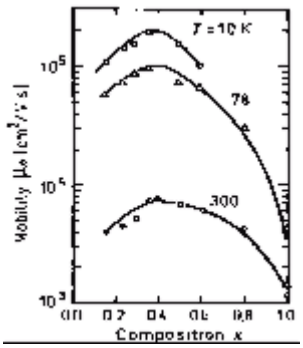

Electron mobility in 2D-electron gas versus Al fraction x at three different temperatures.
(Drummond et al. (1982)).

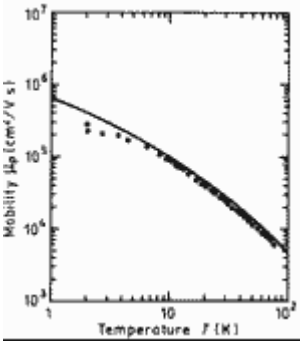

Hole mobility in 2D-hole gas versus temperature.
Solid line shows theoretical calculation.
Points show experimental data for hole surface density $2 \cdot 10^{11}$ cm^{-2} *(Walukiewicz (1996))*.

$Al_x Ga_{1-x} As$

Transport Properties in High Electric Fields

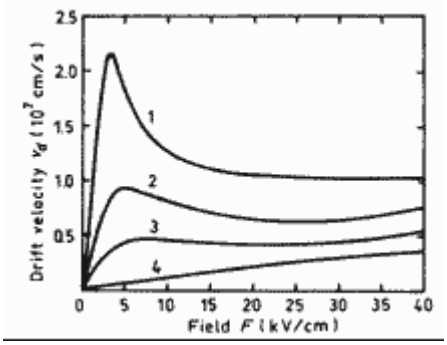

Field dependences of the electron drift velocity for different values of x.
Curves are calculated according displaced Maxwellian approximation.
T=300 K.
1 - x=0;
2 - x=0.225;
3 - x=0.325;
4 - x=0.5.
(Hava and Auslender (1993)).

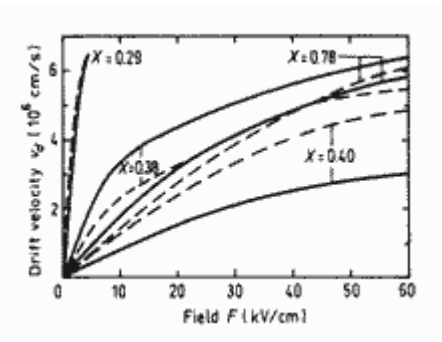

Field dependences of the electron drift velocity for different values of x.
Solid curves - show experimental results (electron concen tration
$n_o=(2\div10)\cdot10^{15}$ cm^{-3}
Dashed curves show results of Monte-Carlo calculations.
(Hill and Robson (1981)).

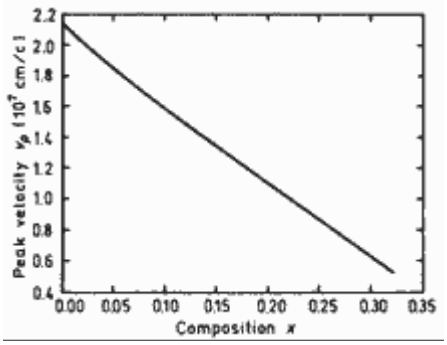

Dependences of peak electron velocity versus x.
(Hava and Auslender (1993)).

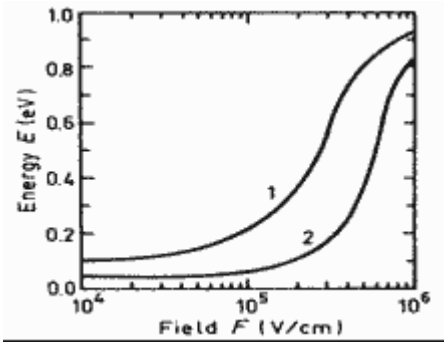

Average electron energy as a function of electric field. T=300 K.
1 - x=0.25;
2 - x=0.45. *(Lippens and Vanbesien (1987))*.

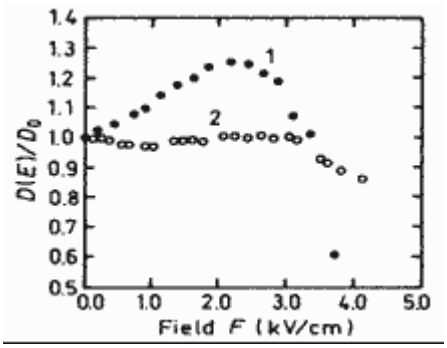

The field dependences of normalized longitudinal diffusion coefficient. T=300 K.
1 - x=0;
2 - x=0.25. *(de Murcia et al. (1993))*.

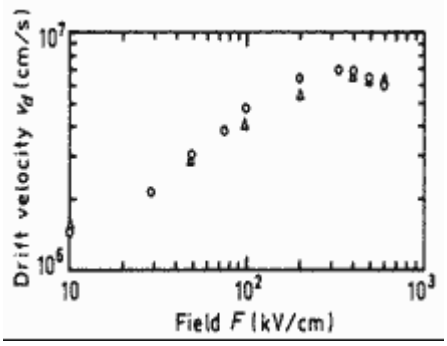

Field dependence of hole drift velocity. Monte-Carlo calculations. T=300 K.
(Brennan and Hess (1986)).

$Al_x Ga_{1-x} As$

Transport properties of electron and hole two-dimensional gas in high electric field

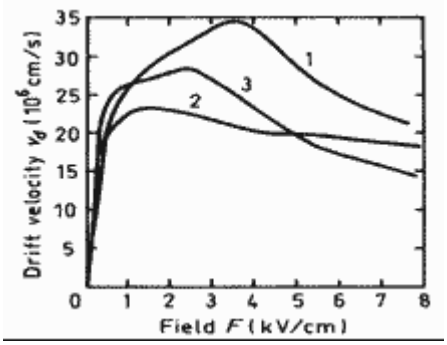

Experimental field dependences dependences of electron velocity. T=77 K.
1 - for bulk GaAs with $n_o=10^{15}$ cm^{-3}
2, 3 - for two-dimensional modulation - doped heterostructures $Al_xGa_{1-x}As/GaAs$.
2 - x=0.3;
3 - x=0.5.
(Masselink (1989)).

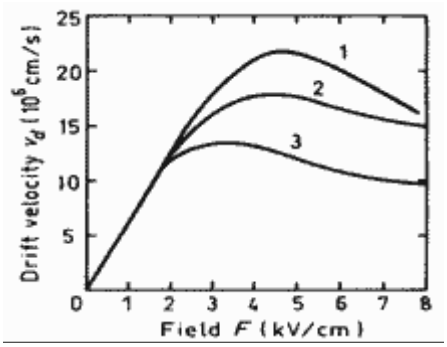

Experimental field dependences dependences of electron velocity. T=300 K.
1 - for bulk GaAs with $n_o=10^{15}$ cm^{-3}
2, 3 - for two-dimensional modulation - doped heterostructures $Al_xGa_{1-x}As/GaAs$.
2 - x=0.3;
3 - x=0.5.
(Masselink (1989)).

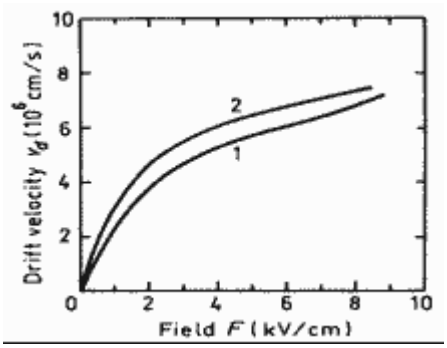

Experimental field dependences of hole velocity for two-dimensional hole gas. Single heterointerface samples. x=0.5. T=77 K.
1 - $p=3.3\cdot10^{11}$ cm^{-2}, $\mu=3300$ cm^2 Vs
2 - $p=4.2\cdot10^{11}$ cm^{-2}, $\mu=4000$ cm^2 Vs
(Masselink et al. (1987)).

$Al_x Ga_{1-x} As$

Impact Ionization

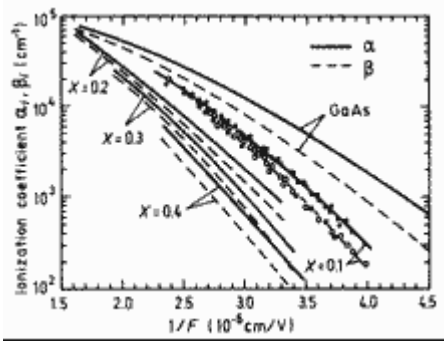

Fits to experimental values of electron and hole ionization coefficients for $Al_xGa_{1-x}As$ with x=0.1÷0.4. T=300 K.
Experimental points are shown only for x=0.1
(Robbins et al. (1988)).

Parametrizations of the electron and hole ionization coefficients. T=300 K.
(Robbins et al.(1988))

For electrons:

$$\alpha_i = \alpha_0 \exp\left[-\left(F_{n_o}/F\right)^m\right]$$

x	α_o (cm^{-1})	F_{no} (V cm^{-1})	m
0.1	$1.81\cdot10^5$	$6.31\cdot10^5$	2.0
0.2	$1.09\cdot10^6$	$1.37\cdot10^6$	1.3
0.3	$2.21\cdot10^5$	$7.64\cdot10^5$	2.0
0.4	$1.74\cdot10^7$	$3.39\cdot10^6$	1.0

For holes:

$$\beta_i = \beta_0 \exp\left[-\left(F_{p_o}/F\right)^m\right]$$

x	β_o (cm^{-1})	F_{po} (V cm^{-1})	m
0.1	$3.05\cdot10^5$	$7.22\cdot10^5$	1.9
0.2	$6.45\cdot10^5$	$1.11\cdot10^6$	1.5
0.3	$2.791\cdot10^5$	$8.47\cdot10^5$	1.9
0.4	$3.06\cdot10^6$	$2.07\cdot10^6$	1.2

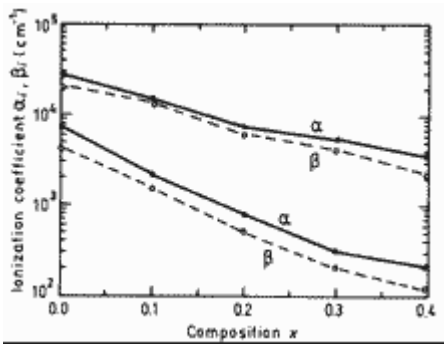

Experimental ionization coefficients versus x for electric fields
Bottom curves - $3\cdot10^5$ V/cm
Upper curves - $4\cdot10^5$ V/cm
T=300 K. *(Robbins et al. (1988))*.

Breakdown voltage and breakdown field of n-GaAs/p-$Al_{0.3}Ga_{0.7}As$ heterojunctions T=300 K.

(Hur et al. (1990))

$N_a=10^{14}$ cm^{-3}	V_i=2.8 kV	$E_i=2.8\cdot10^5$ V cm^{-1}
$N_a=10^{16}$ cm^{-3}	V_i=70 V	$E_i=4.5\cdot10^5$ V cm^{-1}

$Al_x Ga_{1-x} As$

Recombination Parameter

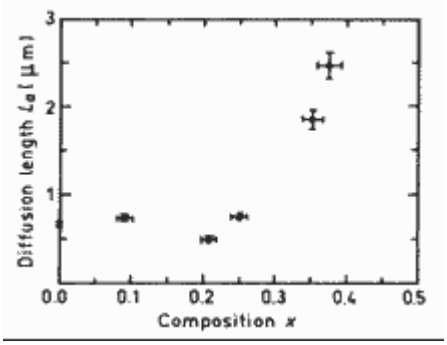

Ambipolar diffusion length at a carrier density of $10^{17} \div 10^{18}$ cm^{-3} versus x. T= 300K.
Determination was accomplished by catodoluminescene technique *(Zarem et al. (1989))*.

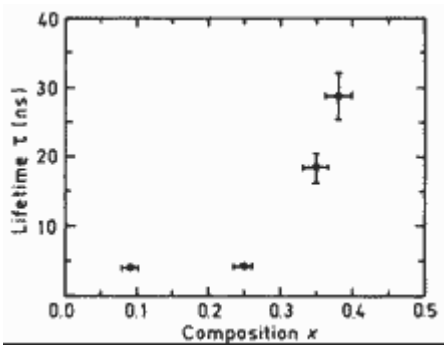

Carrier lifetimes at carrier density of ~$3 \cdot 10^{18}$ cm^{-3} (high injection level) versus versus x. T= 300K.
Determination was accomplished by photoluminiscence decay signal technique.
(Zarem et al. (1989)).

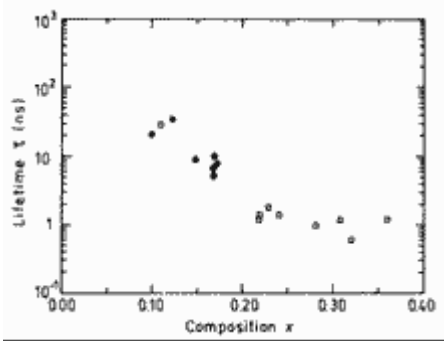

Hole lifetime versus x for n-$Al_xGa_{1-x}As$
N_d-N_a~$10^{15} \div 10^{16}$ cm^{-3}. T= 300K.
(Timmons et al. (1988)).

Radiative recombination coefficient at 300K ~$1.8 \cdot 10^{-10}$ cm^3/s

Auger coefficient at T=300 K *(Timmons (1985))*.

x	C_n (cm^6/s)	C_p (cm^6/s)
0	$1.9 \cdot 10^{-31}$	$12 \cdot 10^{-31}$
0.1	$1.2 \cdot 10^{-31}$	$8.5 \cdot 10^{-31}$
0.2	$0.7 \cdot 10^{-31}$	$6.1 \cdot 10^{-31}$

Cn (for n - doped samples)
Cp (for p - doped samples)

Surface and interface recombination velocities in GaAs and $Al_xGa_{x-1}As$
***(Pavesi and Guzzi (1994))*.**

x	S (cm/s)

0	$4 \cdot 10^5$	free surface
0	45	interface between GaAs/$Al_{0.3}Ga_{0.7}As$
0	450±100	interface between GaAs/$Al_{0.5}Ga_{0.5}As$ p-type
0.08	$4 \cdot 10^5$	free surface
0.08÷0.18	$\sim 3 \cdot 10^4$	interface between $Al_xGa_{1-x}As/Al_{0.88}Ga_{0.22}As$ undoped
0.28	4200	interface between $Al_xGa_{1-x}As/Al_{0.5}Ga_{0.5}As$ undoped

$Al_x Ga_{1-x} As$

Optical properties

Infrared refractive index (300 K)
$n=3.3-0.53x+0.09x^2$

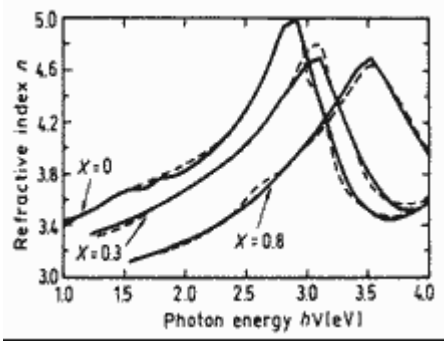

Refractive index *n* versus photon energy for three values of *x*.
Solid lines are calculated.
Dashed lines are experimental data. 300 K.
(Jenkins (1990)).

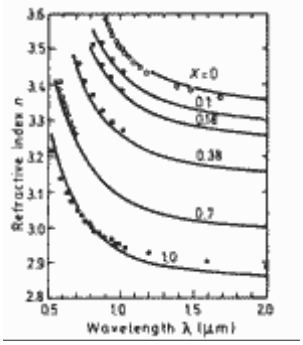

Refractive index *n* versus wavelength for different values of *x*. 300 K.
(Pikhtin and Yas'kov (1980)).

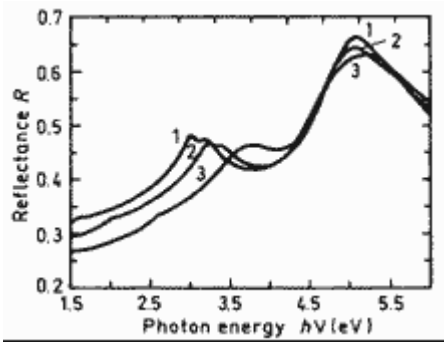

Normal incidence reflectivity versus photon energy. 300 K.
1 x~0.1,
2 x~0.42,
3 x~0.8.
(Aspnes et al. (1986))).

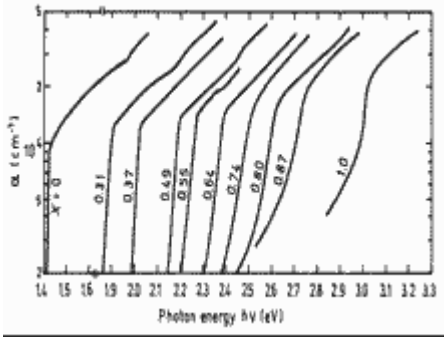

Intrinsic absorption coefficient near the intrinsic absorption edge for different values of *x*. 300 K.
(Monemar et al. (1976)).

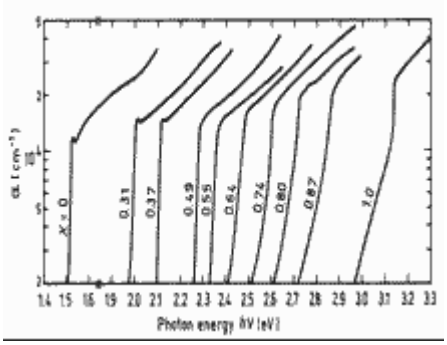

Intrinsic absorption coefficient near the intrinsic absorption edge for different values of *x*. 4 K.
(Monemar et al. (1976)).

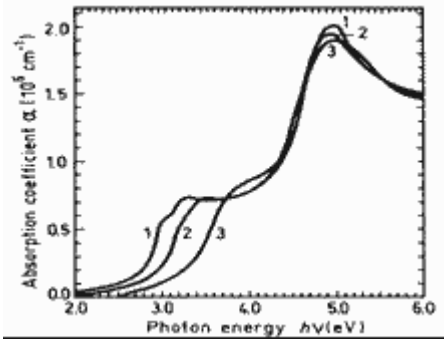

The absorption coefficient versus photon energy. 300 K.
1 x~0.1,
2 x~0.42,
3 x~0.8.
(Aspnes et al. (1986))).

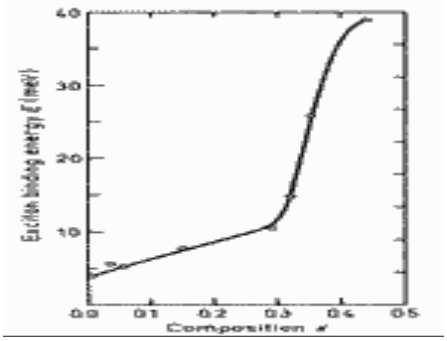

Free exciton binding energy versus Al mole fraction *x*.
(Pearah et al. (1985)).

$Al_x Ga_{1-x} As$

Thermal properties

Bulk modulus	$(7.55+0.26x)\cdot 10^{11}$ dyn cm^{-2}
Melting point	$1240-58x+558x^2$ °C *(solidus curve)* $12401082x+582x^2$ °C *(liquidus curve)*
Specific heat	$0.33+0.12x$ J g^{-1}°C^{-1}
Thermal conductivity	$0.55-2.12x+2.48x^2$ W cm^{-1} °C^{-1}
Thermal diffusivity	$0.31-1.23x+1.46^2$ $cm^2 s^{-1}$
Thermal expansion, linear	$(5.73-0.53x)\cdot 10^{-6}$ °C^{-1}

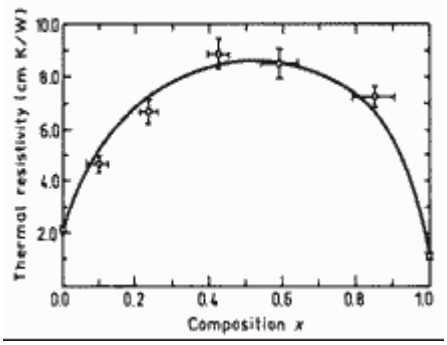

Thermal resistivity versus Al fraction x. 300K.
Solid curve is a theoretical fit to the experimental data.
(Afromowitz [1973]).

Approximate formula for the lattice thermal resistivity:

$R_{th}=2.27+28.83x-30x^2$ cm··W^{-1}

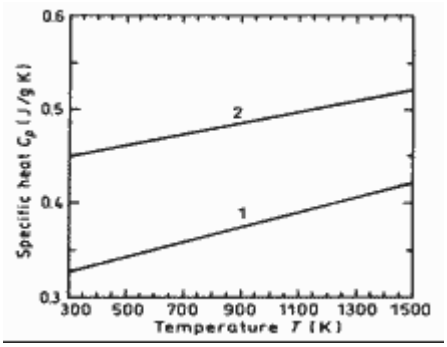

Temperature dependences of specific heat at constant pressure.
1. GaAs *(Lichter and Sommelet [1969])*;
2. AlAs *(Barin et al. [1977])*.

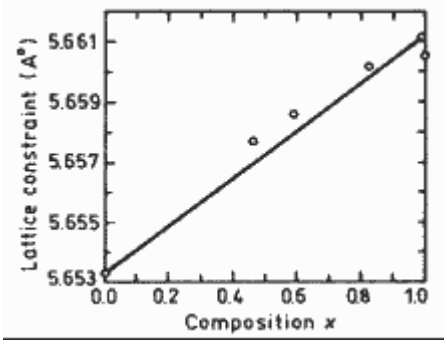

Lattice constant as a function of x. 300K.
(Adachi [1985]).

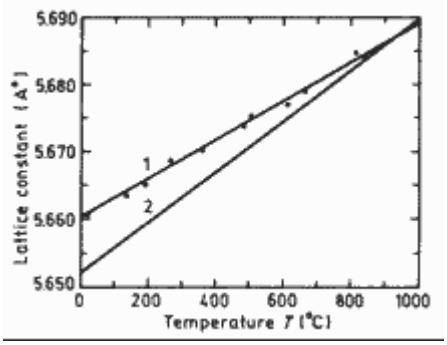

Lattice constants versus temperature.
1. AlAs;
2. GaAs;
(Ettenberg and Paff [1970]).

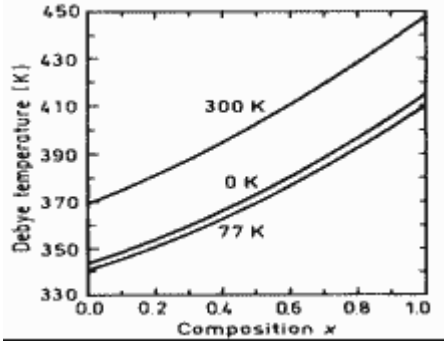

Debye temperature as a function of x for three different temperatures.
(Adachi [1985]).

Melting point:

T_m=1240-58x+558x^2 °C - *(solidus curve)*
T_m=1240+1082x-582x^2 °C *(liquidus curve)*

$Al_x Ga_{1-x} As$

Mechanical properties, elastic constants, lattice vibrations

Basic Parameter

Bulk modulus	$(7.55+0.26x)\cdot 10^{11}$ dyn cm^{-2}
Density	5.32-1.56x g cm^{-3}
Hardness on the Mohs scale	~ 5
Cleavage plane	{110}
Piezoelectric constant	e_{14}= -0.16-0.065x C m^{-2}

Elastic constants 300 K.

C_{11}=$(11.88+0.14x)\cdot 10^{11}$ dyn/cm^2
C_{12}=$(5.38+0.32x)\cdot 10^{11}$ dyn/cm^2
C_{44}=$(5.94-0.05x)\cdot 10^{11}$ dyn/cm^2
(Adachi [1985]).

For T = 300 K

Bulk modulus (compressibility^{-1})	B_s= =$(7.55+0.26x)\cdot 10^{11}$dyn/cm^2
Anizotropy factor	A=0.55-0.01x
Shear modulus	C'=$(3.25-0.09x)\cdot 10^{11}$dyn/cm^2
[100] Young's modulus	Y_o=$(8.53-0.18x)\cdot 10^{11}$dyn/cm^2
[100] Poisson ratio	σ_o=(0.31+0.1x)

(Adachi [1985]).

Acoustic Wave Speeds

Wave propagation Direction	Wave character	Expression for wave speed	Wave speed (in units of 10^5 cm/s)
[100]	V_L	$(C_{11}/\rho)^{1/2}$	$4.73+0.68x+0.24x^2$
	V_T	$(C_{44}/\rho)^{1/2}$	$3.34+0.46x+0.16x^2$
[110]	V_l	$[(C_{11}+C_{12}+2C_{44})/2\rho]^{1/2}$	$5.24+0.78x+0.24x^2$
	$V_{t\|\|}$	$V_{t\|\|}=V_T=(C_{44}/\rho)^{1/2}$	$3.34+0.46x+0.16x^2$
	$V_{t\perp}$	$[(C_{11}-C_{12})/2\rho]^{1/2}$	$2.47+0.33x+0.10x^2$

[111]	V_l'	$[(C_{11}+2C_{12}+4C_{44})/3\rho]^{1/2}$	$5.40+0.79x+0.26x^2$
	V_t'	$[(C_{11}-C_{12}+C_{44})/3\rho]^{1/2}$	$2.79+0.38x+0.12x^2$

Phonon frequencies

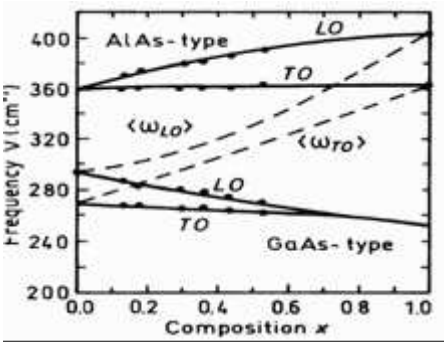

Optical phonon energy as a function of x.
The compositional dependence of the effective phonon energy $<\omega_{L0}>$ and $<\omega_{T0}>$ are shown by the dashed lines.
(Adachi [1985]).

$Al_x Ga_{1-x} As$

References:

- Goldberg Yu.A. *Handbook Series on Semiconductor Parameters*, **vol.2**, M. Levinshtein, S. Rumyantsev and M. Shur, ed., World Scientific, London, 1999, pp. 1-36.

- S.Adachi, *J. Appl. Phys.*, **58**, no.3, pp.R1-R29 (1985).
- M.A.Afromowitz, *J. Appl. Phys.*, **44**, no.3, pp.1292-1294 (1973).
- D.E.Aspnes, *Phys. Rev.*, **B14**, no.12, pp.5331-5343 (1976).
- D.E.Aspnes, S.M.Kelso, R.A.Logan, R.Bhat., *J.Appl.Phys.*, **60**, no.2, pp.754-767 (1986).
- I. Barin, O. Knacke, O. Kubaschewski, *Thermochemical Properties of Inorganic Substances*, Springer, Berlin-Heidelberg-New York, 1977.
- K. Brennan, K. Hess, *J. Appl. Phys.*, **59**, no.3, pp.964-966 (1986).
- T. J. Drummond, W. Kopp, R. Fischer, H. Morkoc, *J. Appl. Phys.*, **53**, no.2, pp.1028-1029 (1982).
- M. Ettenberg, R. J. Paff, *J. Appl. Phys.*, **41**, no.10, pp.3926-3927 (1970).
- M.A. Haase, M.A. Emanuel, S.C. Smith, J.J. Coleman, and G.E. Stillman, *Appl. Phys. Lett.*, **50**, no.7, pp.404-406 (1987).
- J.J. Harris, C.T. Foxon, K.W.J. Barhkam, D.E. Lacklison, J. Hewett, C. White, *J. Appl. Phys.*, **61**, no.3, pp.1219-1221 (1987)
- S. Hava, M. Auslender, *J. Appl. Phys.*, **73**, no.11, pp.7431-7434 (1993).
- R. Heilman, G. Oelgart, *Semicond. Sci. Technol.*, **5**, no 10, pp.1040-1045 (1990).
- G. Hill, and P.N.Robson, *J.de Physique*, **42**, Colloque no.7, Suppl. au no.10, pp.C7-335 - C7-341 (1981).
- J.H. Hur, C.W. Myles, M.A. Gundersen, *J. Appl. Phys.*, 67, no.11, pp.6917-6923 (1990).
- S.C.Jain, J.M.McGregor, D.J.Roulston, *J. Appl. Phys.*, **68**, no.7, pp.3747-3749 (1990).
- S.C.Jain, and D.J.Roulston, *Solid State Electron*, **34**, no.5, pp.453-465 (1991).
- D.W.Jenkins, *J. Appl. Phys.*, **68**, no.4, pp.1848-1853 (1990).
- K.Kaneko, M.Ayabe, and N.Watanabe, *in GaAs and Related Compounds* (Inst.of Phys., London, Ser . 33a, 1977), pp.216-226.
- J.M.Langer, H.Heinrich, *Physica B*, **134** no.1-3, pp.444-450 (1985).
- B.D.Lichter and P.Sommelet, *Trans. Metall. Soc., AIME*, **245**, pp.1021-1027 (1969).
- D.Lippens, O.Vanbesien, *in GaAs and Related Compounds* (Inst.of Phys., Bristol and Philadelphia, Ser. 91, 1987), pp.757-760.
- W.C.Liu, *J. Material Sci.*, **25**, no.3, pp.1765-1772 (1990).
- D.C.Look, D.K.Lorance, J.R.Sizelove, C.E.Stutz, K.R.Evans, D.W.Whitson, *J. Appl. Phys.*, **71**, no.1, pp.260-266 (1992).
- W.T.Masselink, *Semicond. Sci. Technol.*, **4**, no.7, pp.503-512 (1989).
- W.T.Masselink,N.Braslau, D.LaTulipe, W.I.Wang, S.L.Wright, *in GaAs and Related Compounds* (Inst. of Phys.,Bristol and Philadephia, Ser. 91, 1987), pp.665-668.
- B.Monemar, K.K. Shih, and G.D.Pettit, *J. Appl. Phys.*, **47**, no.6, pp.2604-2613 (1976).
- M.de Murcia, D.Gasquet, E.Richard, P.Wolff, J.Zimmermann, J.Vanbremeersch, *AIP Conf. Proc. 285* (Noise in Physical Systems and 1/f fluctuations, St.Louis, USA, 1993), pp.27-30 .
- L. Pavesi, M.Guzzi, *J. Appl. Phys.*, **75**, no.10, pp.4779-4842 (1994).
- P.J.Pearah, W.T.Masselink, J.Klem, T.Henderson, H.Morcoc, C.W.Litton, D.C.Reynolds, *Phys.Rev.*, **B32**, no.6, pp.3857-3862 (1985).
- L.Pfeiffer, K.W.West, H.L.Stormer, K.W.Baldwin, *Appl. Phys. Lett.*, **55**, no.18, pp.1888-1890 (1989).
- A.N.Pikhtin, A.D.Yas'kov, *Sov.Phys.Semicond.*, **14**, no.4, pp.389-392 (1980).
- V.M.Robbins, S.C.Smith, G.E.Stillman, *Appl. Phys. Lett*, **52**, no.4, pp.296-298 (1988).
- A.K. Saxena, *J. Phys. C.*, **13**, no.23, pp. 4323-4334 (1980).
- A. K. Saxena, *Solid St. Comm.*, **39**, no.7, pp. 839-842 (1981).
- A.K.Saxena, *Phys. Rev.*, **B24**, no.6, pp. 3295-3302 (1981).
- M.Shur, *Physics of Semiconductor Devices*, Prentice Hall, 1990.
- A.J. Spring Thorpe, T.D. King, A.J. Beck, *J. Electron. Mater.*, **4**, no.1, pp. 101-118 (1975).
- G.E.Stillman, C.M. Wolfe, and J.O. Dimmock, *J. Phys. Chem. Solids*, **31**, no. 6, pp. 1199-1204 (1970).
- M.Takeshima, *J. Appl. Phys.*, 58, no.10, p.3846 (1985)

- M.L. Timmons, J.A. Hutchby, R.K. Ahrenkiel, D.J. Dunlavy, *in GaAs and Related Compounds* (Inst. of Phys., Bristol and Philadelphia, Ser. 96, 1988), pp. 289-294.
- W.Walukiewicz, *J. Appl. Phys.*, **59**, no.10, pp.3577-3579 (1986).
- Z.Wilamowski, J.Kossut, W.Jantsch, and G.Ostermayer, *Semicond.Sci.Technol.*, **6**, no.10B, pp.B38-B46 (1991).
- J.J.Yang, W.I.Simpson, L.A.Moudy, *in GaAs and Related Compounds* (Inst. of Phys., Bristol and London, Ser.63, 1981), pp.107-112.
- J.J.Yang, L.A.Moudy , W.I.Simpson, *Appl. Phys. Lett.*, **40**, no. 3, pp.244-246 (1982).
- H.A.Zarem, J.A.Lebens, K.B.Nordstrom, P.C.Sercel, S.Sanders, L.E.Eng, A.Yariv, K.J.Vahala, *Appl.Phys.Lett.*, **55**, no. 25, pp.2622-2624 (1989).

3.2 Bildvergrößerungen

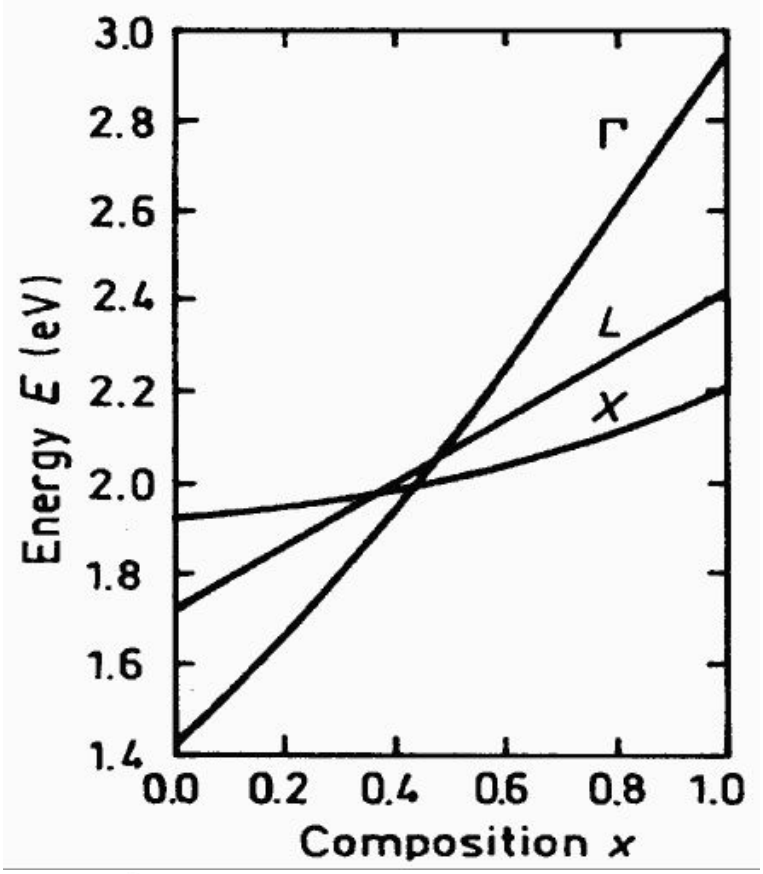

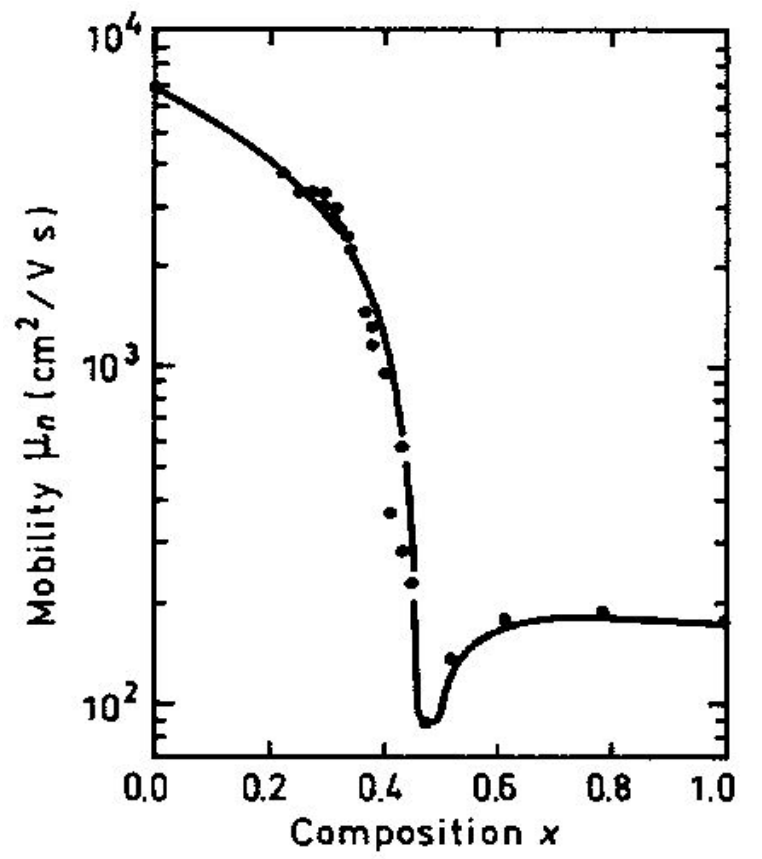

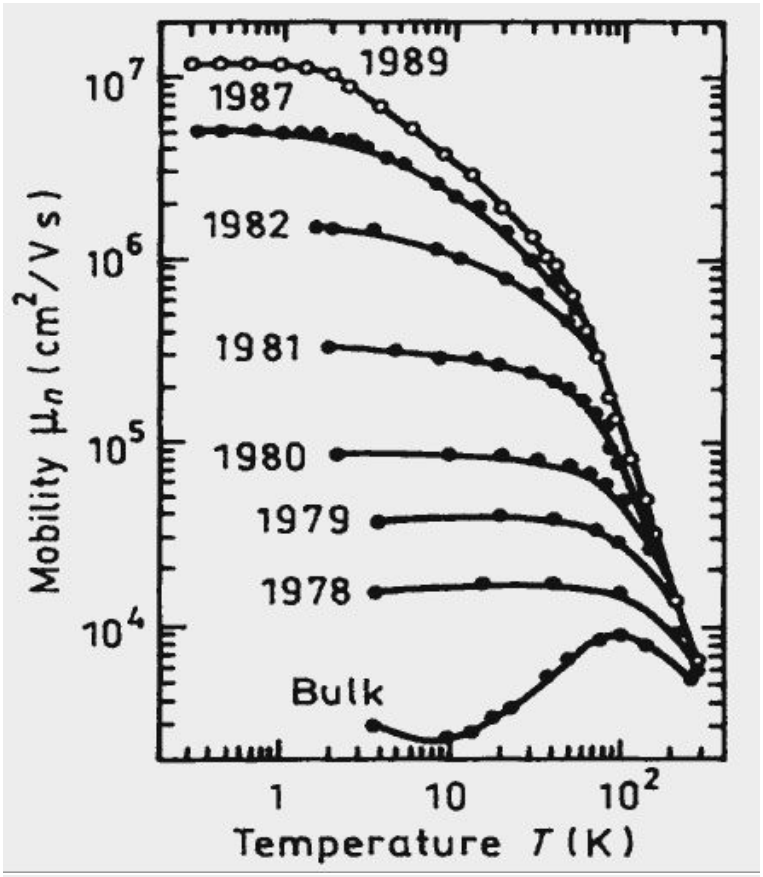
1989
1987
1982
1981
1980
1979
1978
Bulk
10^7
10^6
10^5
10^4
Mobility μ_n ($cm^2/V\,s$)
1
10
10^2
Temperature T (K)

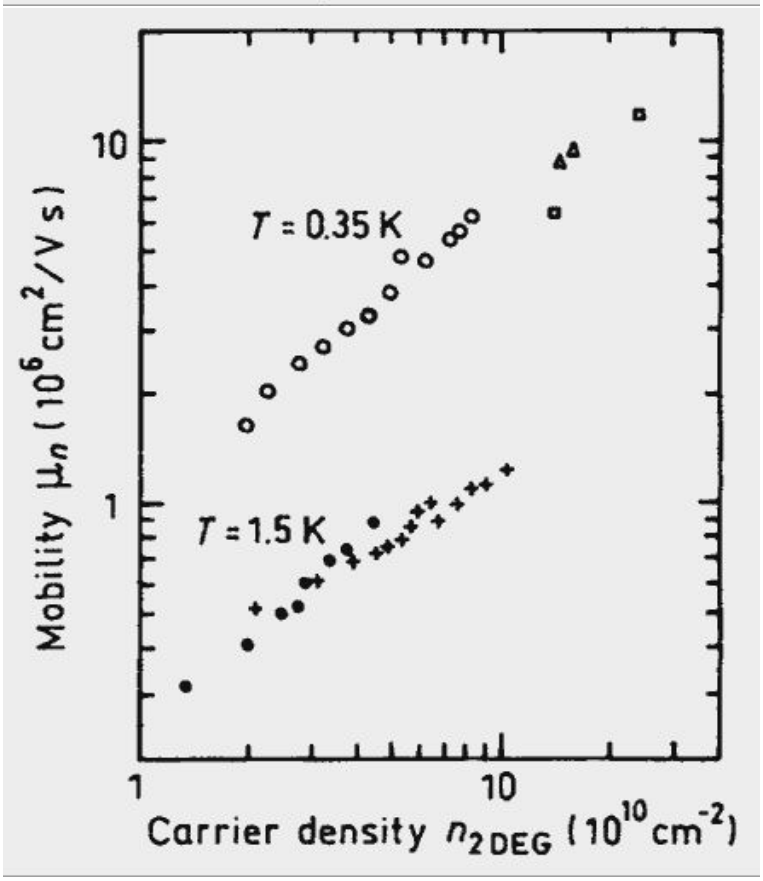
T = 0.35 K
T = 1.5 K
10
1
Mobility μ_n ($10^6 cm^2/V\,s$)
1
10
Carrier density n_{2DEG} ($10^{10} cm^{-2}$)

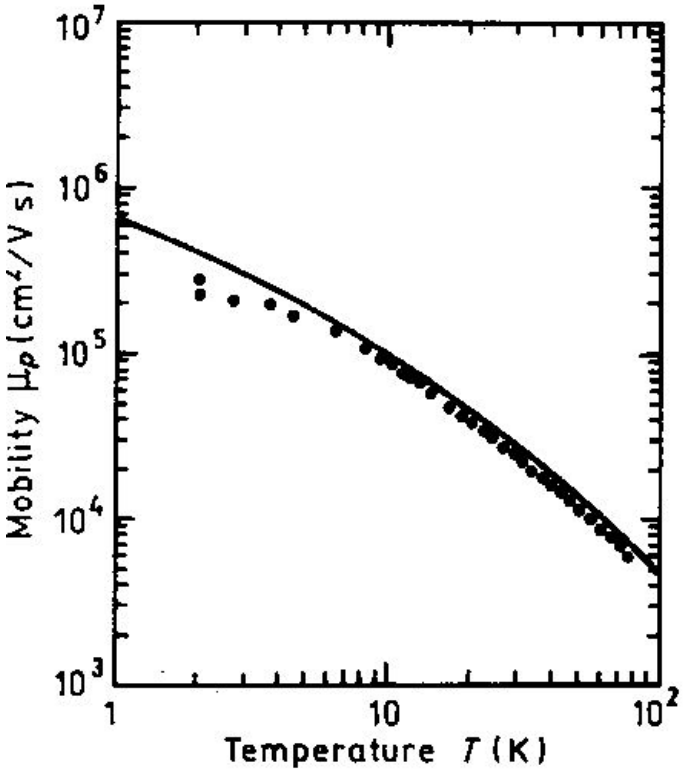
Mobility μ_p (cm²/V s)
10^7
10^6
10^5
10^4
10^3
1
10
10^2
Temperature T (K)

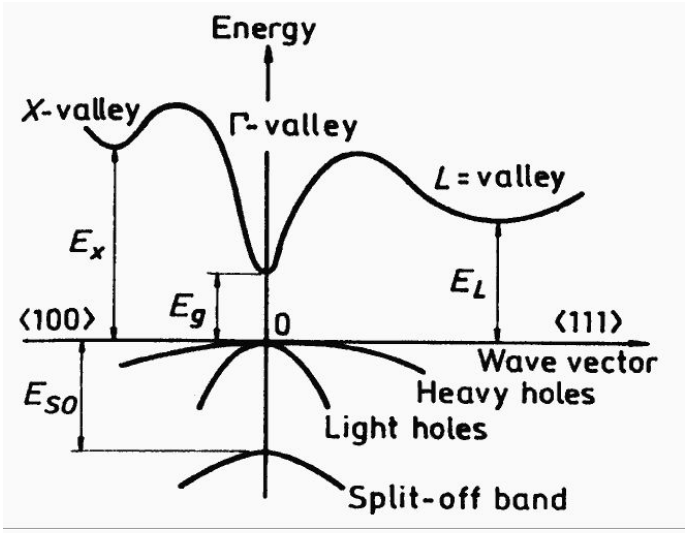
Energy
X-valley
Γ-valley
L = valley
E_x
E_g
E_L
⟨100⟩
0
⟨111⟩
Wave vector
E_{so}
Heavy holes
Light holes
Split-off band

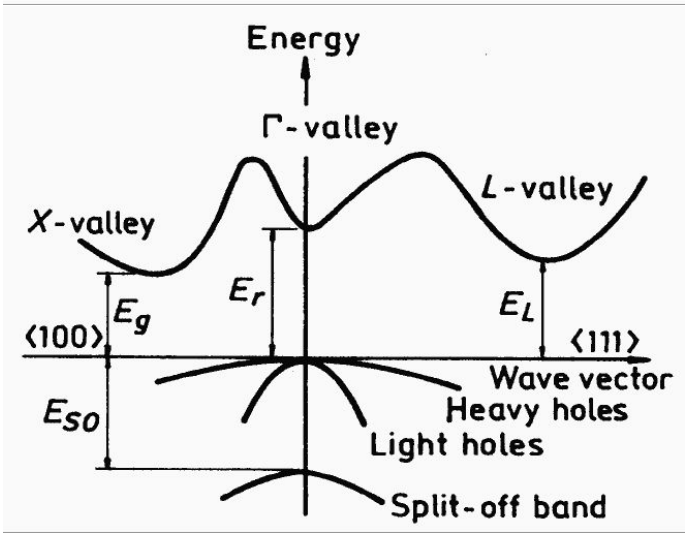
Energy
Γ-valley
L-valley
X-valley
E_r
E_g
E_L
⟨100⟩
⟨111⟩
Wave vector
E_{so}
Heavy holes
Light holes
Split-off band

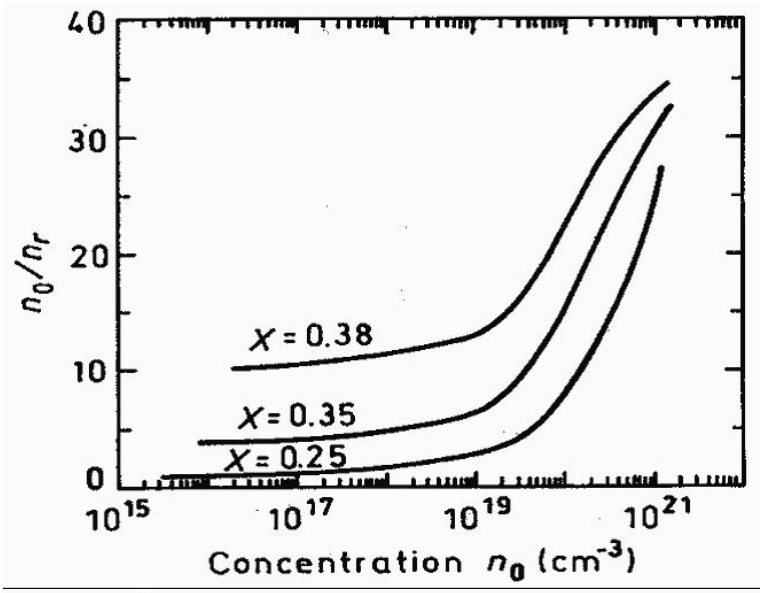
40
30
20
10
0
n_0/n_r
X = 0.38
X = 0.35
X = 0.25
10^{15}
10^{17}
10^{19}
10^{21}
Concentration n_0 (cm^{-3})

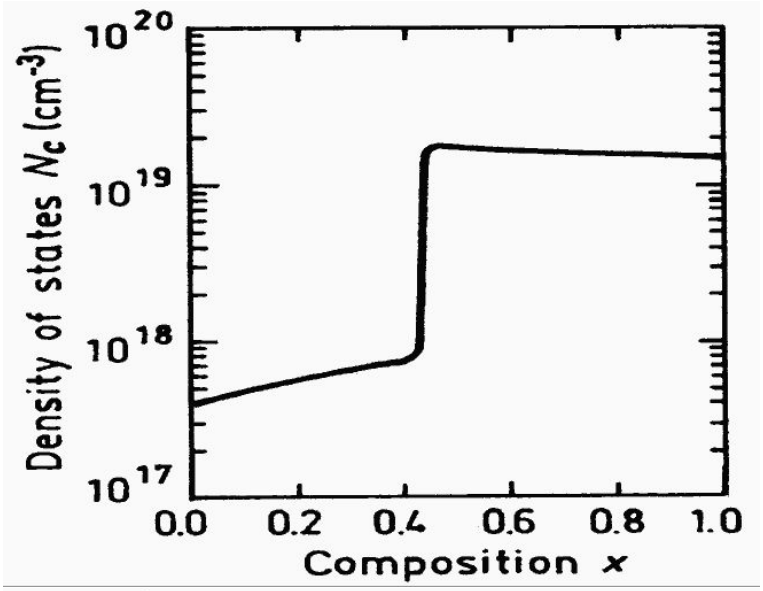
10^{20}
10^{19}
10^{18}
10^{17}
Density of states N_c (cm^{-3})
0.0
0.2
0.4
0.6
0.8
1.0
Composition x

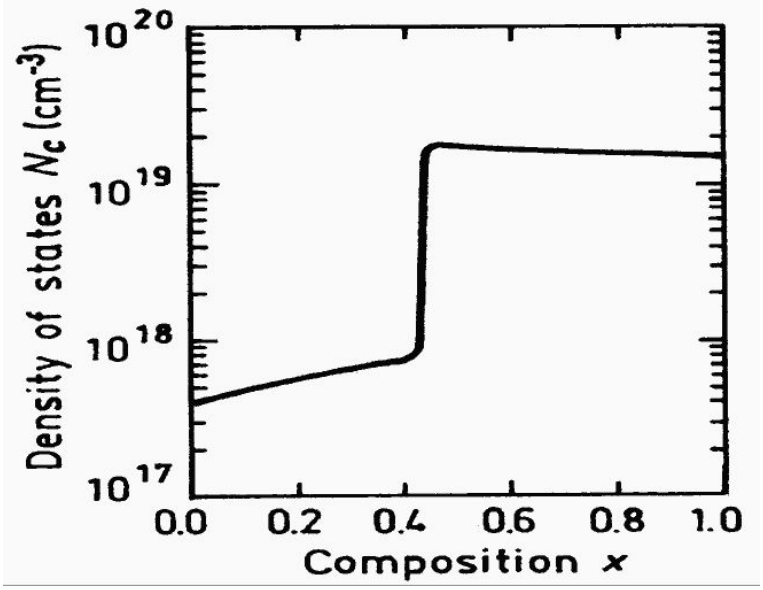
10^{20}
10^{19}
10^{18}
10^{17}
Density of states N_c (cm^{-3})
0.0
0.2
0.4
0.6
0.8
1.0
Composition x

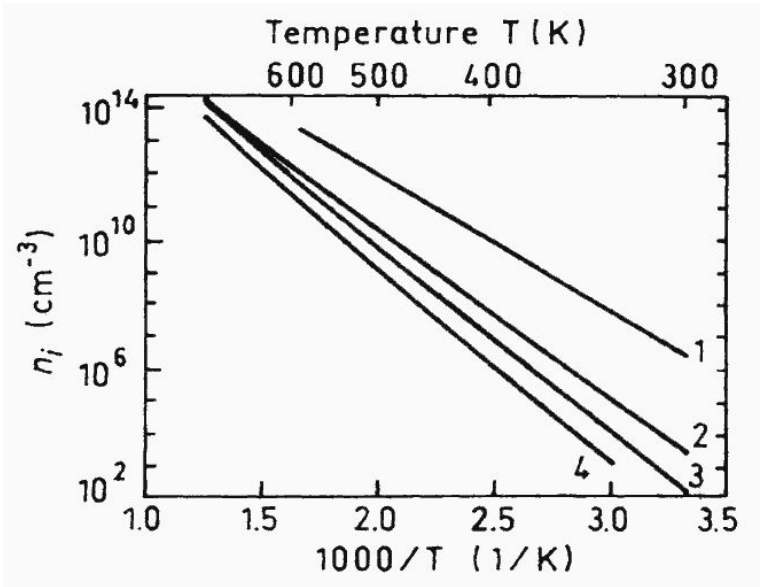
Temperature T (K)
600 500 400 300
10^{14}
10^{10}
10^{6}
10^{2}
n_i (cm^{-3})
1
2
3
4
1.0 1.5 2.0 2.5 3.0 3.5
1000/T (1/K)

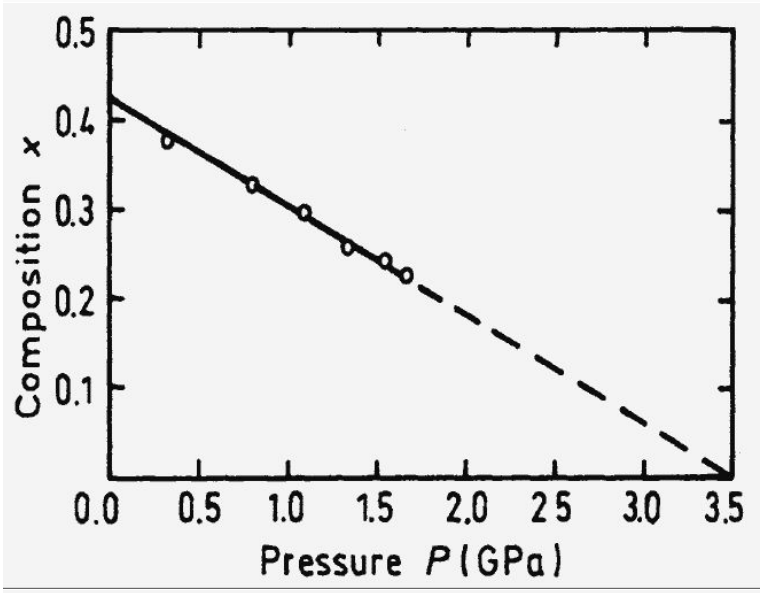
0.5
0.4
0.3
0.2
0.1
Composition x
0.0 0.5 1.0 1.5 2.0 2.5 3.0 3.5
Pressure P (GPa)

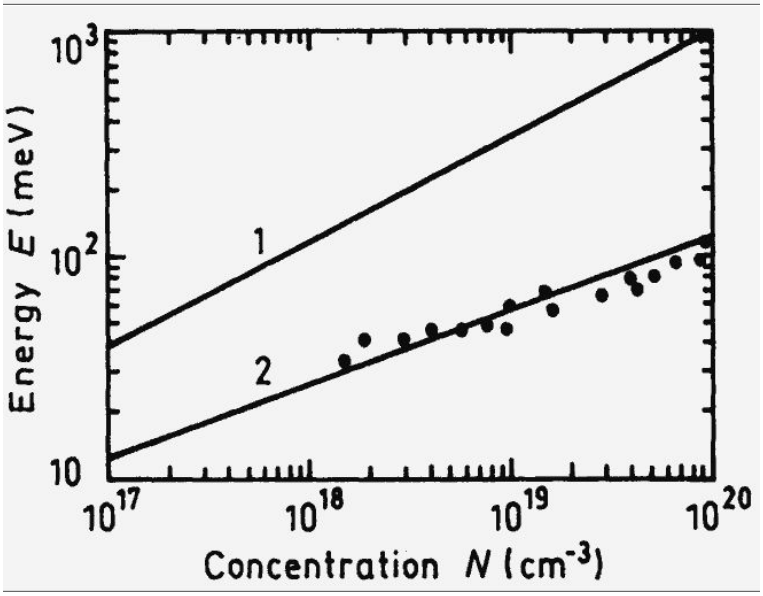
10^{3}
10^{2}
10
Energy E (meV)
1
2
10^{17} 10^{18} 10^{19} 10^{20}
Concentration N (cm^{-3})

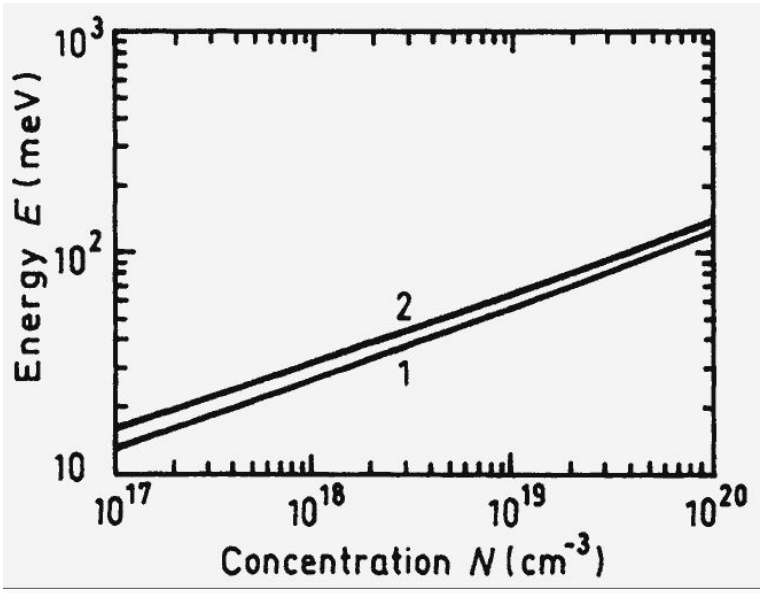
Energy E (meV)
10^3
10^2
10
2
1
10^17
10^18
10^19
10^20
Concentration N (cm^-3)

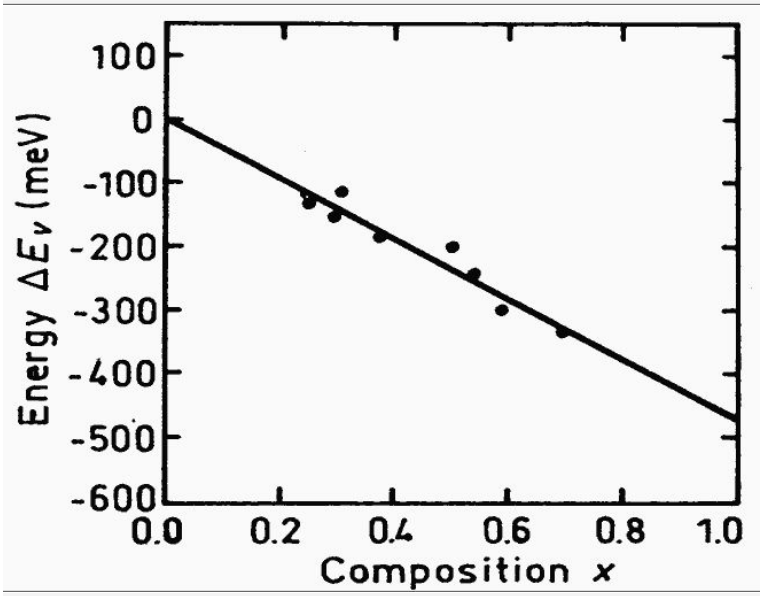
Energy ΔE_v (meV)
100
0
-100
-200
-300
-400
-500
-600
0.0
0.2
0.4
0.6
0.8
1.0
Composition x

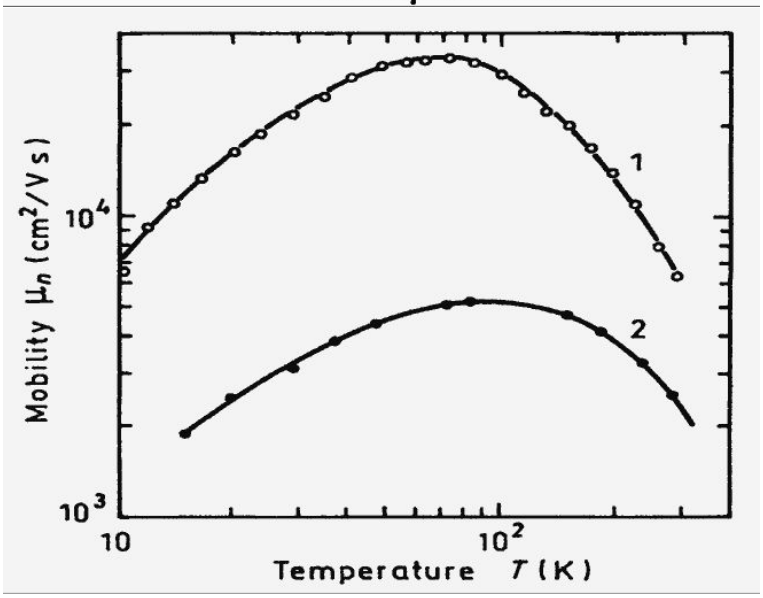
Mobility μ_n (cm^2/Vs)
10^4
10^3
1
2
10
10^2
Temperature T (K)

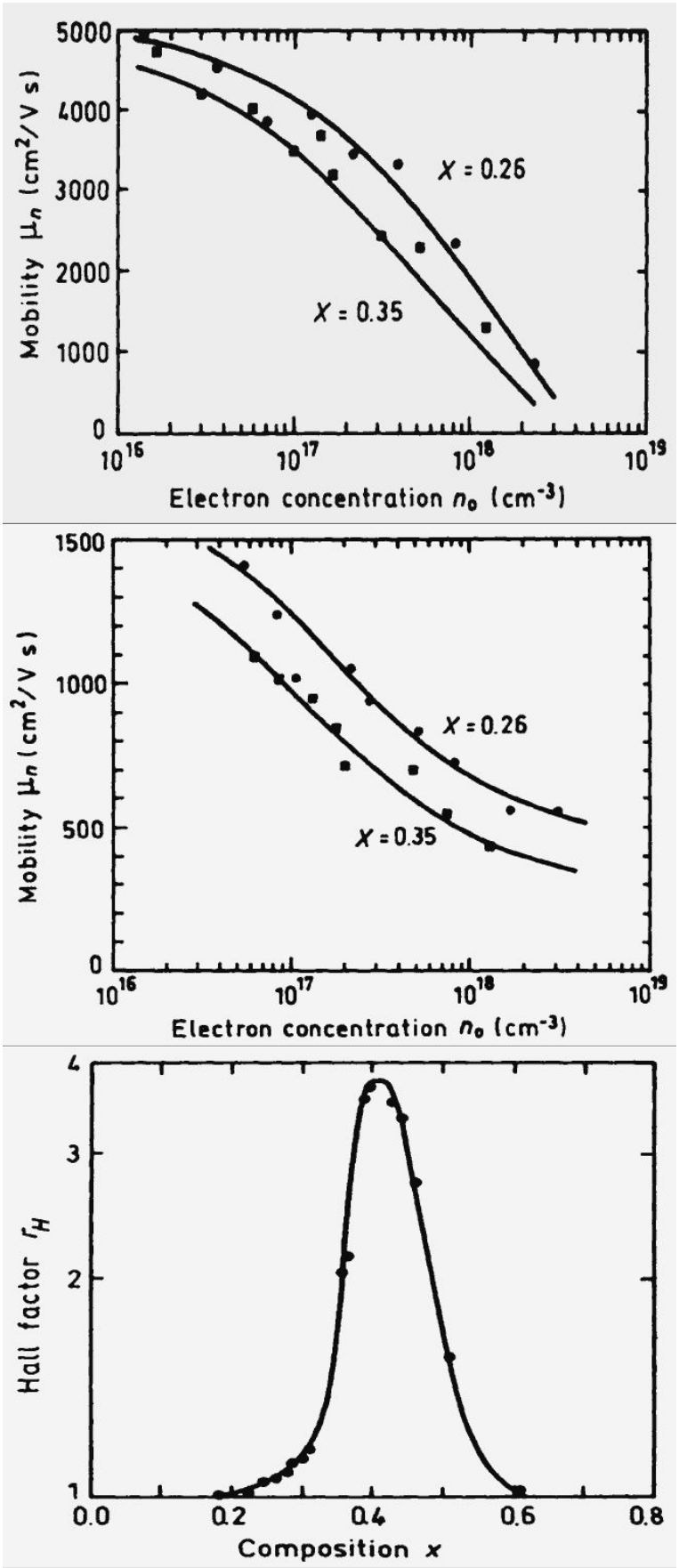
5000
4000
3000
2000
1000
0
Mobility μ_n (cm²/V s)
X = 0.26
X = 0.35
10^{16}
10^{17}
10^{18}
10^{19}
Electron concentration n_0 (cm^{-3})
1500
1000
500
0
Mobility μ_n (cm²/V s)
X = 0.26
X = 0.35
10^{16}
10^{17}
10^{18}
10^{19}
Electron concentration n_0 (cm^{-3})
4
3
2
1
Hall factor r_H
0.0
0.2
0.4
0.6
0.8
Composition x

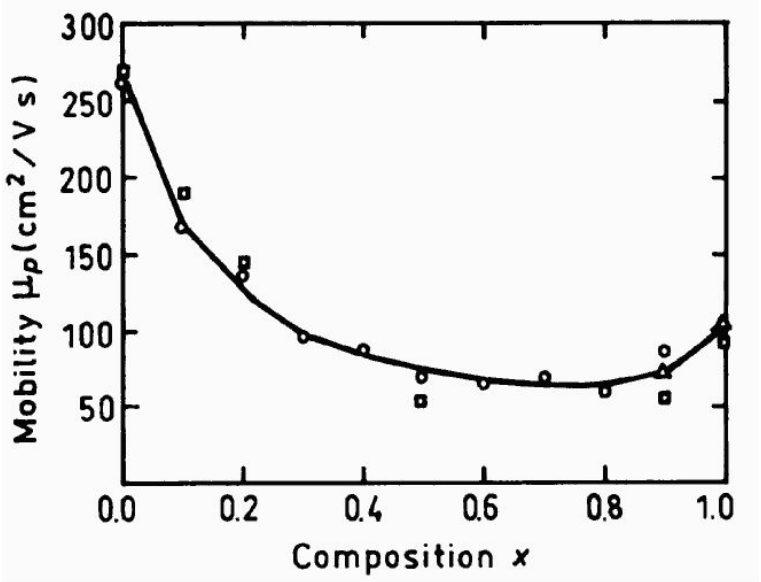
Mobility μ_p (cm^2/V s)
300
250
200
150
100
50
0.0
0.2
0.4
0.6
0.8
1.0
Composition x

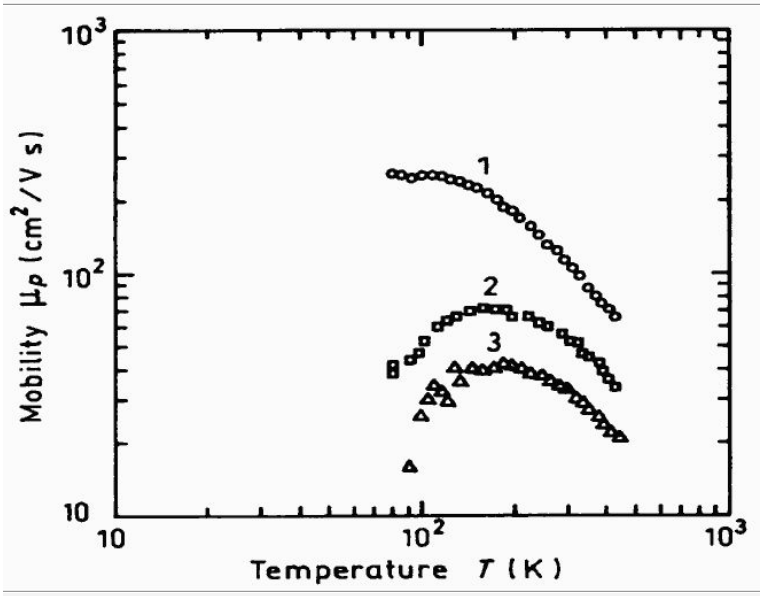
Mobility μ_p (cm^2/V s)
10^3
10^2
10
1
2
3
10
10^2
10^3
Temperature T (K)

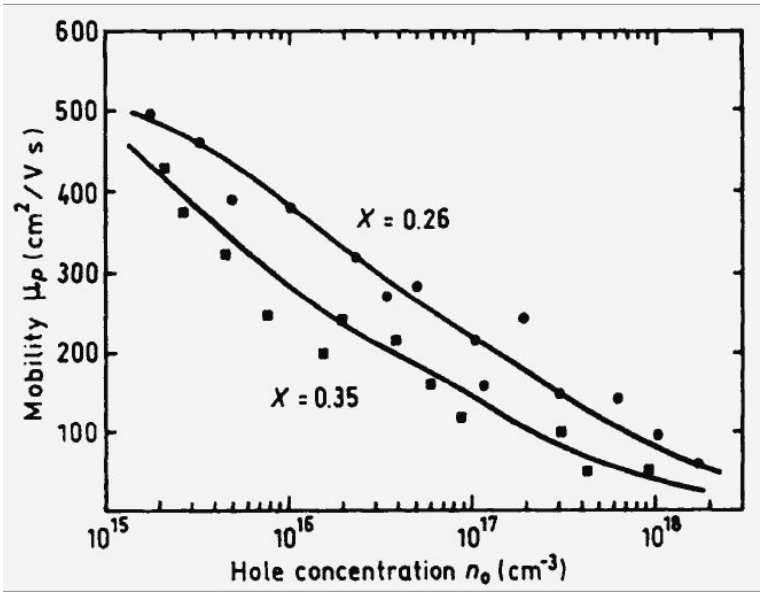
Mobility μ_p (cm^2/V s)
600
500
400
300
200
100
X = 0.26
X = 0.35
10^{15}
10^{16}
10^{17}
10^{18}
Hole concentration n_0 (cm^{-3})

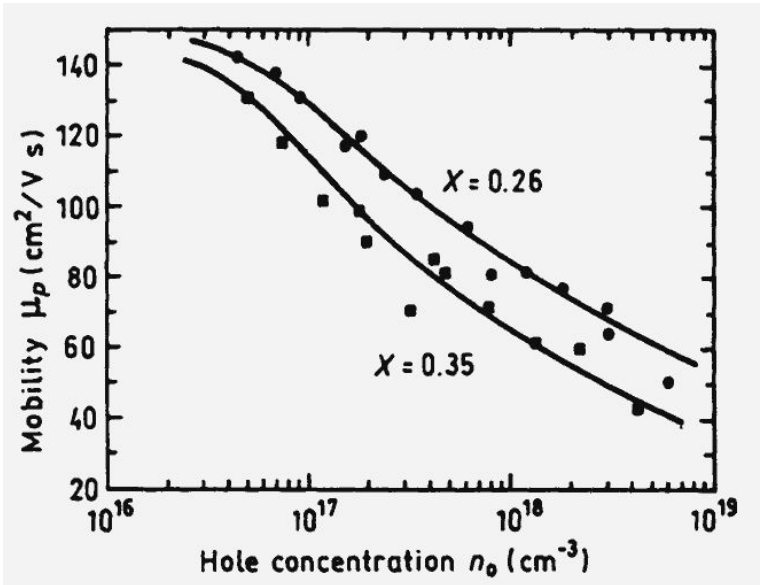
Mobility μ_p (cm^2/V s)
140
120
100
80
60
40
20
10^{16}
10^{17}
10^{18}
10^{19}
Hole concentration n_o (cm^{-3})
X = 0.26
X = 0.35

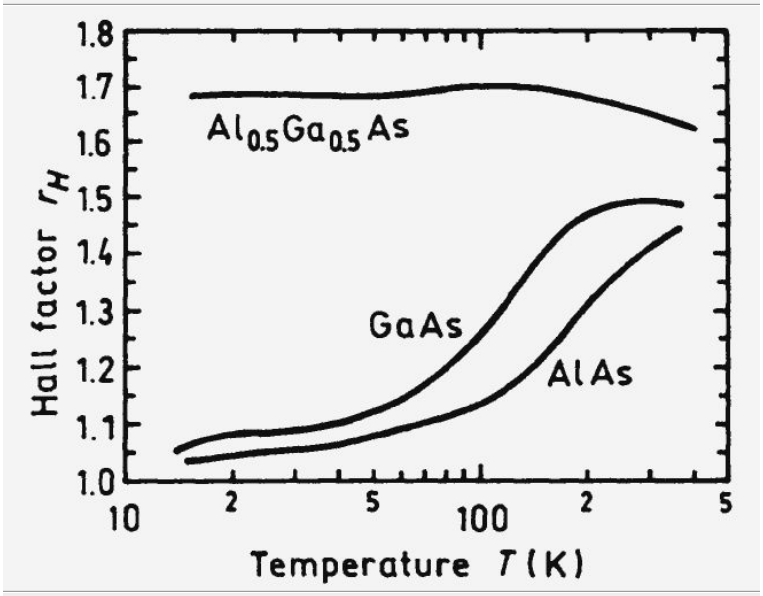
Hall factor r_H
1.8
1.7
1.6
1.5
1.4
1.3
1.2
1.1
1.0
10
2
5
100
2
5
Temperature T (K)
$Al_{0.5}Ga_{0.5}As$
GaAs
AlAs

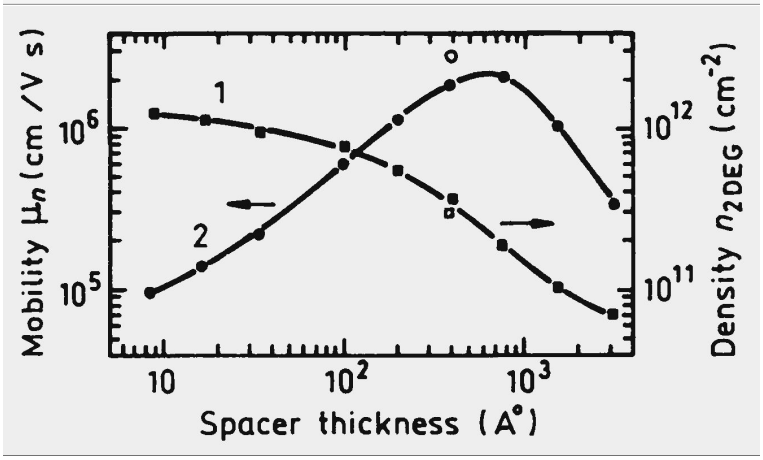
Mobility μ_n (cm /V s)
10^6
10^5
Density n_{2DEG} (cm^{-2})
10^{12}
10^{11}
10
10^2
10^3
Spacer thickness (A°)
1
2

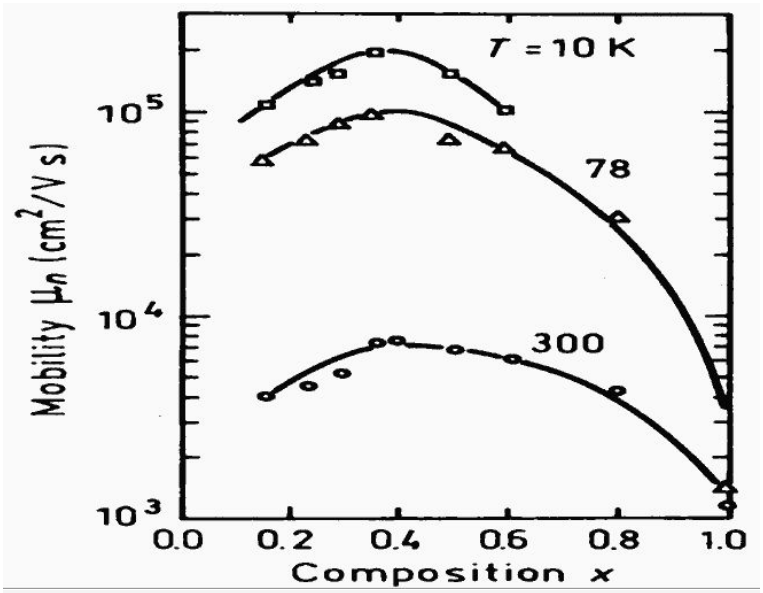
T = 10 K
78
300
Mobility μ_n (cm^2/V s)
10^5
10^4
10^3
0.0
0.2
0.4
0.6
0.8
1.0
Composition x

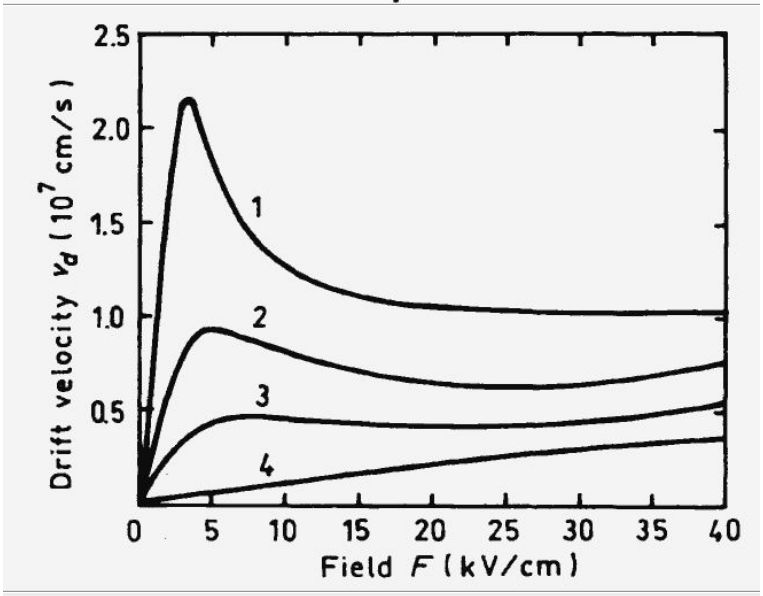
Drift velocity v_d (10^7 cm/s)
2.5
2.0
1.5
1.0
0.5
1
2
3
4
0
5
10
15
20
25
30
35
40
Field F (kV/cm)

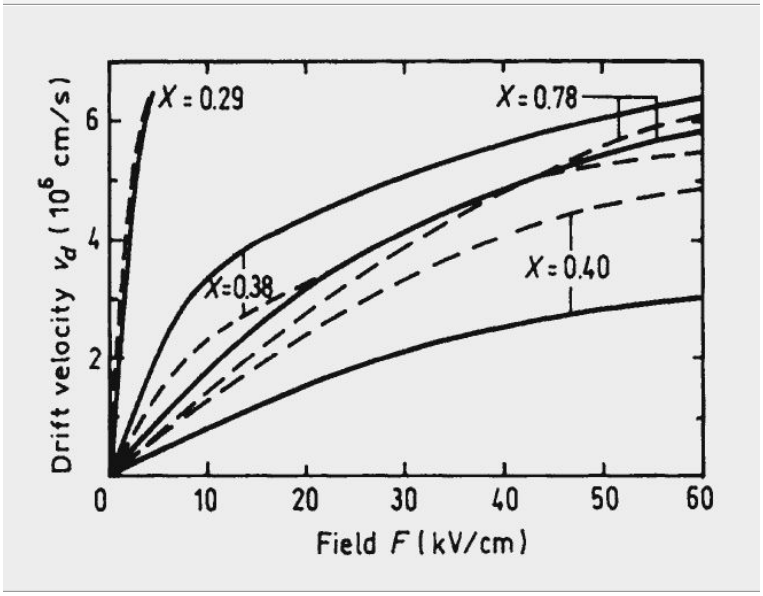
Drift velocity v_d (10^6 cm/s)
6
4
2
X = 0.29
X = 0.78
X = 0.38
X = 0.40
0
10
20
30
40
50
60
Field F (kV/cm)

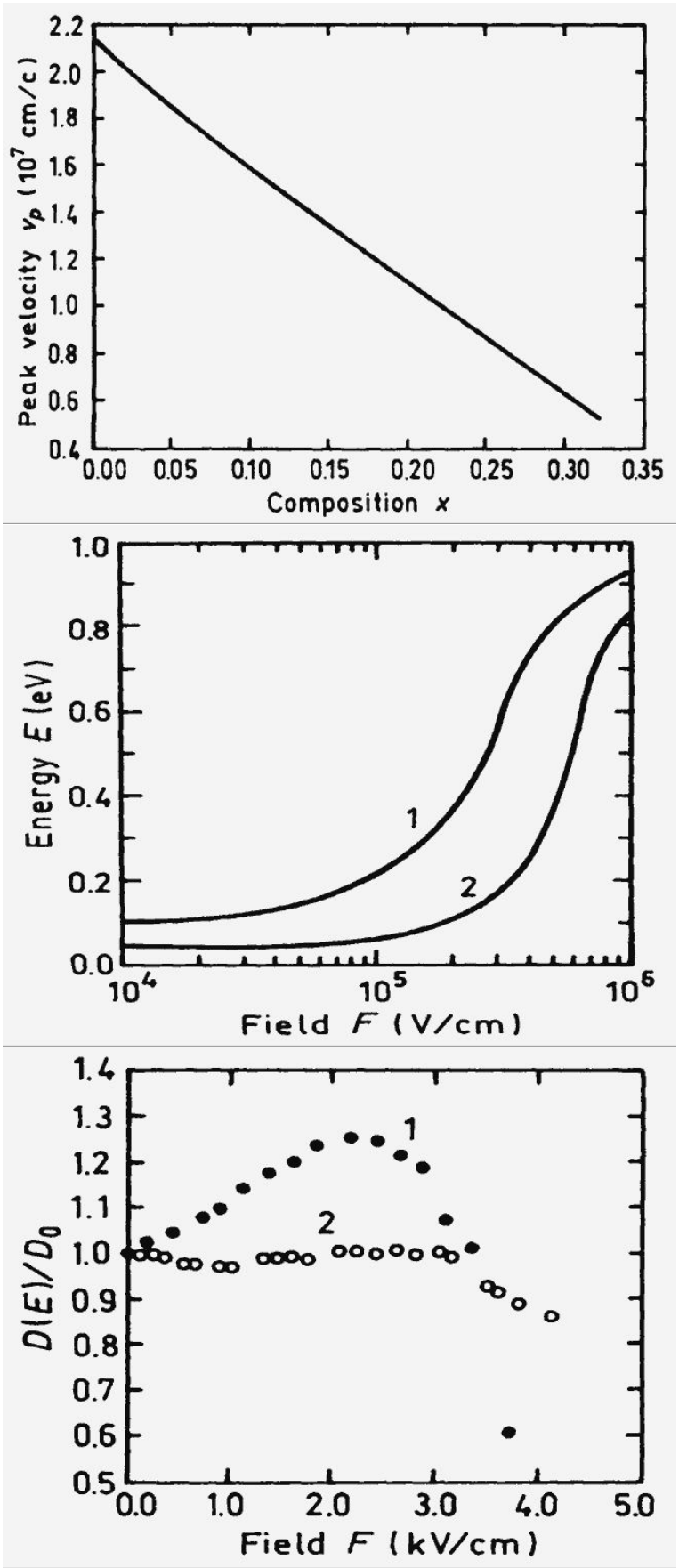
Peak velocity v_p (10^7 cm/c)
2.2
2.0
1.8
1.6
1.4
1.2
1.0
0.8
0.6
0.4
0.00 0.05 0.10 0.15 0.20 0.25 0.30 0.35
Composition x
Energy E (eV)
1.0
0.8
0.6
0.4
0.2
0.0
1
2
10^4
10^5
10^6
Field F (V/cm)
$D(E)/D_0$
1.4
1.3
1.2
1.1
1.0
0.9
0.8
0.7
0.6
0.5
1
2
0.0 1.0 2.0 3.0 4.0 5.0
Field F (kV/cm)

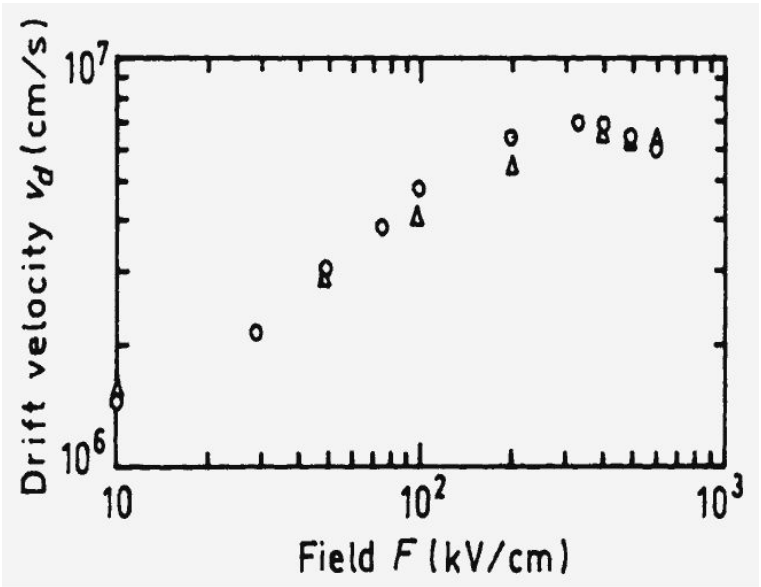
Drift velocity v_d (cm/s)
10^7
10^6
10
10^2
10^3
Field F (kV/cm)

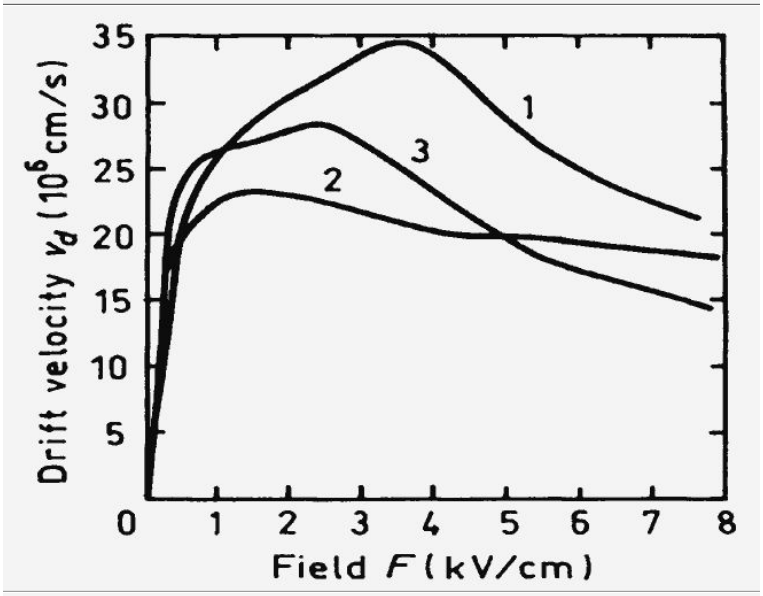
Drift velocity v_d (10^6cm/s)
35
30
25
20
15
10
5
0
1
2
3
4
5
6
7
8
Field F (kV/cm)
1
2
3

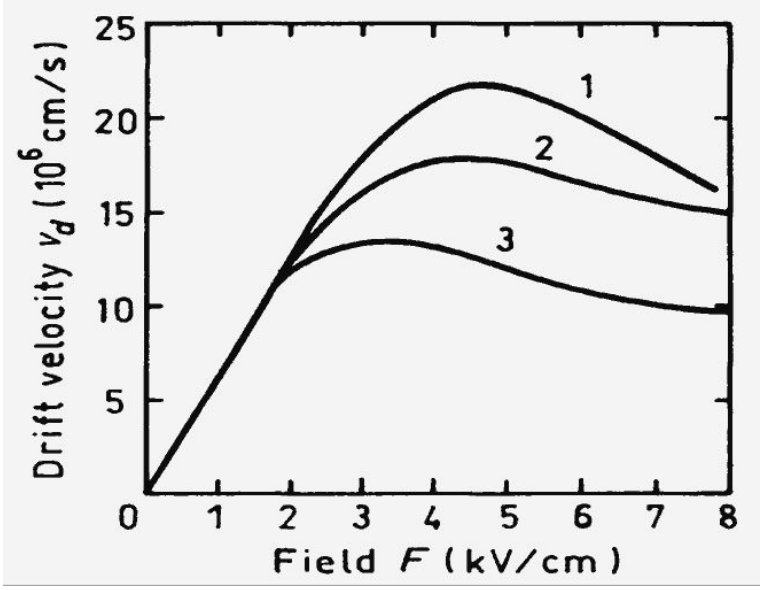
Drift velocity v_d (10^6cm/s)
25
20
15
10
5
0
1
2
3
4
5
6
7
8
Field F (kV/cm)
1
2
3

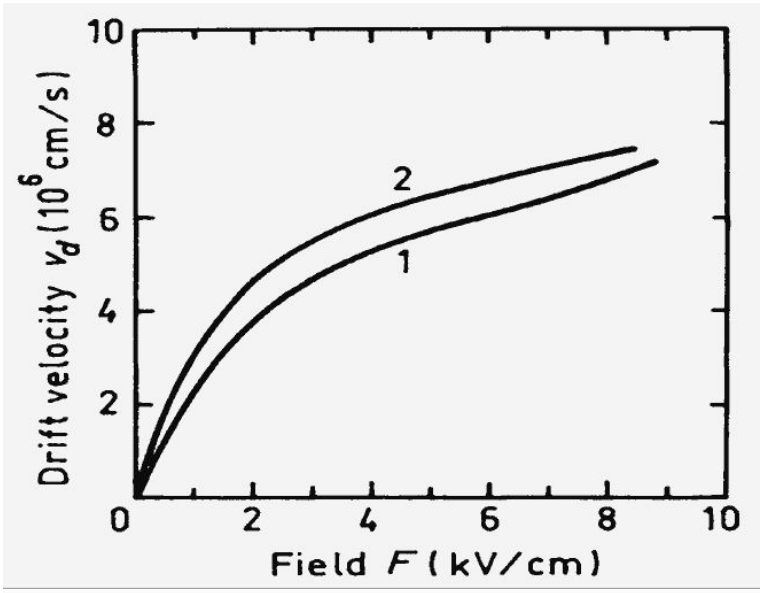
Drift velocity v_d (10^6 cm/s)
Field F (kV/cm)
1
2

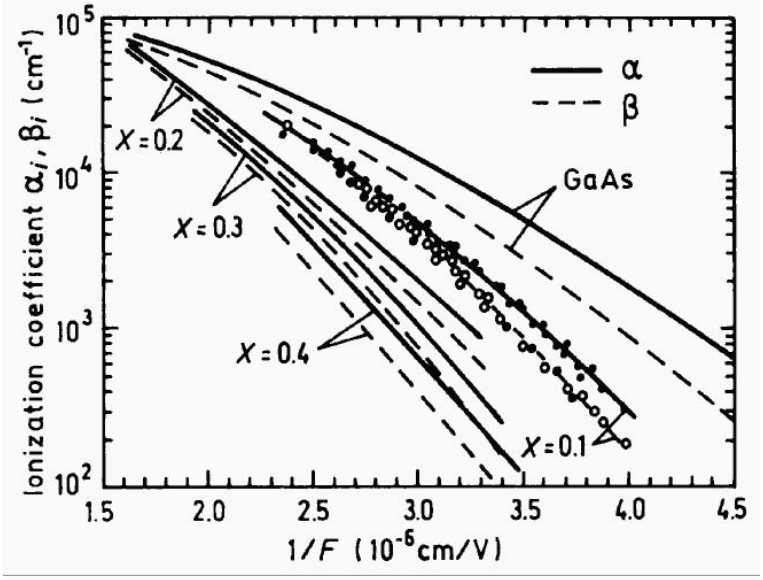
Ionization coefficient α_i, β_i (cm^{-1})
$1/F$ (10^{-6}cm/V)
α
β
GaAs
X = 0.2
X = 0.3
X = 0.4
X = 0.1

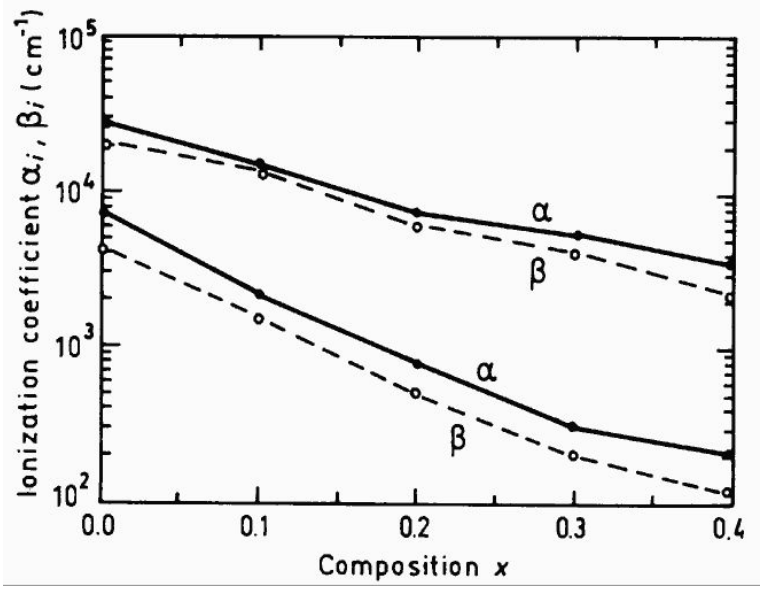
Ionization coefficient α_i, β_i (cm^{-1})
Composition x
α
β
α
β

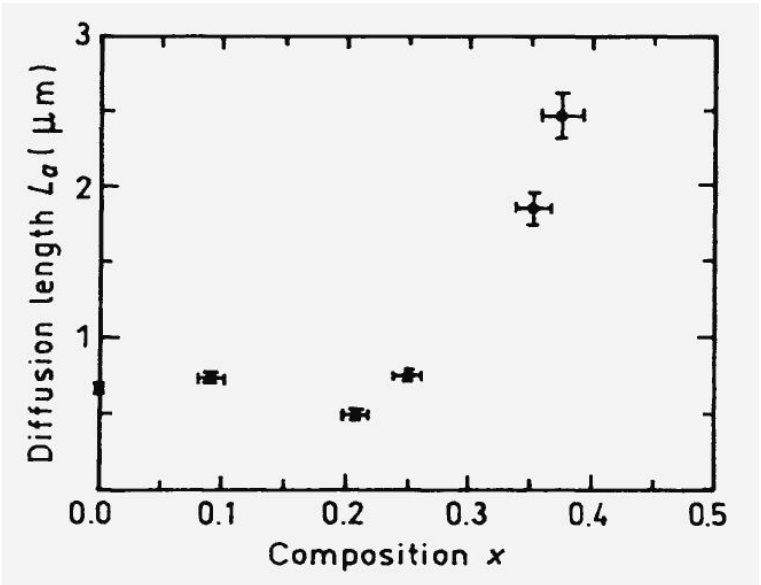
Diffusion length L_a (µm)
3
2
1
0.0
0.1
0.2
0.3
0.4
0.5
Composition x

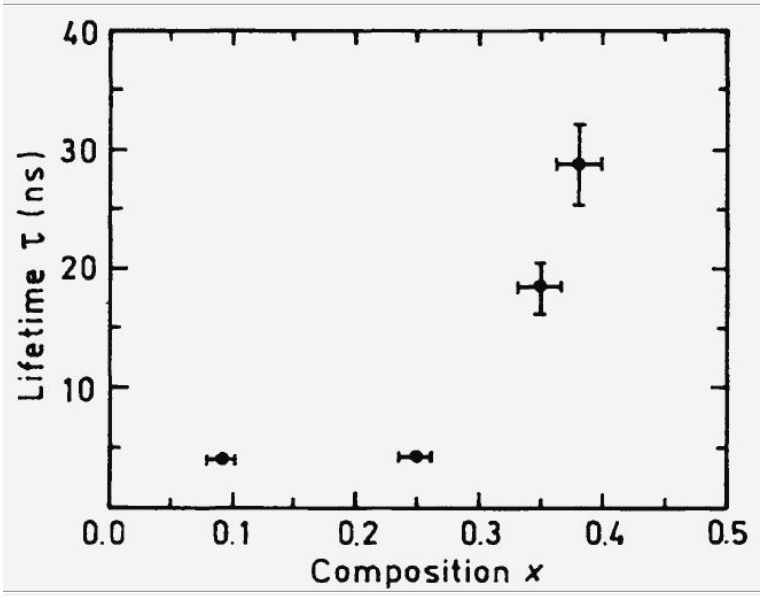
Lifetime τ (ns)
40
30
20
10
0.0
0.1
0.2
0.3
0.4
0.5
Composition x

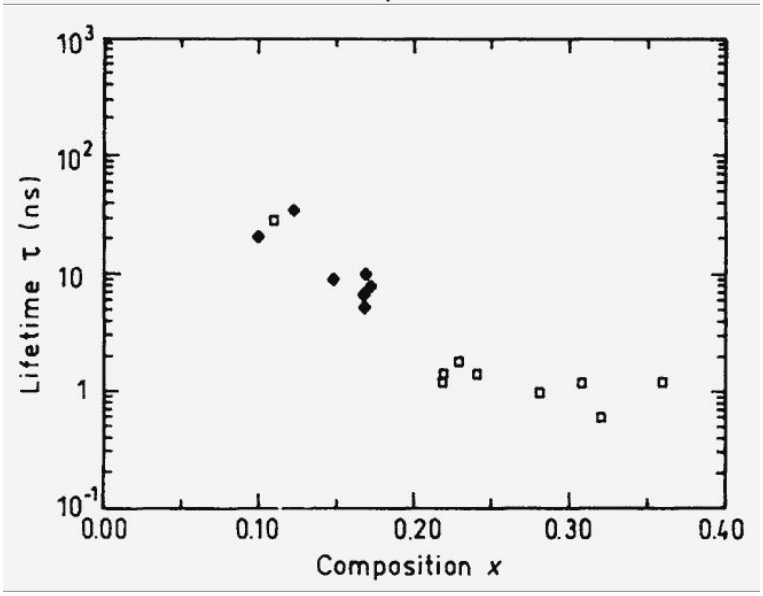
Lifetime τ (ns)
10^3
10^2
10
1
10^{-1}
0.00
0.10
0.20
0.30
0.40
Composition x

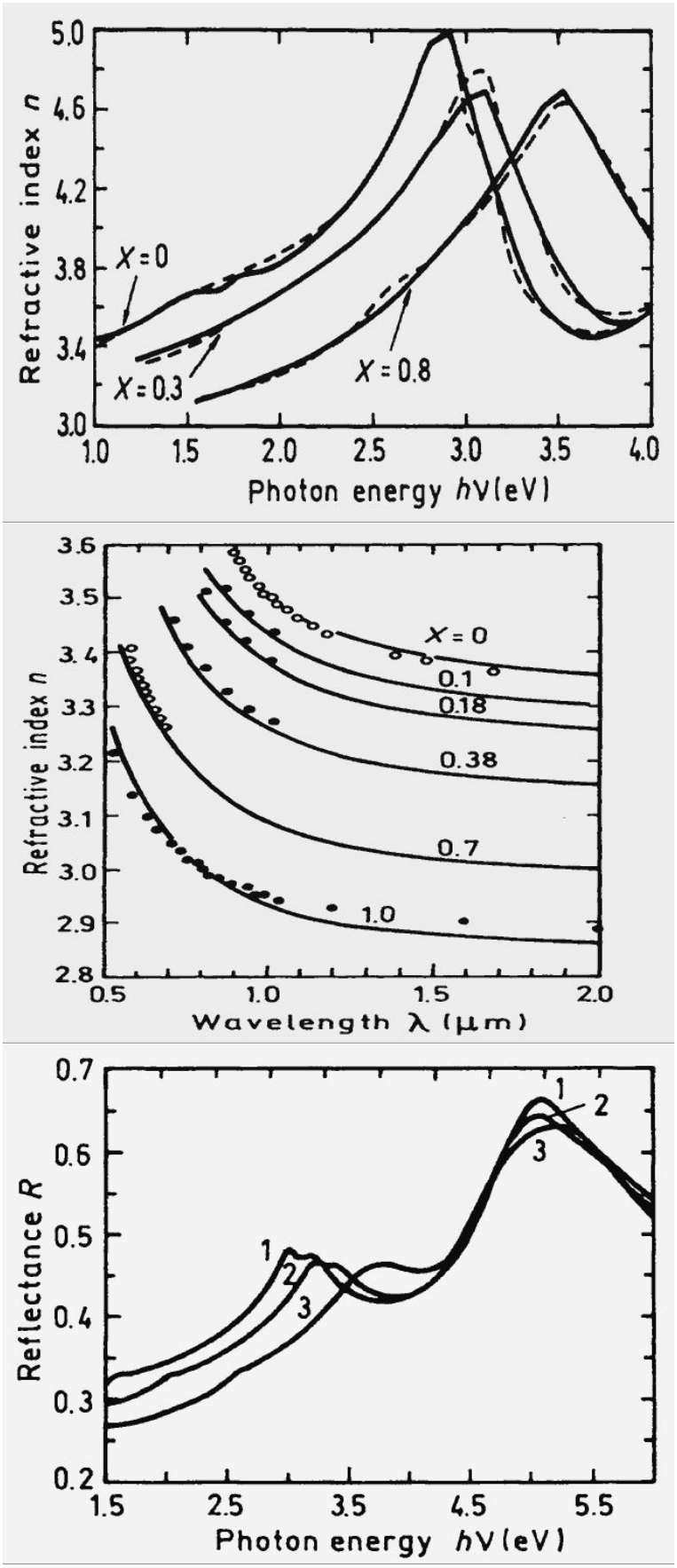
Refractive index n
5.0
4.6
4.2
3.8
3.4
3.0
X = 0
X = 0.3
X = 0.8
1.0
1.5
2.0
2.5
3.0
3.5
4.0
Photon energy hV (eV)
Refractive index n
3.6
3.5
3.4
3.3
3.2
3.1
3.0
2.9
2.8
X = 0
0.1
0.18
0.38
0.7
1.0
0.5
1.0
1.5
2.0
Wavelength λ (μm)
Reflectance R
0.7
0.6
0.5
0.4
0.3
0.2
1
2
3
1
2
3
1.5
2.5
3.5
4.5
5.5
Photon energy hV (eV)

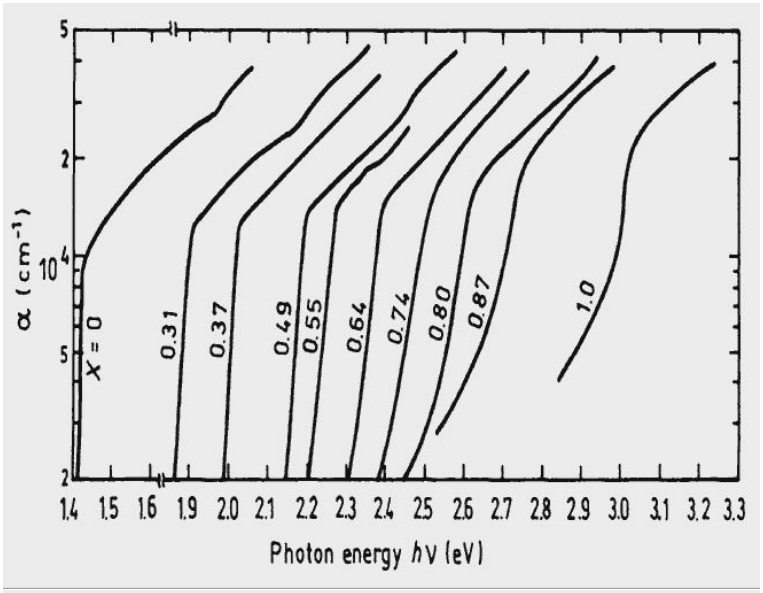
α (cm⁻¹)
X = 0
0.31
0.37
0.49
0.55
0.64
0.74
0.80
0.87
1.0
Photon energy hν (eV)

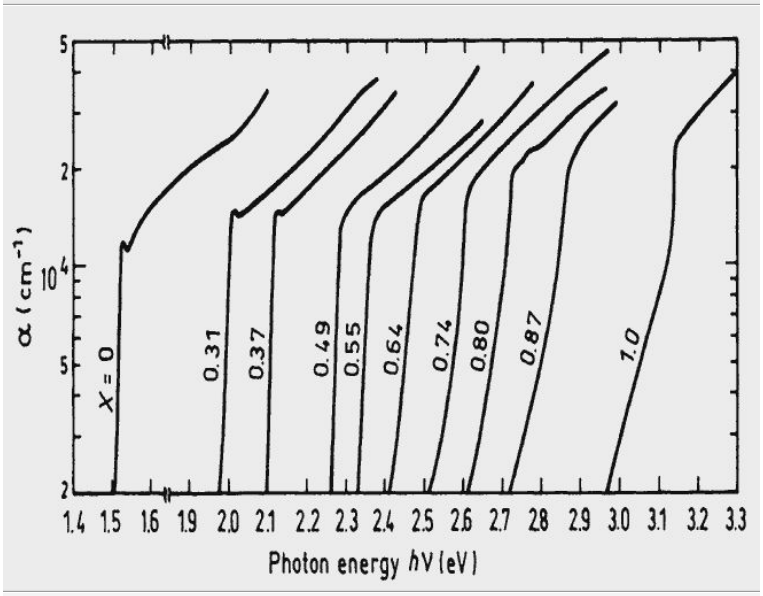
α (cm⁻¹)
X = 0
0.31
0.37
0.49
0.55
0.64
0.74
0.80
0.87
1.0
Photon energy hν (eV)

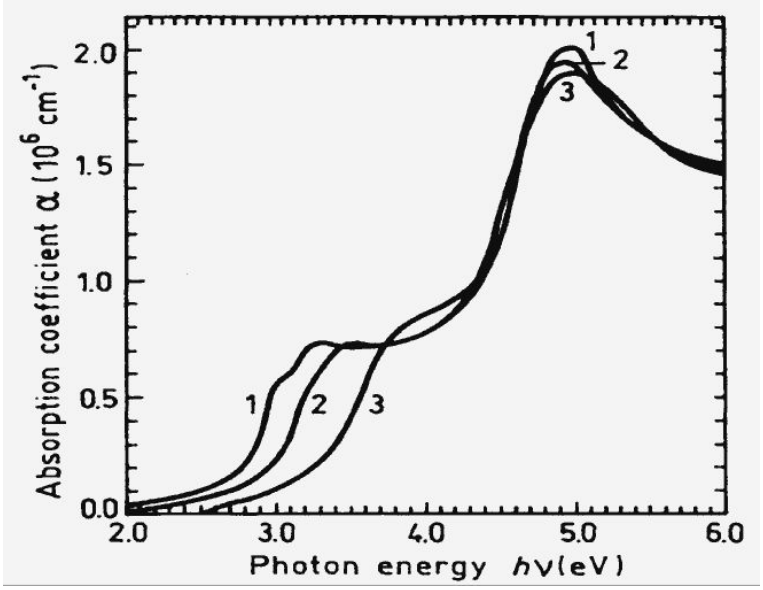
Absorption coefficient α (10⁶ cm⁻¹)
Photon energy hν (eV)

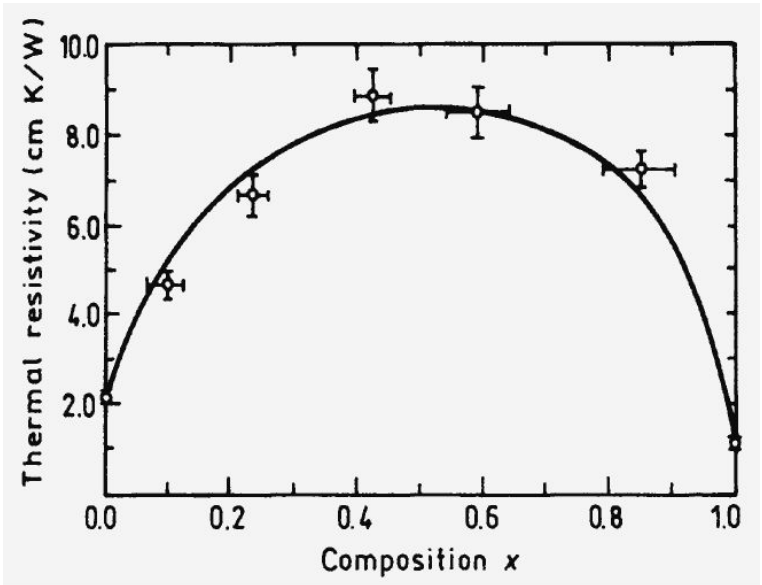
Thermal resistivity (cm K/W)
10.0
8.0
6.0
4.0
2.0
0.0
0.2
0.4
0.6
0.8
1.0
Composition x

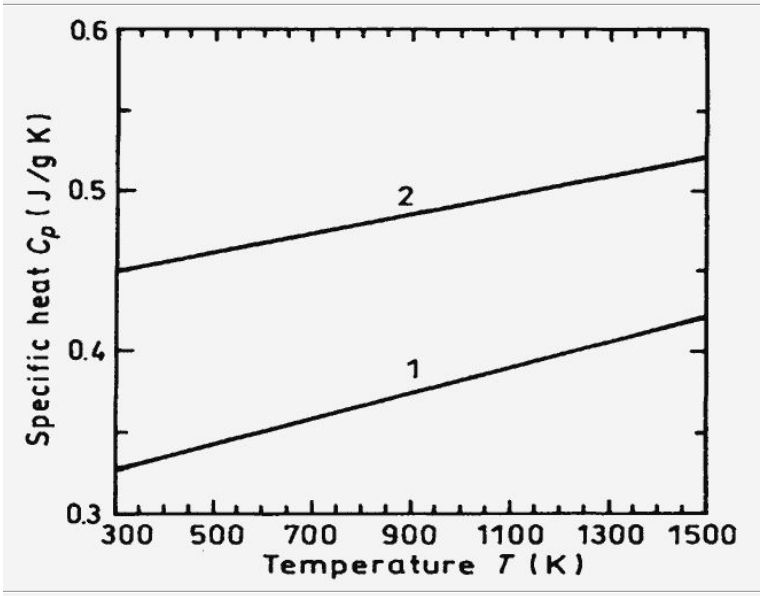
Specific heat C_p (J/g K)
0.6
0.5
0.4
0.3
2
1
300
500
700
900
1100
1300
1500
Temperature T (K)

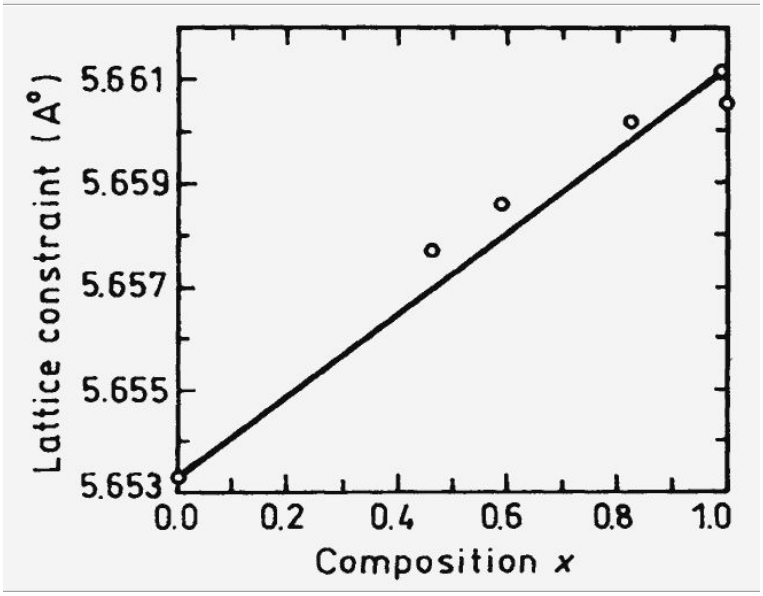
Lattice constraint (A°)
5.661
5.659
5.657
5.655
5.653
0.0
0.2
0.4
0.6
0.8
1.0
Composition x

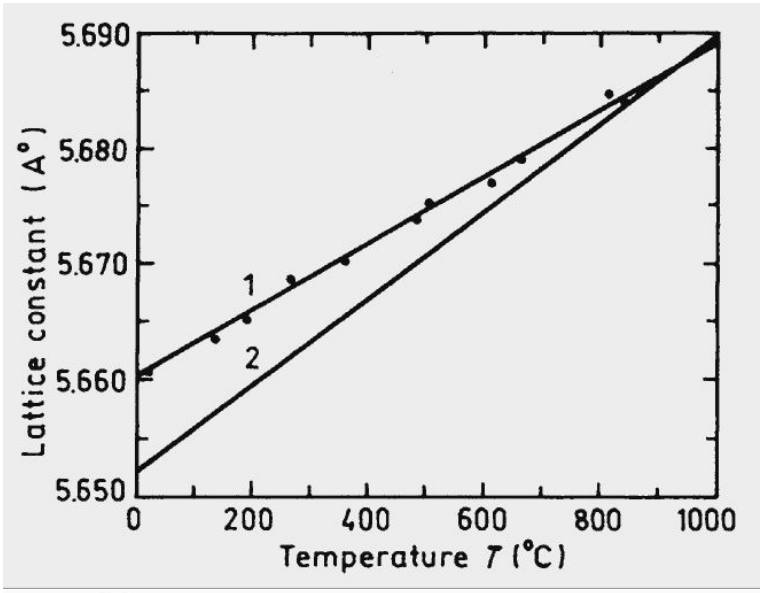
Lattice constant (A°)
5.690
5.680
5.670
5.660
5.650
1
2
0
200
400
600
800
1000
Temperature T (°C)

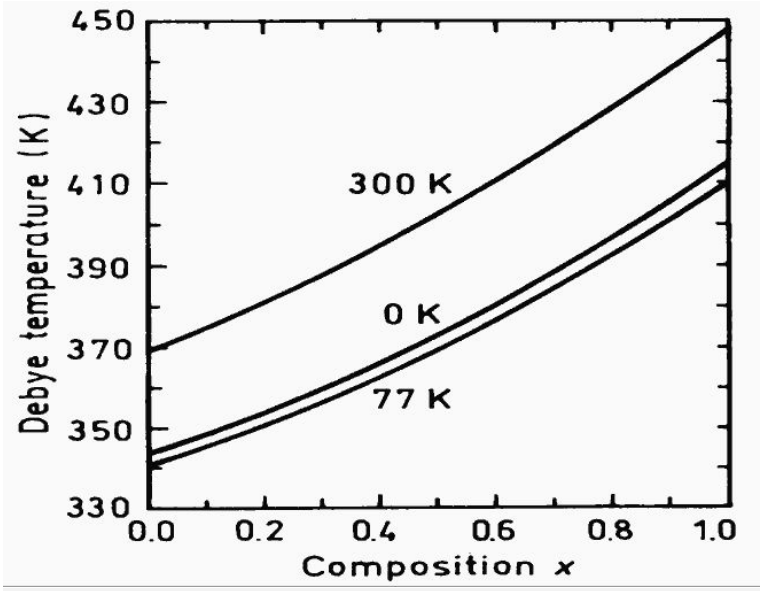
Debye temperature (K)
450
430
410
390
370
350
330
300 K
0 K
77 K
0.0
0.2
0.4
0.6
0.8
1.0
Composition x

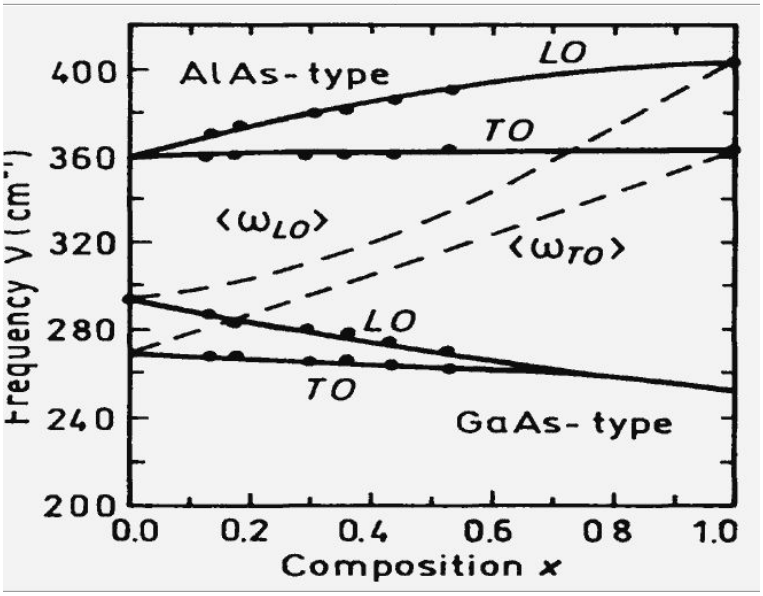
Frequency ν (cm⁻¹)
400
360
320
280
240
200
AlAs-type
LO
TO
⟨ωLO⟩
⟨ωTO⟩
LO
TO
GaAs-type
0.0
0.2
0.4
0.6
0.8
1.0
Composition x

4 InP

[002]ff.

4.1 Originaltexte

Dokument nächste Seite folgend.

InP - Indium Phosphide

InP - Indium Phosphide

Basic Parameters at 300 K

Crystal structure	Zinc Blende
Group of symmetry	T_d^2-F43m
Number of atoms in 1 cm^3	$3.96 \cdot 10^{22}$
Debye temperature	425 K
Density	4.81 g/cm^3
Dielectric constant (static)	12.5
Dielectric constant (high frequency)	9.61
Effective electron mass	$0.08m_o$
Effective hole masses m_h	$0.6m_o$
Effective hole masses m_{lp}	$0.089m_o$
Electron affinity	4.38 eV
Lattice constant	5.8687 A
Optical phonon energy	0.043 eV

InP - Indium Phosphide

Band structure and carrier concentration

Basic Parameters

Energy gap	1.344 eV
Energy separation ($E_{\Gamma L}$) between Γ and L valleys	0.59 eV
Energy separation ($E_{\Gamma X}$) between Γ and X valleys	0.85 eV
Energy spin-orbital splitting	0.11 eV
Intrinsic carrier concentration	$1.3 \cdot 10^{7}$ cm^{-3}
Intrinsic resistivity	$8.6 \cdot 10^{7} \Omega \cdot cm$
Effective conduction band density of states	$5.7 \cdot 10^{17}$ cm^{-3}
Effective valence band density of states	$1.1 \cdot 10^{19}$ cm^{-3}

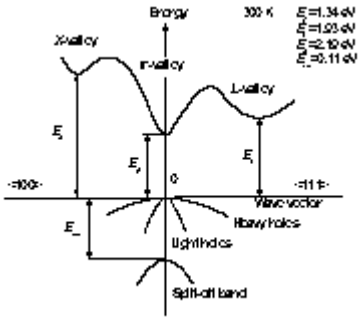

Band structure and carrier concentration of InP.
Important minima of the conduction band and maxima of the valence band. 300 K.
E_g = 1.34eV;
E_L = 1.93 eV;
E_X = 2.19 eV;
E_{so} = 0.11 eV

Temperature Dependences

Temperature Dependences Temperature dependence of the energy gap

$E_g = 1.421 - 4.9 \cdot 10^{-4} \cdot T^2/(T+327)$ (eV),
where T is temperature in degrees K (0 < T < 800).

Temperature dependence of the energy separation between Γ and X valleys

$E_{\Gamma X} = 0.96 - 3.7 \cdot 10^{-4} \cdot T$ (eV),
where T is temperature in degrees K (0 < T < 300).

Effective density of states in the conduction band

$N_c \approx 1.1 \cdot 10^{14} \cdot T^{3/2}$ (cm^{-3}).

Effective density of states in the valence band

$N_v \approx 2.2 \cdot 10^{15} \cdot T^{3/2}$ (cm^{-3}).

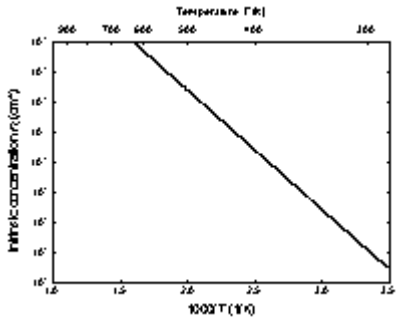

The temperature dependence of the intrinsic carrier concentration.

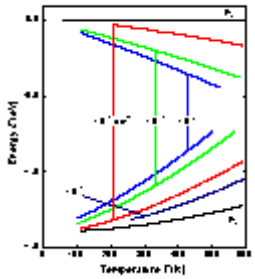

Fermi level versus temperature for different concentrations of shallow donors and acceptors.

Dependences on Hydrostatic Pressure

$E_g = E_g(0) + 8.4 \cdot 10^{-3}P - 1.8 \cdot 10^{-5}P^2$ (eV)
$E_L = E_L(0) + 4.6 \cdot 10^{-3}P$ (eV),
$E_X = E_X(0) + 2 \cdot 10^{-3}P$ (eV),
where P is pressure in kbar.

Energy Gap Narrowing at High Doping Levels

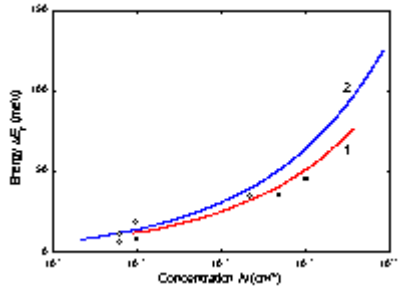

Energy gap narrowing versus donor (curve 1 and experimental points) and acceptor (curve 2) doping density, T = 300 K.
Curve 1 and experimental points *(Bugajski and Lewandowski [1985])*;
Curve 2 *(Jain et al. [1990])*.

For *n*-type InP:

$\Delta E_g \approx 22.5 \cdot 10^{-9} \cdot N_d^{1/3}$ (eV)
(Bugajski and Lewandowski [1985])

For *p*-type InP

$\Delta E_g \approx 10.3 \cdot 10^{-9} \cdot N_a^{1/3} + 4.43 \cdot 10^{-7} \cdot N_a^{1/4} + 3.38 \cdot 10^{-12} \cdot N_a^{1/2}$ (eV)
(Jain et al. [1990]).

Effective Masses

Electrons:

For Γ-valley	$m_\Gamma = 0.08 m_o$
The are 4 equivalent L-valleys in the conduction band:	
in one L-valley	$m_L = 0.25 m_o$
for all L-valley	$m_{Ld} = 0.63 m_o$
The are 3 equivalent X-valleys in the conduction band:	
in one X-valley	$m_X = 0.32 m_o$
for all X-valley	$m_{Xd} = 0.66 m_o$

Holes:

Heavy	$m_h = 0.6 m_o$
Light	$m_{lp} = 0.089 m_o$
Split-off band	$m_{so} = 0.17 m_o$
Effective mass of density of states	$m_v = 0.6 m_o$

Donors and Acceptors

Ionization energies of shallow donors (eV) ~0.0057:

S, **Si**, **Sn**, **Ge**

Ionization energies of shallow acceptors (eV):

C	Hg	Zn	Cd	Si	Cu	Be	Mg	Ge	Mn
0.04	0.098	0.035	0.057	0.03	0.06	0.03(MBE)	0.03(MBE)	0.021	0.27

InP - Indium Phosphide

Electrical properties

Basic Parameters

Breakdown field	$\approx 5 \cdot 10^5$ V cm^{-1}
Mobility electrons	≤ 5400 cm^{2}V^{-1}s^{-1}
Mobility holes	≤ 200 cm^2 V^{-1}s^{-1}
Diffusion coefficient electrons	≤ 130 cm^2 s^{-1}
Diffusion coefficient holes	≤ 5 cm^2 s^{-1}
Electron thermal velocity	$3.9 \cdot 10^5$ m s^{-1}
Hole thermal velocity	$1.7 \cdot 10^5$ m s^{-1}

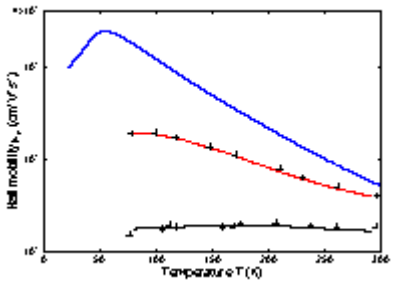

Electron Hall mobility versus temperature for different doping levels.
Bottom curve - $n_o=N_d-N_a=8 \cdot 10^{17}$ cm^{-3};
Middle curve - $n_o=2 \cdot 10^{15}$ cm^{-3};
Top curve - $n_o=3 \cdot 10^{13}$ cm^{-3}.
(Razeghi et al. [1988]) and *(Walukiewicz et al [1980])*.

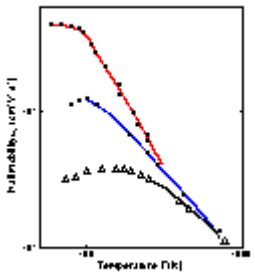

Electron Hall mobility versus temperature (high temperatures):
Bottom curve - $n_o=N_d-N_a \sim 3 \cdot 10^{17}$ cm^{-3};
Middle curve - $n_o \sim 1.5 \cdot 10^{16}$ cm^{-3};
Top curve - $n_o \sim 3 \cdot 10^{15}$ cm^{-3}.
(Galavanov and Siukaev[1970]).

For weakly doped *n*-InP at temperatures close to 300 K electron drift mobility:

$\mu_n = (4.2 \div 5.4) \cdot 10^3 \cdot (300/T)$ (cm^{2}V^{-1} s^{-1})

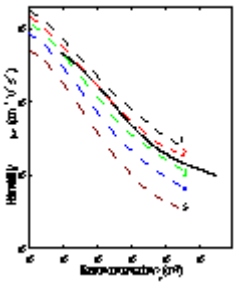

Hall mobility versus electron concentration for different compensation ratios.
$\theta = N_a/N_d$, 77 K.
Dashed curves are theoretical calculations: **1**. $\theta = 0$; **2**. $\theta = 0.2$; **3**. $\theta = 0.4$; **4**. $\theta = 0.6$; **5**. $\theta = 0.8$;
(Walukiewicz et al. [1980]).
Solid line is mean observed values *(Anderson et al. [1985])*.

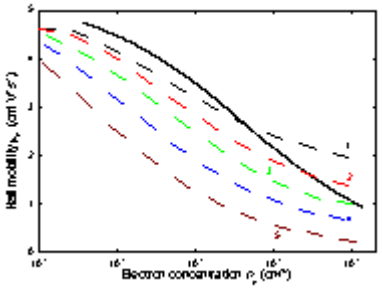

Hall mobility versus electron concentration for different compensation ratios
$\theta = N_a/N_d$, 300 K.
Dashed curves are theoretical calculations: **1**. $\theta = 0$; **2**. $\theta = 0.2$; **3**. $\theta = 0.4$; **4**. $\theta = 0.6$; **5**. $\theta = 0.8$;
(Walukiewicz et al. [1980]).
Solid line is mean observed values *(Anderson et al. [1985])*.

Approximate formula for electron Hall mobility

$\mu=\mu_{OH}/[1+(N_d/10^7)^{1/2}]$,
where $\mu_{OH}=5000$ cm^2V^{-1} s^{-1},
N_d- in cm^{-3} *(Hilsum [1974])*

At 300 K, the electron Hall factor $\mathbf{r_n \approx 1}$ in *n*-InP.
for $N_d > 10^{15}$ cm^{-3}.

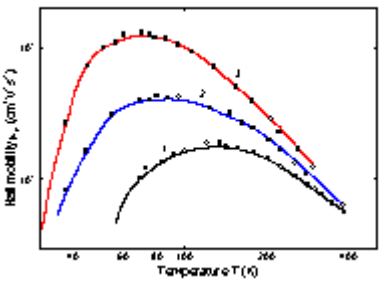

Hole Hall mobility versus temperature for different doping (Zn) levels.
Hole concentration at 300 K: **1**. $1.75\cdot10^{18}$ cm^{-3}; **2**. $3.6\cdot10^{17}$ cm^{-3}; **3**. $4.4\cdot10^{16}$ cm^{-3}.
$\theta=N_a/N_d\sim0.1$.
(Kohanyuk et al. [1988]).

For weakly doped *p*-InP at temperature close to 300 K the Hall mobility

$\mu_{pH}\sim150\cdot(300/T)^{2.2}$ (cm^2V^{-1} s^{-1}).

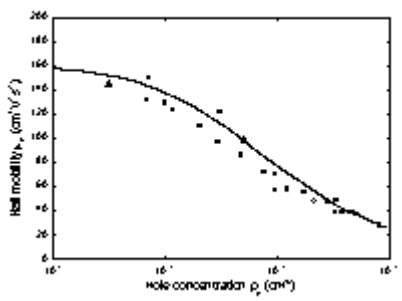

Hole Hall mobility versus hole density, 300 K (Wiley [1975]).
The approximate formula for hole Hall mobility:
$\mu_p=\mu_{po}/[1 + (N_a/2\cdot10^{17})^{1/2}]$, where $\mu_{po}\sim150$ cm^2V^{-1} s^{-1}, N_a- in cm^{-3}

At 300 K, the hole factor in pure *p*-InP: $\mathbf{r_p \sim 1}$

Transport Properties in High Electric Fields

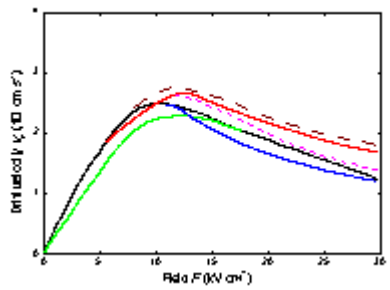

Field dependences of the electron drift velocity in InP, 300 K.
Solid curve are theoretical calculation.
Dashed and dotted curve are measured data.
(Maloney and Frey [1977]) and *(Gonzalez Sanchez et al. [1992])*.

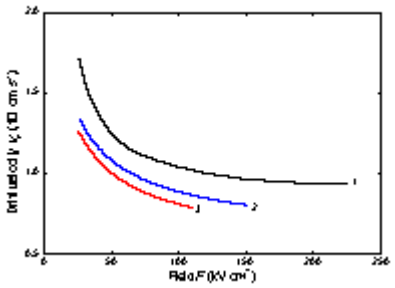

The field dependences of the electron drift velocity for high electric fields.
T(K): **1**. 95; **2**. 300; **3**. 400.
(Windhorn et al. [1983]).

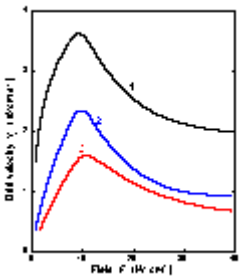

Field dependences of the electron drift velocity at different temperatures.
Curve 1 -77 K *(Gonzalez Sanchez et al. [1992])*.
Curve 2 - 300 K, Curve 3 - 500 K *(Fawcett and Hill [1975])*.

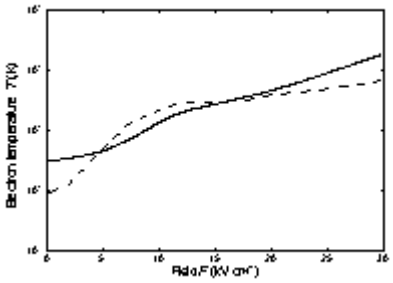

Electron temperature versus electric field for 77 K and 300 K.
(Maloney and Frey [1977])

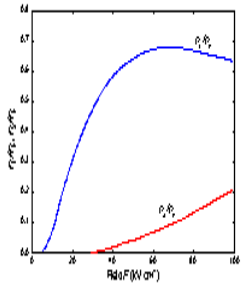

Fraction of electrons in L and X valleys n_L/n_0 and n_X/n_0 as a function of electric field, 300 K.
(Borodovskii and Osadchii [1987]).

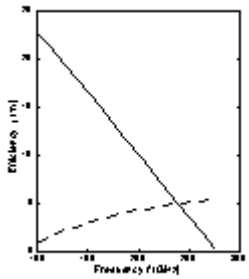

Frequency dependence of the efficiency η at first (solid line) and at the second (dashed line) harmonic in LSA mode.
Monte Carlo simulation.
$F = F_o + F_1 \cdot \sin(2\pi \cdot ft) + F_2 \cdot [\sin(4\pi \cdot ft)+3\pi/2]$,
$F_o=F_1=35$ kV cm^{-1},
$F_2=10.5$ kV cm^{-1}
(Borodovskii and Osadchii [1987]).

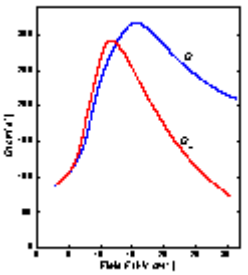

Longitudinal (D || F) and transverse (D ⊥ F) electron diffusion coefficients at 300 K.
Ensemble Monte Carlo simulation.
(Aishima and Fukushima [1983]).

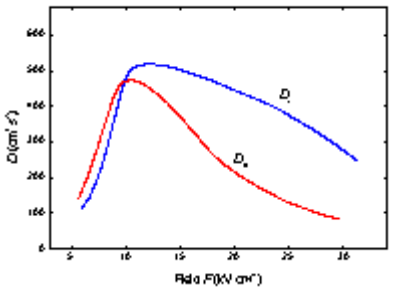

Longitudinal (D || F) and transverse (D ⊥ F) electron diffusion coefficients at 77K.
Ensemble Monte Carlo simulation.
(Aishima and Fukushima [1983]).

Impact Ionization

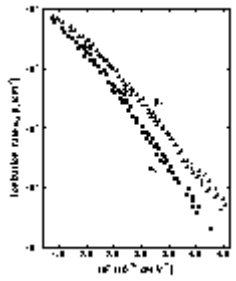

The dependence of ionization rates for electrons α_i and holes β_i versus 1/F, 300 K.
(Cook et al. [1982]).

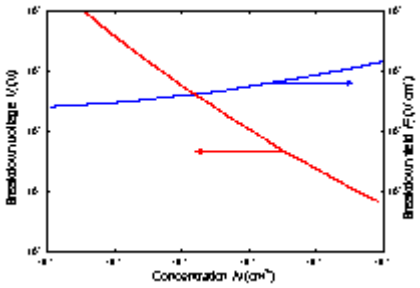

Breakdown voltage and breakdown field versus doping density for an abrupt *p-n* junction, 300 K
(Kyuregyan and Yurkov [1989]).

Recombination Parameters

Pure *n*-type material ($n_o \sim 10^{-14} cm^{-3}$)

The longest lifetime of holes	$\tau_p \sim 3 \cdot 10^{-6}$ s
Diffusion length $L_p = (D_p \cdot \tau_p)^{1/2}$	$L_p \sim 40$ µm.

Pure *p*-type material($p_o \sim 10^{15} cm^{-3}$)

(a)Low injection level

The longest lifetime of electrons	$\tau_n \sim 2 \cdot 10^{-9}$ s
Diffusion length $L_n = (D_n \cdot \tau_n)^{1/2}$	$L_n \sim 8$ µm

(b) High injection level (filled traps)

The longest lifetime of electrons	$\tau \sim 10^{-8}$ s
Diffusion length L_n	$L_n \sim 25$ µm

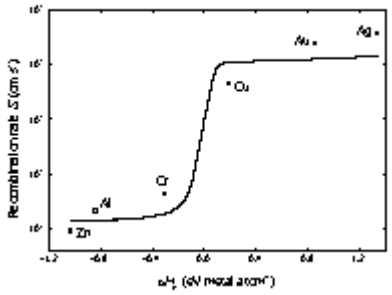

Surface recombination velocity versus the heat of reaction per atom of each metal phosphide ΔH_R
(Rosenwaks et al. [1990]).

If the surface Fermi level E_{FS} is pinned close to midgap ($E_{FS} \sim E_g/2$) the surface recombination velocity increases from $\sim 5 \cdot 10^{-3}$cm/s for doping level $n_o \sim 3 \cdot 10^{15}$ cm^{-3} to $\sim 10^6$ cm/s for doping level $n_o \sim 3 \cdot 10^{18} cm^{-3}$ *(Bothra et al. [1991])*.

Radiative recombination coefficient (300 K) $1.2 \cdot 10^{-10}$ cm^3/s

Auger coefficient (300 K) $\sim 9 \cdot 10^{-31}$ cm^6/s

InP - Indium Phosphide

Optical properties

Infrared refractive index	3.1
Radiative recombination coefficient	$1.2 \cdot 10^{-10}$ cm^3/s

Infrared refractive index

$n = k^{1/2} = 3.075 \cdot (1+2.7 \cdot 10^{-5}T)$

Long-wave TO phonon energy at 300 K $h\nu_{TO}$ = 38.1 meV
Long-wave LO phonon energy at 300 K $h\nu_{LO}$ = 42.6 meV

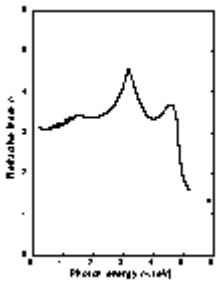

Refractive index n versus photon energy.
Solid curve is theoretical calculation.
Points represent experimental data, 300 K
(Adachi [1989]).

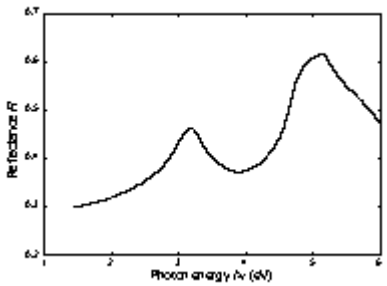

Normal incidence reflectivity versus photon energy, 300 K
(Aspnes and Studna [1983]).

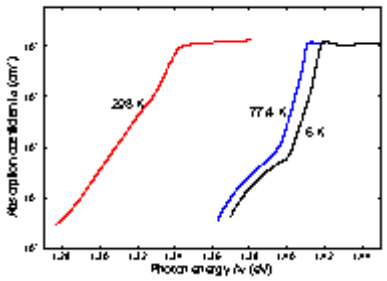

Intrinsic absorption coefficient near the intrinsic absorption edge for different temperatures.
n-InP. $n_o = 5 \cdot 10^{15}$ cm^{-3}
(Turner et al. [1964]).

A ground state Rydberg energy R_{X1} = 5.0 meV.

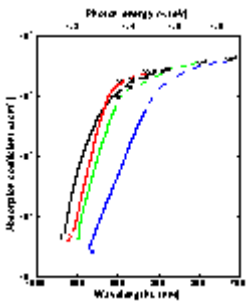

Intrinsic absorption edge at 296 K at different doping levels

1. *p*-type sample, $p_o = 1.1 \cdot 10^{18}$ cm^{-3}

3. *n*-type sample, $n_o = 1.9 \cdot 10^{18}$ cm^{-3}

2. *n*-type sample, $n_o = 7.4 \cdot 10^{16}$ cm^{-3}

4. *n*-type sample, $n_o = 7 \cdot 10^{18}$ cm^{-3}

(Burkhard et al. 1982]).

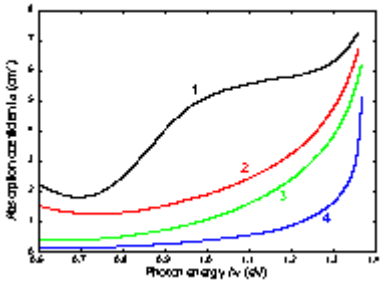

Intrinsic absorption edge at 77 K for *n*-InP at different doping levels

1. $n_o = 10^{19}$ cm^{-3};

2. $n_o = 5 \cdot 10^{18}$ cm^{-3};

3. $n_o = 2 \cdot 10^{18}$ cm^{-3};

4. $n_o = 9.6 \cdot 10^{16}$ cm^{-3}

(Bugajski and Lewandowski [1985]).

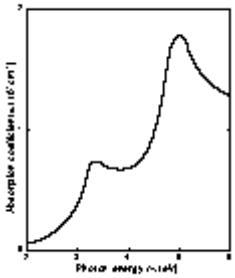

The absorption coefficient versus photon energy, 300 K

(Aspnes and Studna [1983]).

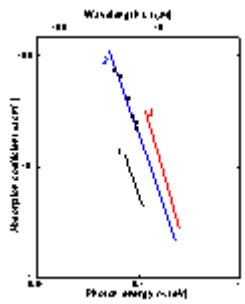

Free carrier absorption versus photon energy ai different doping levels, 300 K.

Electron concentration n_o (cm^{-3}): **1**. $4 \cdot 10^{16}$; **2**. $2 \cdot 10^{17}$; **3**. $4 \cdot 10^{17}$

(Newman [1958]).

InP - Indium Phosphide

Thermal properties

Bulk modulus	$7.1 \cdot 10^{11}$ dyn cm^{-2}
Melting point	1060 °C
Specific heat	0.31 J g^{-1} $°C^{-1}$
Thermal conductivity	0.68 W cm^{-1} $°C^{-1}$
Thermal diffusivity	0.372 cm^2 s^{-1}
Thermal expansion, linear	$4.60 \cdot 10^{-6}$ $°C^{-1}$

Melting point T_m = 1333 K

For 0 < P < 40 kbar

$T_m = 1333 - 2.0 \cdot P$ (P in kbar)

(Glasov et al. [1977]).

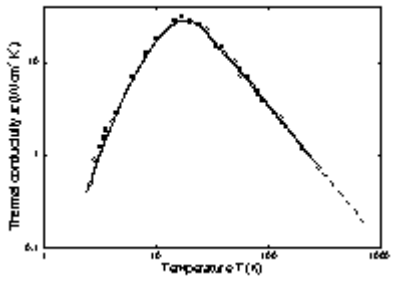

Temperature dependence of thermal conductivity.

n-type samples, $n_o = 2 \cdot 10^{16}$ cm^{-3}

(Aliev et al [1965]).

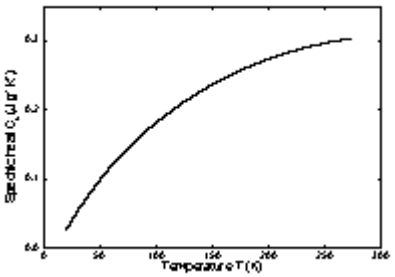

Temperature dependence of specific heat at constant pressure

(Piesbergen [1963]).

For 298< T < 910 K

$C_p = 0.28 + 10^{-4} \cdot T$ (J g^{-1} K^{-1})

(Barin et al. [1977]).

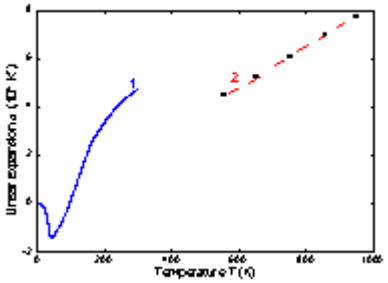

Temperature dependence of linear expansion coefficient α.

1. *(Soma et al. [1982])*,

2. *(Glazov et al. [1977])*.

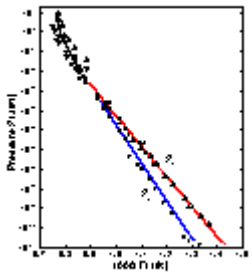

Temperature dependence of saturation vapor pressure.
(Panish and Arthur[1970]).

InP - Indium Phosphide

Mechanical properties, elastic constants, lattice vibrations

Basic Parameter

Bulk modulus	$7.1 \cdot 10^{11}$ dyn cm^{-2}
Density	4.81 g cm^{-3}
Surface microhardness (using Knoop's pyramid test)	~460 kg mm^{-2}
Cleavage plane	{100}
Piezoelectric constant	e_{14}= $-3.5 \cdot 10^{-2}$ C m^{-2}

Elastic constants at 300 K

C_{11} = $10.11 \cdot 10^{11}$ dyn/cm^2
C_{12} = $5.61 \cdot 10^{11}$ dyn/cm^2
C_{44} = $4.56 \cdot 10^{11}$ dyn/cm^2
(Nichols et al. [1980]).

Bulk modulus (compressibility^{-1})	B_s= $7.11 \cdot 10^{11}$ dyn/cm^2
Shear modulus	C'= $2.25 \cdot 10^{11}$ dyn/cm^2
[100] Young's modulus	Y_o= $6.11 \cdot 10^{11}$ dyn/cm^2
[100] Poisson ratio	σ_o = 0.36

Acoustic Wave Speeds

Wave propagation Direction	Wave character	Expression for wave speed	Wave speed (in units of 10^5 cm/s)
[100]	V_L	$(C_{11}/\rho)^{1/2}$	4.58
	V_T	$(C_{44}/\rho)^{1/2}$	3.08
[100]	V_l	$[(C_{11}+C_{l2}+2C_{44})/2\rho]^{1/2}$	5.08
	$V_{t\|\|}$	$V_{t\|\|}=V_T=(C_{44}/\rho)^{1/2}$	3.08
	$V_{t\perp}$	$[(C_{11}-C_{12})/2\rho]^{1/2}$	2.16
[111]	V_l'	$[(C_{11}+2C_{12}+4C_{44})/3\rho]^{1/2}$	5.23
	V_t'	$[(C_{11}-C_{12}+C_{44})/3\rho]^{1/2}$	2.51

Phonon frequencies (in units of 10^{12} Hz)

$\nu_{TO}(\Gamma)$ 9.2 $\nu_{LO}(X)$ 9.95

$\nu_{LO}(\Gamma)$	10.3	$\nu_{TA}(L)$	1.65
$\nu_{TA}(X)$	2.05	$\nu_{LA}(L)$	5.0
$\nu_{LA}(X)$	5.8	$\nu_{TO}(L)$	9.5
$\nu_{TO}(X)$	9.7	$\nu_{LO}(L)$	10.2

(Suto and Nashizawa [1990]).

InP - Indium Phosphide

References:

- Shmidt *Handbook Series on Semiconductor Parameters*, **vol.1**, M. Levinshtein, S. Rumyantsev and M. Shur, ed., World Scientific, London, 1996, pp. 169-190.
- Dargys A. and J. Kundrotas *Handbook on Physical Properties of Ge, Si, GaAs and InP*, Vilnius, Science and Encyclopedia Publishers, 1994

- Adachi, S., *J. Appi Phys.* **66**, 12 (1989) 6030-6040.
- Aliev, S. A., A. Ya. Nashelskii, and S. S. Shalyt, *Sov. Phys. Solid State* **7**, (1965) 1287.
- Anderson, D. A., N. Apsley, P. Davies, and P. L. Giles, J. *Appi Phys.* **58**, 8 (1985) 3059-3067.
- Aishima, A. and Y. Fukushima, *Jpn. J. Appi Phys.* **22**, 8 (1983) 1290-1293.
- Aspnes, D. E. and A. A. Studna, *Phys. Rev.* **B27**, 2 (1983) 985-1009.
- Barin, I., 0. Knacke, and O. Kubaschewski, *Thermal Properties of Inorganic Substances*, Springer, Berlin, 1977.
- Borcherds, P. H., G. F. Alfrey, D. H. Sauudcrson, and A. D. B. Woods, *J. Phys.* **C8**, 13 (1975) 2022-2030.
- Borodovskii, P. A. and V. M. Osadchii, *Intervalley Transfer of Electrons in AsBs Semiconductors*, Inst. of Semiconductor Physics, Novosibirsk, 1987, p. 170 (in Russian).
- Bothra, S., S. Tyagi, S. K. Chandhi, and J. M. Borrego, *Solid State Electron.* **34**, 1 (1991) 47-50.
- Bugajski, M. and W. Lewandowski, J. *Appl. Phys.* **57**, 2 (1985) 521-530.
- Burkhard, H., H. W. Dinges, and E. Kuphal, *J. Appl. Phys.* **53**, 1 (1982) 655-662.
- Cook, L. W., G. E. Bulman, and G. E. Stillman, *Appl. Phys. Lett.* **40**, 7 (1982) 589-591.
- Fawcett, W. and G. Hill, *Electron. Lett* **11**, 4 (1975) 80-81.
- Galavanov, V. V. and N. V. Siukaev, *Phys. Status Solid* **38**, 2 (1970) 523-530.
- Glazov, V. M., K. Davletov, A. Ya. Nashelskii, and M. M. Mamedov, *Zh. Fiz. Khim.* **51**, 10 (1977) 2558-2561 (in Russian).
- Gonzalez Sanchez, T., J. E. Velazquez Perez, P. M. Gutierrez Conde, and D. Pardo, *Semicond. Sci. Technol.* **7**, 1 (1992) 31-36.
- Hilsum, C., *Electron. Lett.* **10**, **13** (1974) 259-260.
- Jain, S. C., J. M. M. Gregor, and D. J. Roulston, *J. Appl. Phys.* **68**, 7 (1990) 3747-3749.
- Kohanyuk, M. B., G. L. Lyakhu, I. P. Molodyan, and E. V. Russu, *Indium Phosphide in Semiconductor Electronics*, S. I. Radaucan, ed., Shtinca, Kishinev, 1988, pp. 200-222 (in Russian).
- Kushwaha, M. S. and S. S. Kushwaha, *Can. J. Phys.* **58**, 3 (1980) 351-358.
- Kyuregyan, A. S. and S. N. Yurkov, *Sov. Phys. Semicond.* **23**, 10 (1989) 1126-1132.
- Maloney, T. J. and J. Prey, *J. Appl. Phys.* **48**, 2 (1977) 781-787.
- Newman, R., *Phys. Rev.* **Ill**, 6 (1958) 1518-1521.
- Nichols, D. N., D. S. Rimai, and R. J. Sladek, *Solid State Commun.* **36**, 8 (1980) 667-669.
- Panish, M. B. and J. R. Arthur, *J. Chem. Thermodyn.* **2**, (1970) 299.
- Piesbergen, U., Z. *Naturforschung* **18a**, 2 (1963) 141-147.
- Razeghi, M., Ph. Maurel, M. Defour, F. Omnes, G. Neu, and A. Kozacki, *Appl. Phys. Lett.* **52**, 2 (1988) 117-119.
- Rosenwaks, Y., Y. Shapira, and D. Huppert, *Appl. Phys. Lett.* **57**, 24 (1990) 2552-2554.
- Soma, T., J. Satoh, and H. Matsuo, *Solid State Commun.* **42**, 12 (1982) 889-892.
- Turner, W. J., W. E. Reese, and G. D. Pettit, *Phys. Rev.* **136**, 5A (1964) A1467-1470.
- Walukiewicz, W., J. Lagowskii, L. Jastrzebski, P. Rava, M. Lichtensteiger, C. H. Gatos, and H.C. Gatos, *J. Appl. Phys.* **51**, 5 (1980) 2659-2668
- Wiley, J. D., *Semiconductor and Semimetals*, R. K. Willardson and A. C. Beer, eds., Academic Press, N.Y., vol. 10, 1975, p. 162.
- Windhorn, T. H., L. W. Cook, M. A. Haase, and G. E. Stillman, *Appl.Phys. Lett.* **42**, 8 (1983) 725-727.

4.2 Bildvergrößerungen

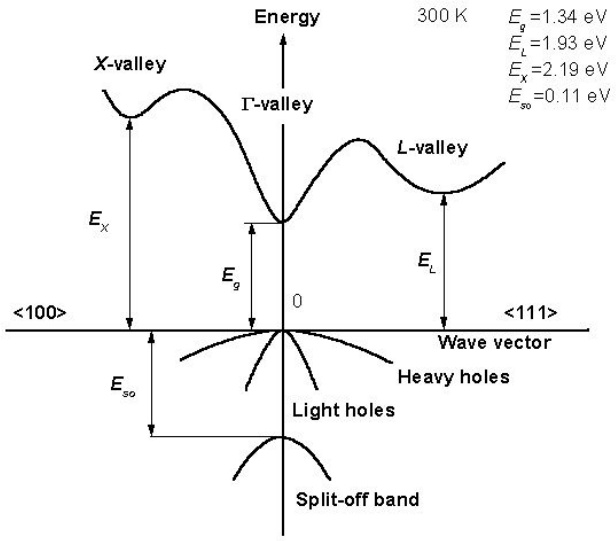

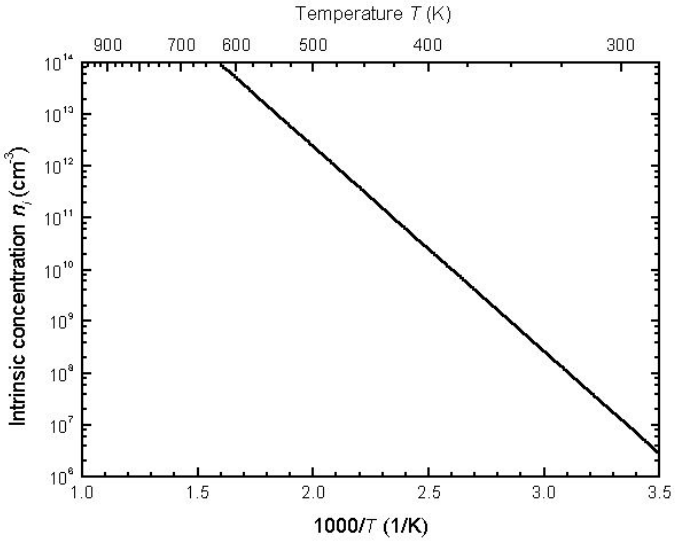

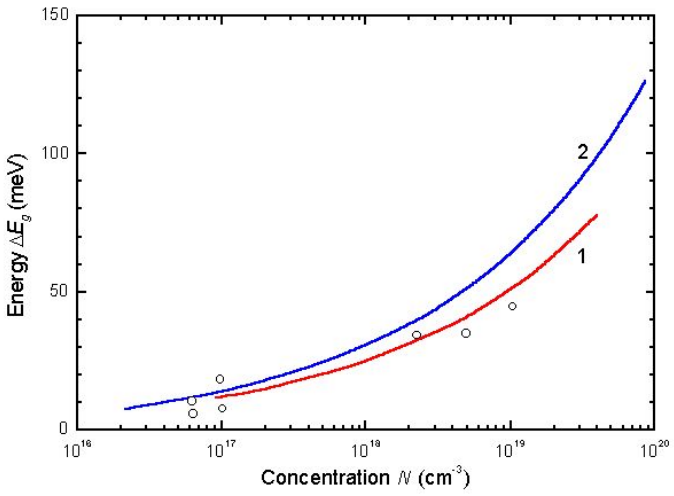

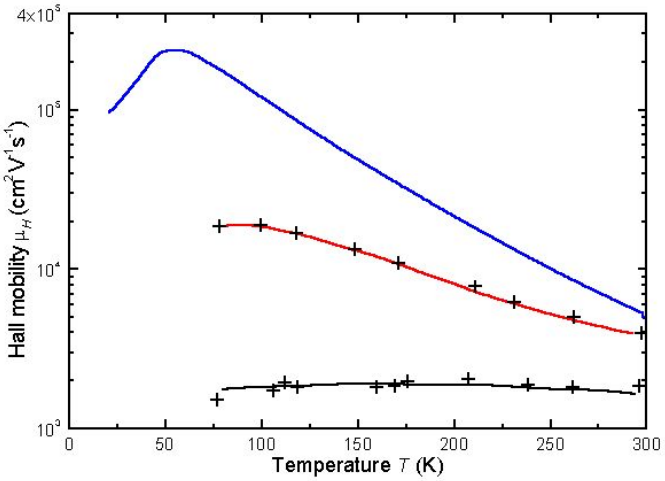
4×10^5
10^5
10^4
10^3
Hall mobility μ_H (cm^2V^-1s^-1)
0
50
100
150
200
250
300
Temperature T (K)

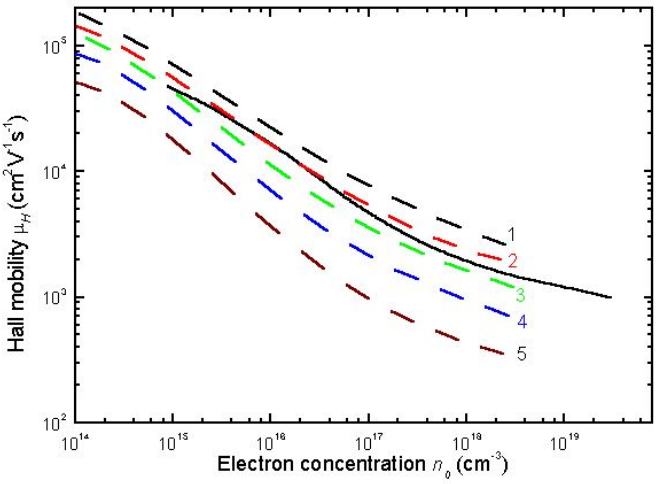
10^5
10^4
10^3
10^2
Hall mobility μ_H (cm^2V^-1s^-1)
1
2
3
4
5
10^14
10^15
10^16
10^17
10^18
10^19
Electron concentration n_0 (cm^-3)

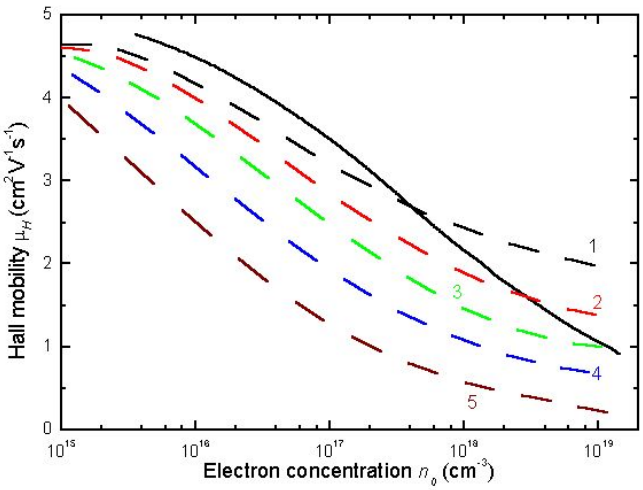
5
4
3
2
1
0
Hall mobility μ_H (cm^2V^-1s^-1)
1
2
3
4
5
10^15
10^16
10^17
10^18
10^19
Electron concentration n_0 (cm^-3)

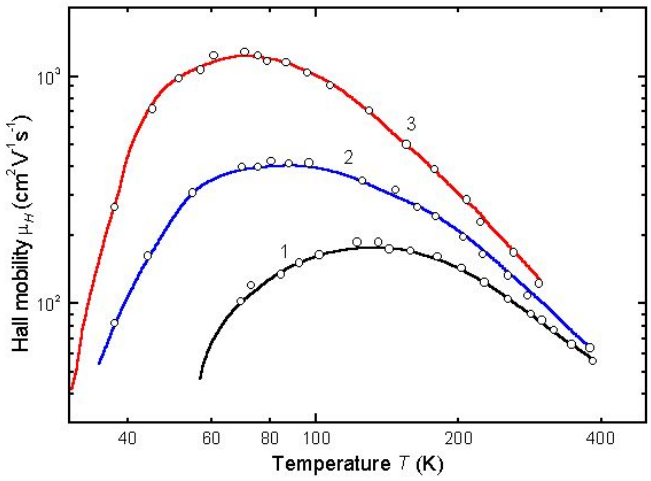
Hall mobility μ_H ($cm^2V^{-1}s^{-1}$)
10^3
10^2
1
2
3
40
60
80
100
200
400
Temperature T (K)

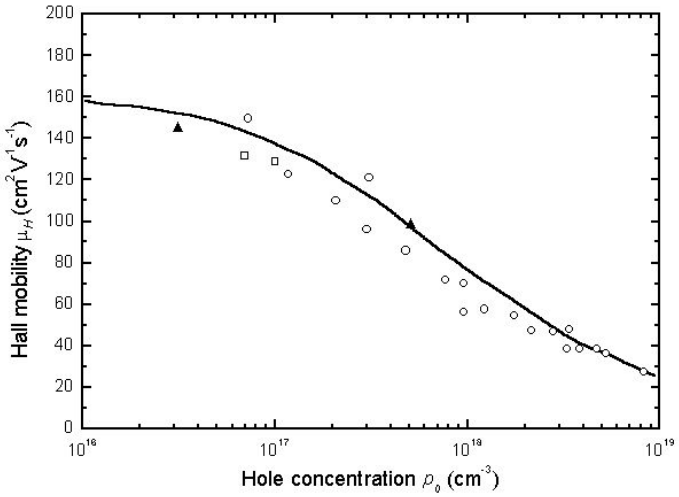
Hall mobility μ_H ($cm^2V^{-1}s^{-1}$)
200
180
160
140
120
100
80
60
40
20
0
10^{16}
10^{17}
10^{18}
10^{19}
Hole concentration p_0 (cm^{-3})

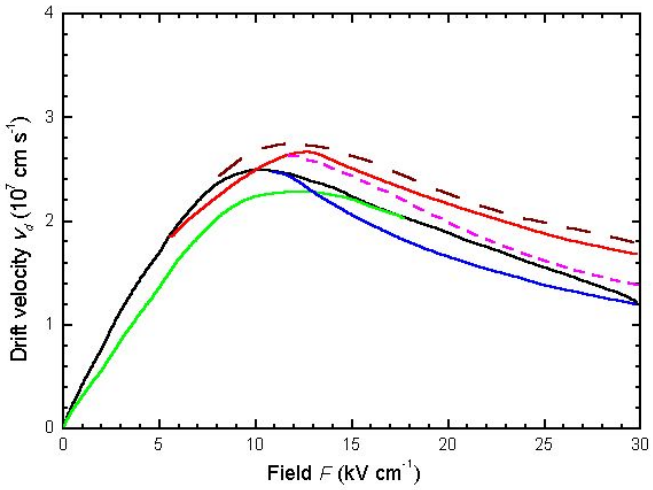
Drift velocity v_d (10^7 cm s^{-1})
4
3
2
1
0
0
5
10
15
20
25
30
Field F (kV cm^{-1})

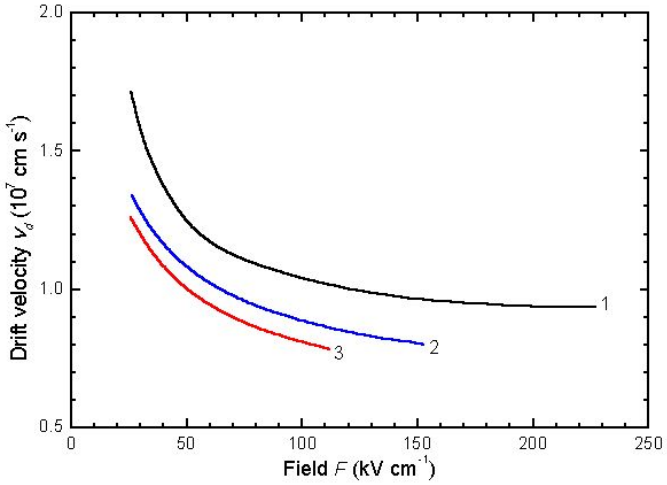
Drift velocity v_d (10^7 cm s^{-1})
Field F (kV cm^{-1})
1
2
3

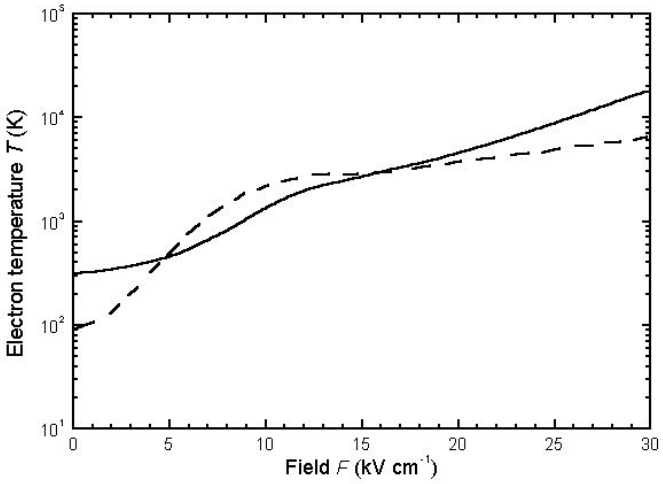
Electron temperature T (K)
Field F (kV cm^{-1})

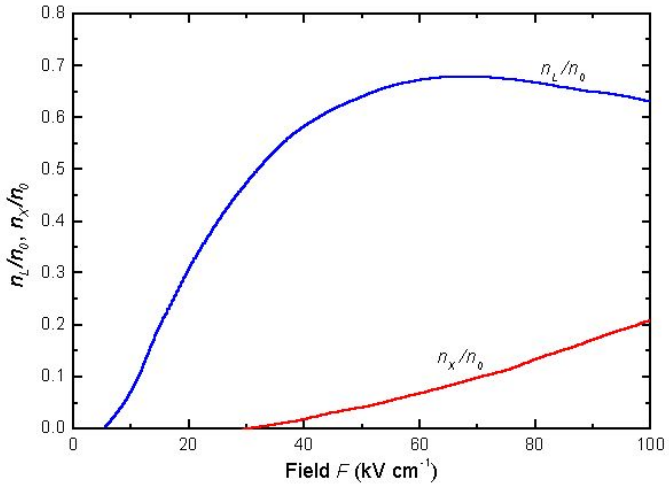
n_L/n_0, n_X/n_0
n_L/n_0
n_X/n_0
Field F (kV cm^{-1})

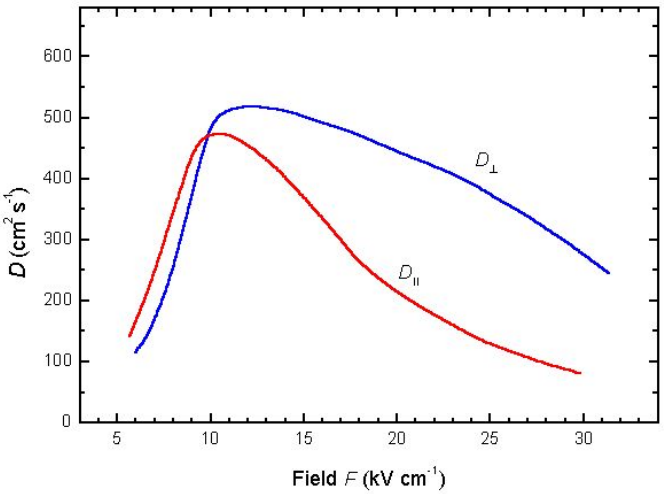
D (cm² s⁻¹)
Field F (kV cm⁻¹)
D⊥
D∥

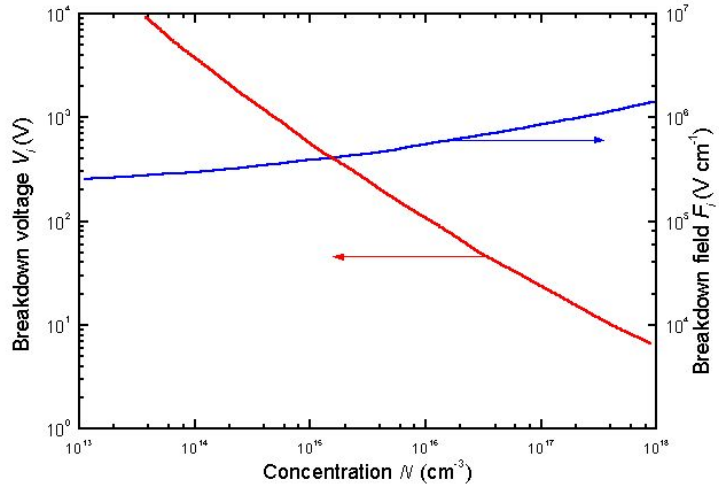
Breakdown voltage V_i (V)
Breakdown field F_i (V cm⁻¹)
Concentration N (cm⁻³)

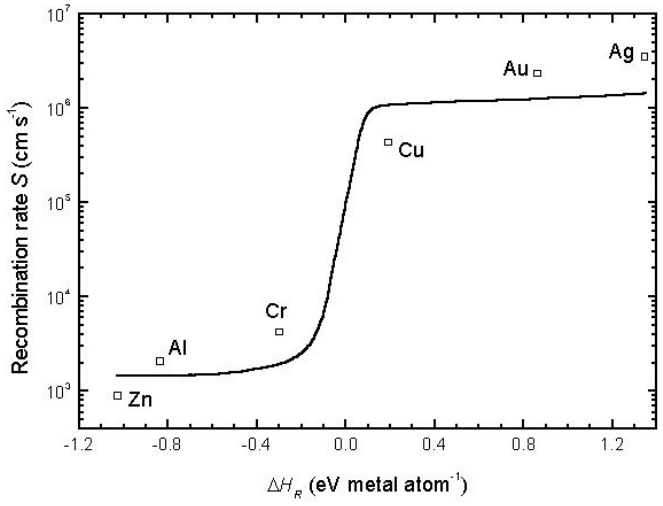
Recombination rate S (cm s⁻¹)
ΔH_R (eV metal atom⁻¹)
Ag
Au
Cu
Cr
Al
Zn

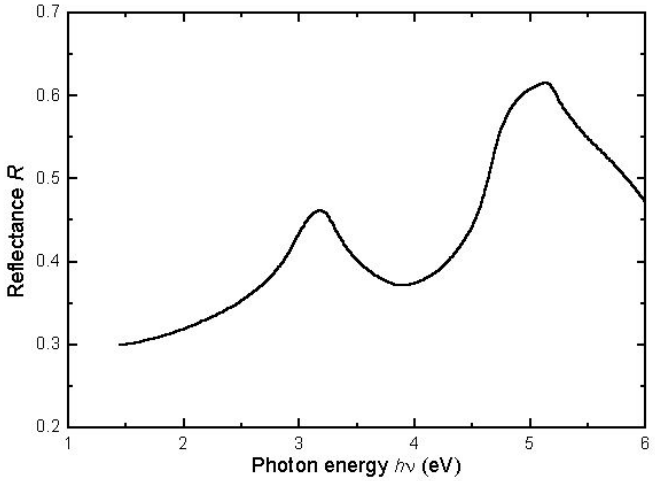
Reflectance R
Photon energy hν (eV)

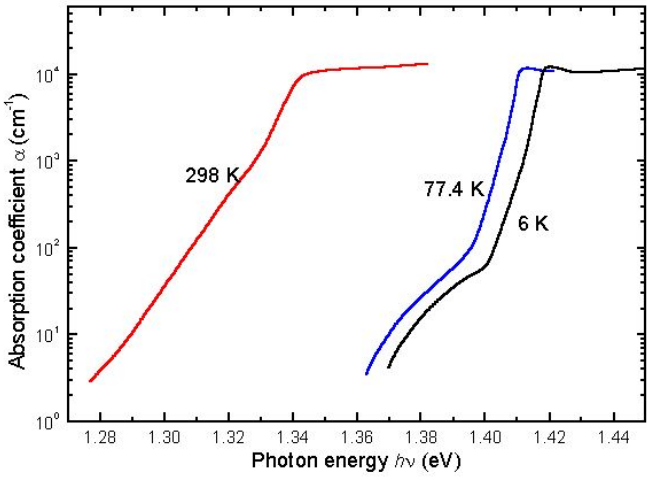
Absorption coefficient α (cm-1)
298 K
77.4 K
6 K
Photon energy hν (eV)

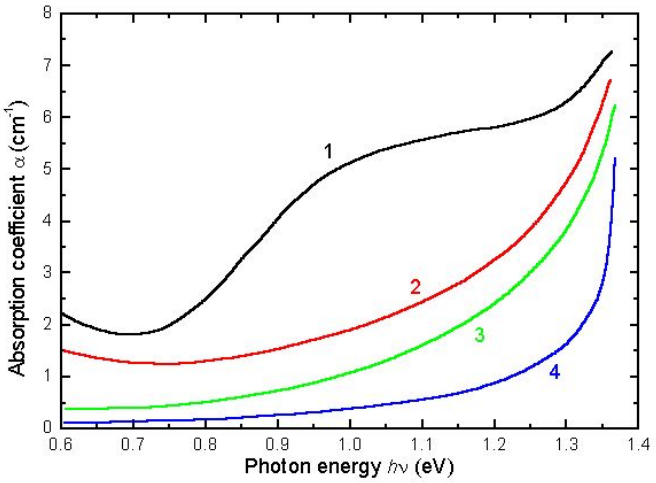
Absorption coefficient α (cm-1)
1
2
3
4
Photon energy hν (eV)

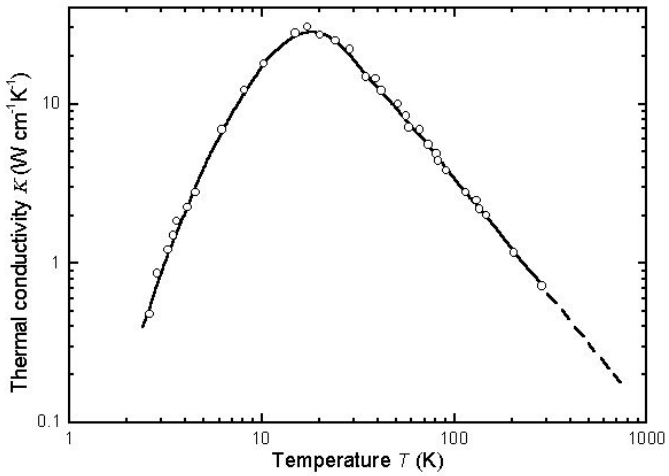
Thermal conductivity κ (W cm-1K-1)
10
1
0.1
1
10
100
1000
Temperature T (K)

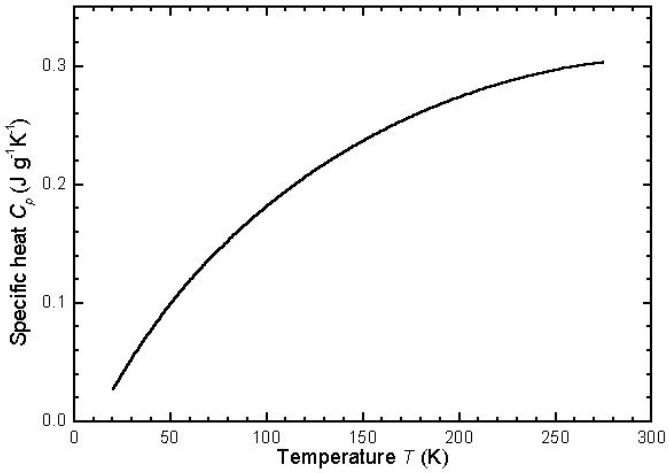
Specific heat Cp (J g-1K-1)
0.3
0.2
0.1
0.0
0
50
100
150
200
250
300
Temperature T (K)

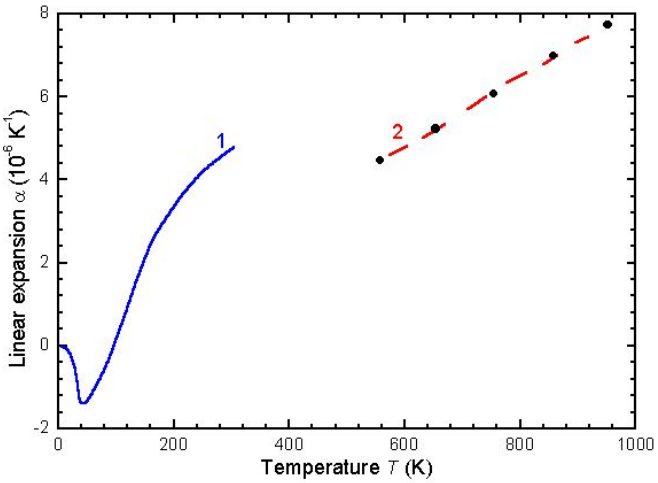
Linear expansion α (10-6 K-1)
8
6
4
2
0
-2
0
200
400
600
800
1000
Temperature T (K)
1
2

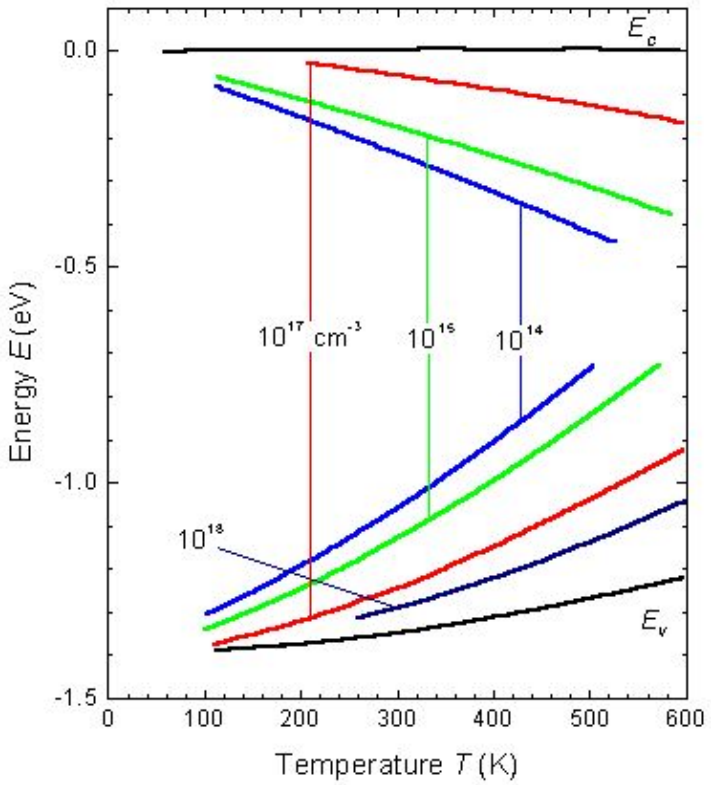
E_c
E_v
10^{17} cm^{-3}
10^{15}
10^{14}
10^{13}
Energy E (eV)
Temperature T (K)
0.0
-0.5
-1.0
-1.5
0
100
200
300
400
500
600

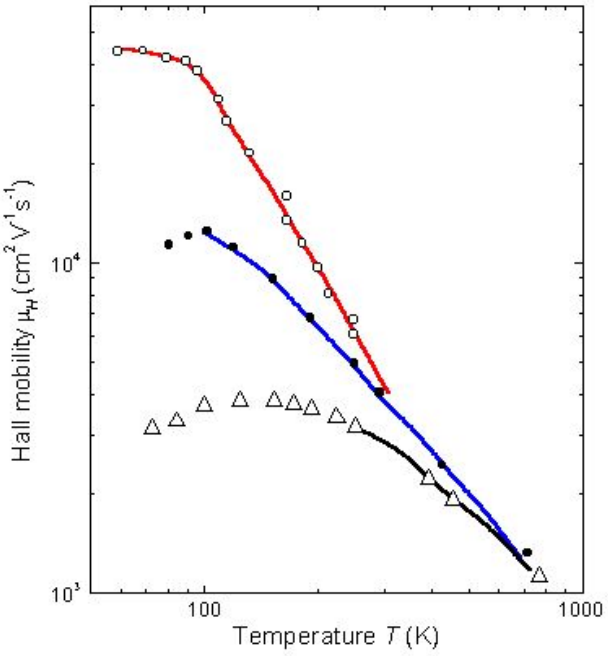
Hall mobility μ_H (cm^{2}V^{-1}s^{-1})
Temperature T (K)
10^4
10^3
100
1000

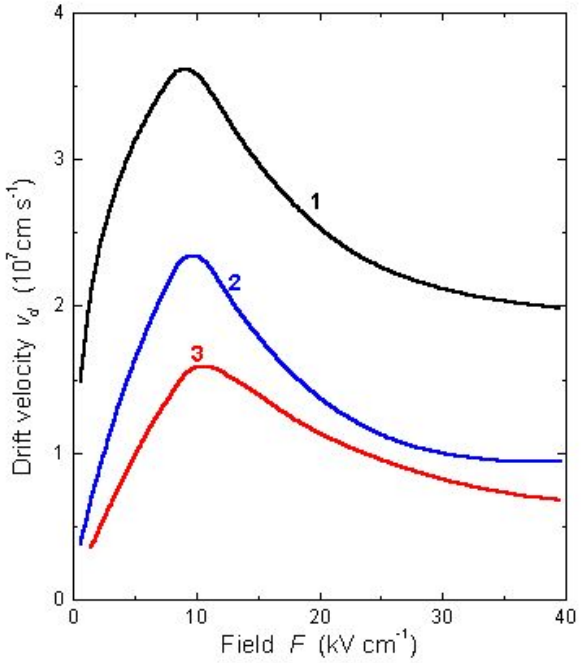
Drift velocity v_d (10^7cm s^{-1})
Field F (kV cm^{-1})
1
2
3
0
1
2
3
4
0
10
20
30
40

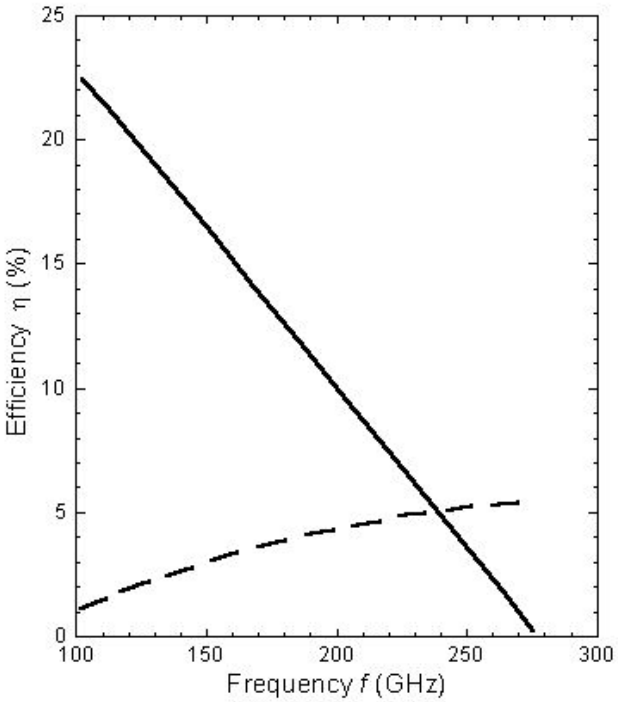
Efficiency η (%)
Frequency f (GHz)
0
5
10
15
20
25
100
150
200
250
300

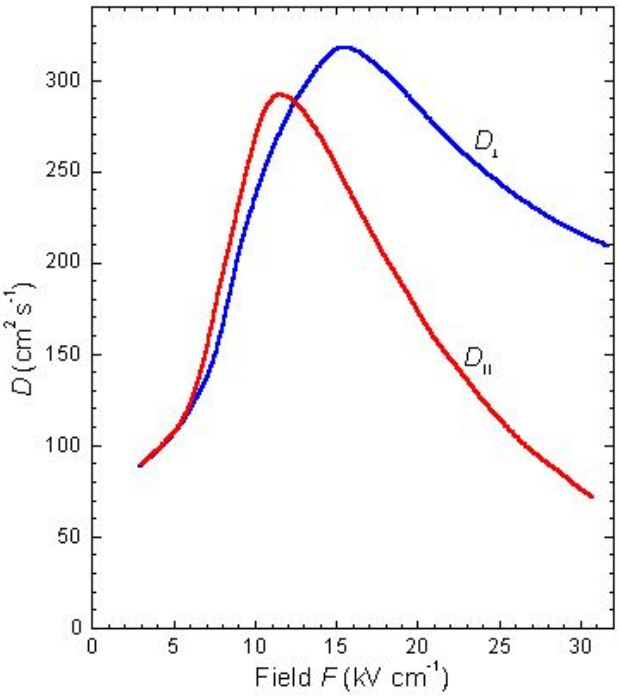
300
250
200
150
100
50
0
0
5
10
15
20
25
30
D (cm² s⁻¹)
Field F (kV cm⁻¹)
D⊥
D∥

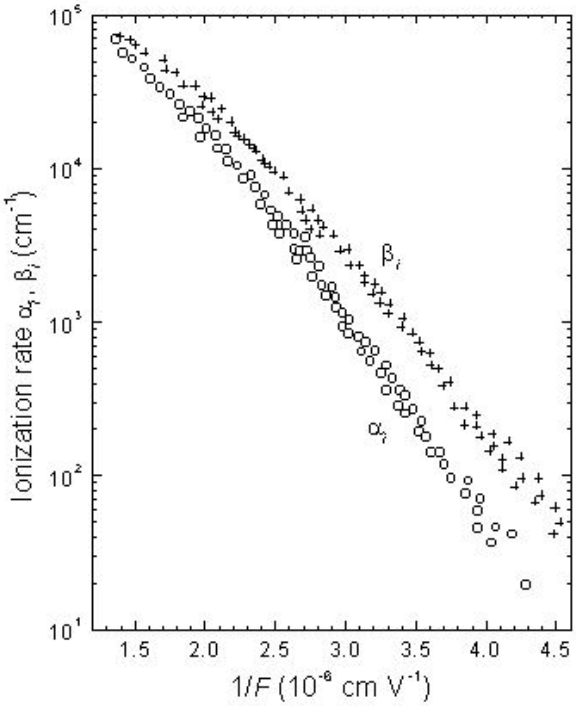
10⁵
10⁴
10³
10²
10¹
1.5
2.0
2.5
3.0
3.5
4.0
4.5
Ionization rate αi, βi (cm⁻¹)
1/F (10⁻⁶ cm V⁻¹)
βi
αi

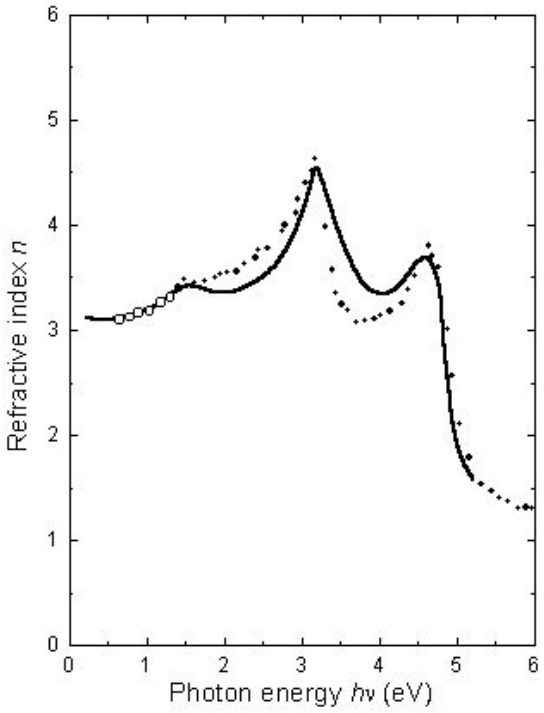
Refractive index n
Photon energy hν (eV)
0
1
2
3
4
5
6

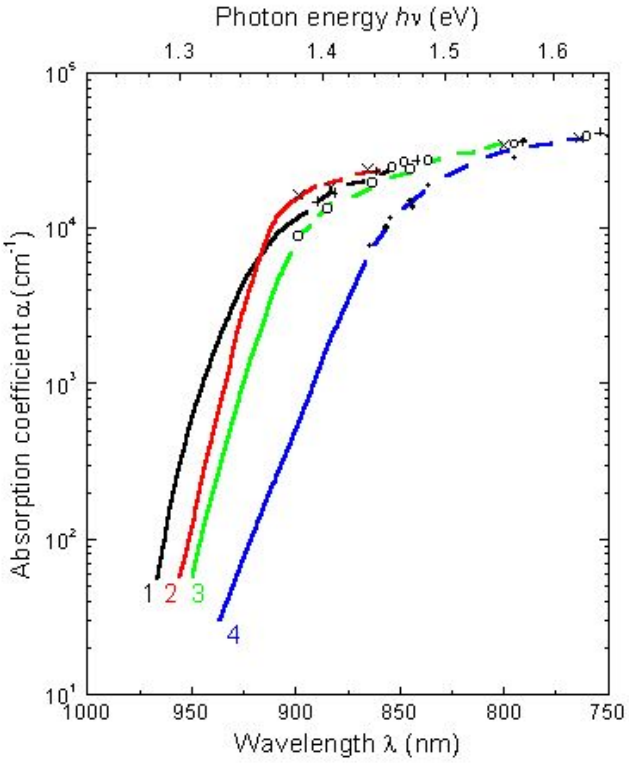
Photon energy hν (eV)
1.3
1.4
1.5
1.6
Absorption coefficient α (cm-1)
Wavelength λ (nm)
1000
950
900
850
800
750
1
2
3
4

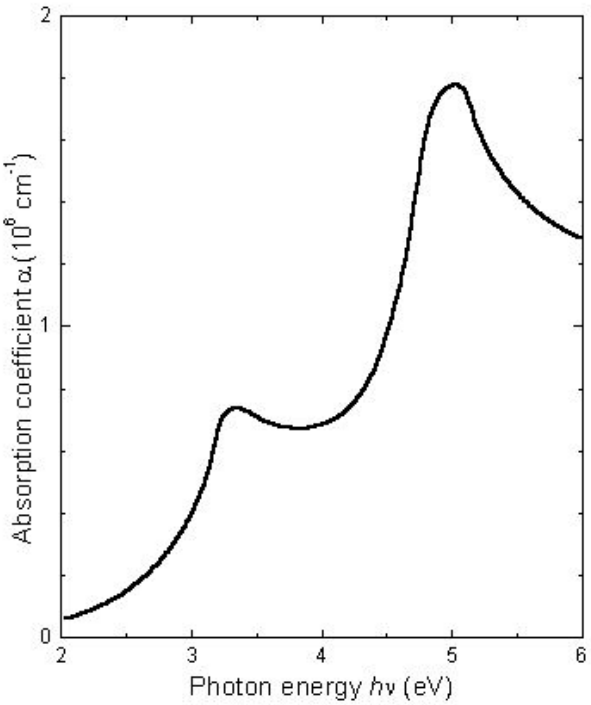
Absorption coefficient α (10^6 cm^-1)
Photon energy hν (eV)
0
1
2
2
3
4
5
6

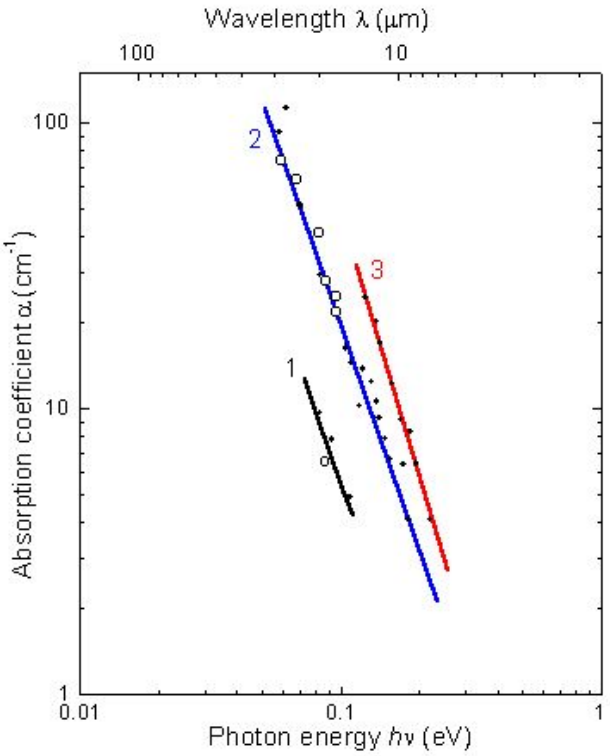
Wavelength λ (μm)
100
10
Absorption coefficient α (cm^-1)
Photon energy hν (eV)
100
10
1
0.01
0.1
1
1
2
3

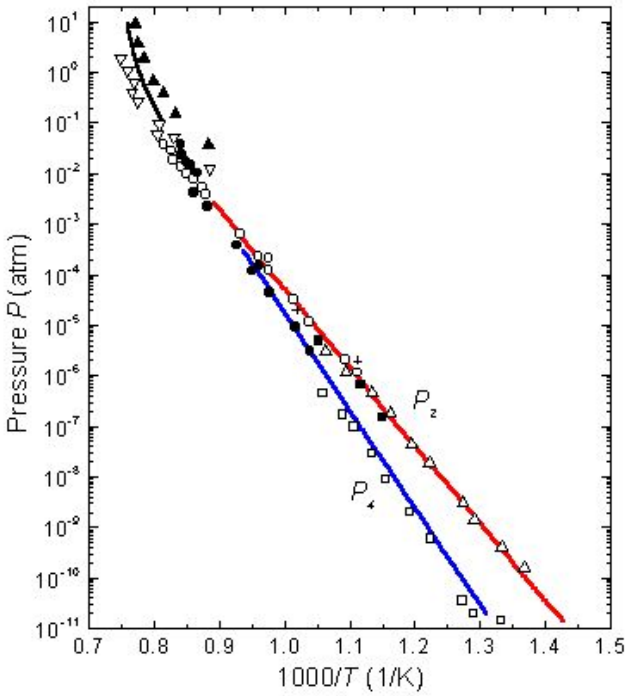

LaTeX 2ε